ABSTRACT

WANG, GUANGQUAN. Peptide ligands that bind to staphylococcal enterotoxin B (SEB). (Under the direction of Dr. Ruben G. Carbonell.)

Staphylococcal enterotoxin B (SEB) is a primary toxin that causes food poisoning. It also acts as a superantigen that interacts with the major histocompatibility complex class II molecule (MHCII) and T cell receptor (TCR) to activate large amounts of T cells leading to autoimmune diseases. Highly purified SEB is needed in research and can be used as a standard in current detection methods for SEB. SEB is also a contaminant in protein A purification from *Staphylococcal aureus* fermentation broth. Inexpensive, robust ligands with high affinity would be suitable replacements for antibodies in biosensors for the detection of SEB. Affinity adsorption processes using short peptides as ligands show great promise in purifying and detecting proteins in comparison with other methods due to their high stability and low cost. By screening a solid-phase combinatorial peptide library, a short peptide ligand, YYWLHH, has been discovered that binds with high affinity and selectivity to SEB, but only weakly to other staphylococcal enterotoxins that share sequence and structural homology with SEB. Using column affinity chromatography with an immobilized YYWLHH stationary phase, it was possible to separate SEB quantitatively from *Staphylococcus aureus* fermentation broth, a complex mixture of proteins, carbohydrates and other biomolecules. The immobilized peptide was also used to purify native SEB from a mixture containing denatured and hydrolyzed SEB, and showed little cross reactivity with other SEs. To our knowledge this is the first report of a highly specific short peptide ligand

for SEB. Such a ligand is a potential candidate to replace antibodies for detection, removal and purification strategies for SEB.

Modeling the transport and kinetic processes in peptide affinity chromatography allows for a direct measurement of the rate of binding of SEB to peptide ligands. It can also provide design parameters for columns that can be used to either remove or detect SEB as well as other pathogens. The mass transfer parameters of SEB were either measured using pulse experiments or determined from correlations. The adsorption isotherms of SEB on YYWLHH resins with different peptide densities were fitted to bi-Langmuir isotherms. The general rate (GR) model was used to fit experimental breakthrough curves to obtain the intrinsic rate constants of the adsorption-desorption kinetics of the protein on the peptide ligands. An analysis of the number of transfer units in the column revealed that both intraparticle mass transfer and intrinsic adsorption rates were important rate-limiting steps for adsorption to the resin particles.

The substitution level of peptide on the resin's surface has a significant impact on the resin's performance. The effects of peptide density on both equilibrium (batch format) and dynamic adsorption (column format) were investigated. The results revealed that the binding mechanism might change from univalent to multivalent adsorption with an increase in peptide density, thus explaining the variation of dissociation constants, maximum capacity, and rate constants with increases in peptide density.

Adsorption processes can play an important role in helping to remove infectious pathogens such as SEB from solution without affecting other desirable components in a product stream. However, little work has been done on the design of adsorption columns

specifically for the removal of several logs of infectious components. This requirement is much more stringent than the normal design of affinity separation columns where at most two logs of removal are sufficient. A column design strategy was developed, aimed at the removal of several logs of an infectious agent from a known volume of a process stream in a fixed amount of time. Two design options are analyzed with the general rate (GR) model, one fixing the column length and varying the fluid velocity, the other fixing the fluid velocity and varying the column length. The results indicate that the reduction in pathogen concentration is highly dependent on the residence time in the column, which is in turn dependent on the flow rate and column geometry. The theory, with no adjustable parameters, is shown to predict with great accuracy the effect of residence time on the log removal of SEB from an aqueous stream using an affinity resin with the peptide YYWLHH. Using a conventional Enzyme-Linked Immunosorbent Assay (ELISA) method, up to 5 log removal of SEB was detected, and the experimental log removal results agreed well with the theoretical prediction.

The detection of minute amounts of SEB using High Performance Liquid Chromatography (HPLC), ELISA or Mass Spectrometry (MS) requires a concentration step prior to analysis. This can be accomplished by solid-phase affinity extraction on a peptide ligand column. It was shown that the YYWLHH resin has a great potential in sample preparation for SEB detection due to its high affinity and capacity. The peptide column was shown to capture all the SEB in highly diluted samples and it was possible to release SEB in a small volume of elution buffer. The enrichment of SEB from the YYWLHH column enabled an ELISA method to be able to work on diluted samples that cannot be analyzed

without the peptide-affinity solid-phase extraction. The detection sensitivity of the ELISA method was improved from ng/ml to pg/ml using the YYWLHH column for SEB concentration.

PEPTIDE LIGANDS THAT BIND TO STAPHYLOCOCCAL ENTEROTOXIN B (SEB)

by

Guangquan Wang

A dissertation submitted to the Graduate Faculty of
North Carolina State University
in partial fulfillment of the
requirements for the Degree of
Doctor of Philosophy

Department of Chemical Engineering

Raleigh, NC

January 2004

APPROVED BY:

Peter K. Kilpatrick	Robert M. Kelly	Steven W. Peretti

Zhilin Li	Ruben G. Carbonell
Minor Representative	Chair of Advisory Committee

To my parents

and Yijing

BIOGRAPHY

Guangquan Wang was born on April 20, 1972 in Boxing, Shandong Province, China, the first child of Dafa Wang and Xi-ai Guo. He attended elementary and high school at his hometown. He went to Dalian University of Technology, Dalian, Liaoning Province, China, in August 1990 and obtained his B. S. degree in Chemical Engineering in July 1994. He began his graduate studies at the Chinese Academy of Sciences in August 1994. After one-year of course work at the Graduate School of the Chinese Academy of Sciences in Beijing, he spent two years at the Institute of Chemical Physics at Dalian, Chinese Academy of Sciences, to finish his M. S. in Chemical Engineering. He then worked in the same institute as a research assistant for more than one year.

In July of 1998, the author came to the United States for graduate studies. After one-year stint at New Jersey Institute of Technology, he transferred to the Department of Chemical Engineering at North Carolina State University in August 1999. The author joined the Bioseparation Group under the direction of Dr. Ruben G. Carbonell in May 2000 and defended a M. S. degree in December 2001.

ACKNOWLEDGEMENTS

I would like to thank my advisor, Dr. Ruben Carbonell, for his belief in my ability, his encouragement, and more importantly, for his endless guidance to help me overcome all the technical obstacles in this thesis. I would also like to thank Dr. Peter Kilpatrick for his continuous encouragement and support. In addition, I want to express my appreciations to Dr. Robert Kelly, Dr. Steven Peretti, and Dr. Zhilin Li for serving on my advisory committee. A special note of thanks to Dr. Xiao-Biao Lin for sitting in on the oral defense during Dr. Zhilin Li's unavoidable absence.

I wish to acknowledge the members of the Bioseparation Group, Honglue Shen, Viterose Wiltshire, Patrick Gurgel, and Jeff Salm, for their kind help and thoughtful discussions. In addition, appreciation is also expressed to the secretaries, Carol Carroll, Peggy Wilkins, Sandra Bailey and Ena Meng, for their help and compassion.

I wish to thank the financial support from Sandia National Laboratories and the American Red Cross for my research. A very special thank goes to Dr. Raoul Reiser at Toxin Technology, Inc. who provided me cell extracts and answered me so many technical questions of toxins. In addition, I also wish to thank scientists at Peptide International, Tosoh Bioseparation, and Texas A&M University for their good services.

I would like to extend my deepest thanks to my wife, Yijing Yu, for her love, understanding, and boundless support. My parents and two little sisters, Yan and Xiao-xia, also deserve special thanks for their continued support and encouragement. Last but not

least, I would also like to thank Zhiqiang, Jianguo, Hao, Jingsan, and Linquan in my hometown, still my best friends after all these years.

TABLE OF CONTENTS

LIST OF TABLES

LIST OF FIGURES

Page

CHAPTER 1

INTRODUCTION

1.1 Motivation

Staphylococcal enterotoxins (SEs) comprise a family of serologically distinct toxins (labeled A-K), all of which are secreted by *Staphylococcus aureus* and share significant homology in primary structure. These toxins are primary causes of food poisoning (Bergdoll, 1983). In addition, they act as superantigens to stimulate enhanced T cell production leading to highly overactive cytokine release and autoimmune diseases (Johnson et al., 1991; Marrack and Kappler, 1990; Swaminathan et al., 1992).

Due to the extreme toxicity of SEs, and their inherent stability, they are considered a significant bioterrorism threat as either an aerosol or food and water contaminant (Franz et al., 1997), and are listed by the Center for Diseases Control (CDC) as select agents (Enserink and Malakoff, 2001). Therefore, it is desirable to develop a sensitive and convenient analytical method to detect such toxins. Furthermore, SEs contaminate other proteins produced from Staphylococcal bacteria, such as protein A. Protein A plays an important role in purification and therapeutic removal of IgG and IgG-containing immune complexes in the treatment of certain cancers and autoimmune diseases (Balint et al., 1989). An affinity separation step might be a convenient way to remove trace SEs and reduce loss of activity and yield of protein A. Homogeneous and highly purified preparations of SEs are required in

studies of their biological activity, identification and quantification (Bhatti et al., 1994; Lopes et al., 1996). Hence an efficient and convenient purification method is desired to recover enterotoxins from fermentation broth and cell culture. Affinity chromatography is used in laboratory and some industrial scale separations to recover a wide variety of biological molecules, especially when the concentration of product of interest is low and when it is found in solution with many contaminants with similar physical properties. Thus affinity chromatography could be a promising method to detect, remove or purify SEs.

The key in affinity chromatography is to create or find a proper adsorbent. Ideally, a ligand should be specific, inexpensive, and stable during multiple operational cycles. To recover biological molecules while retaining their activity, the interaction between ligands and target molecules should be moderate so that harsh elution conditions can be avoided (Chase, 1983; Sproule et al., 2000). The primary affinity ligands used in practice are immobilized metal atoms, dyes and polyclonal and monoclonal antibodies. Both metal and dye ligands are pseudo-affinity ligands. These ligands tend to have lower specificity than antibodies. In addition, dyes and metals have the potential to leach from the column to contaminate the products. Monoclonal antibodies have been widely used in protein purification because of their high affinity and specificity. However, monoclonal antibodies must be purified extensively prior to use as affinity ligands. In addition, immobilized antibodies are sensitive to operating conditions. Harsh conditions are usually required to break antigen-antibody interactions in the elution step and even harsher conditions are necessary (ex. 0.1M sodium hydroxide) to clean and generate the columns prior to the next operating cycle. These conditions can denature the antibodies over time so that only a

limited number operating cycles can be carried out. Both the difficult purification and relatively short life of antibodies result in high cost of antibodies as affinity ligands. Furthermore, the leakage of the antibody into the product could elicit an immune response (Bastek et al., 2000; Huang and Carbonell, 1995). As a result, low cost, more robust ligands that have moderate interaction with the target could have widespread potential application. Short peptides derived from combinatorial peptide libraries have been demonstrated to be good candidates as ligands in affinity chromatography (Baumbach and Hammond, 1992; Huang and Carbonell, 1995; Lam et al., 1991).

SEB is the most widely studied member of the SEs (Swaminathan et al., 1992). It is a good model of a toxin that can be used in biological warfare and other environmental problems. We use SEB as target molecule to find affinity ligands from a solid phase combinatorial peptide library, and then use such ligands to detect, remove and purify SEB by affinity chromatography. In addition, the derived peptide ligands could help us understand the interactions of SEB as a superantigen with the major histocompatibility complex class II molecule (MHCII) and T cell receptor (TCR). As far as we are aware, this is the first time an attempt has been made to identify affinity ligands for a toxin using solid phase combinatorial peptide libraries.

1.2 Goals

The primary objective of this thesis is try to find and then characterize a peptide ligand that can be used to purify, detect or remove SEB from a complex matrix such as cell

fermentation broth and food samples. The first goal of this research is to identify affinity peptide ligands that selectively bind SEB by screening a combinatorial peptide library. The second goal is to understand the rates of binding of SEB to peptide ligands since there is little information on the behavior of small affinity ligands on columns. The contributions of mass transfer and kinetics steps, i.e. axial convection and dispersion, film mass transfer, and pore diffusion, and intrinsic binding kinetics, to the apparent adsorption rate is to be evaluated by the use of mathematical modeling. The third goal is to uncover the binding mechanism of the protein to the resin, which can be deduced from the effects of peptide density on the adsorption isotherm and rate of binding. Besides their application in protein purification, peptides ligands can be employed for pathogen removal. The characterization of the peptide ligand resin provides design parameters for a column that can be used to either remove or detect SEB as well as other pathogens. The fourth goal of this research is to provide strategies for column design of a prescribed number of log removal of SEB or other pathogens. The ultimate goal of this research deals with the application of peptide ligands in SEB detection. The peptide ligands can be employed in a solid-phase concentration step to improve the sensitivity of ELISA and western blotting, or directly used in an on-bead assay.

1.3 Overviews of Contents of This Thesis

This dissertation focuses on biorecovery and bioprocessing using short peptides as the affinity ligands to capture SEB.

Chapter 2 presents a literature review of SEB and peptide ligands. Following a description of the characteristics of SEB, currently used detection and purification methods for SEB are reviewed to show their advantages and disadvantages. For peptide ligands, we first present their potential advantages over other affinity ligands. After a short discussion of the advantages and disadvantages of solid phase combinatorial peptide libraries over phage libraries, the details of the construction and screening of solid phase combinatorial peptide libraries are addressed. This section lists some proteins that have been successfully purified by peptide ligands. The final part in Chapter 2 discusses how to characterize peptide ligands to understand the binding mechanism for the target protein.

Chapter 3 describes the library screening and discovery process used to identify an SEB binding peptide. A short peptide that shows high affinity and selectivity to SEB, YYWLHH, was identified by using a well-established multi-tier screening process. The potential application of the selected peptide in SEB purification is investigated by loading various protein solutions including *E. coli* lysate, BSA, and *Staphylococcal aureus* fermentation broth that have been spiked with SEB in a column format. Finally, according to the binding behavior of native and nicked SEB, an argument is provided for the potential binding site of the peptide on SEB.

Chapter 4 presents the characterization of the mass transfer and binding kinetics in a chromatography column packed with the affinity peptide ligand YYWLHH. The methods used to characterize peptide ligands in this chapter are general and thereby can be used in other protein-peptide systems. By using the general rate model, the contribution of each step involved in the adsorption process in a column is evaluated so that the rate-limiting step can

be determined. The final part in Chapter 4 describes the effects of peptide density on the adsorption isotherms and rates of binding. According to the variances of dissociation constants and rate constants with peptide density, a possible transition of the binding mechanism from single point binding to multipoint binding is discussed.

Pathogen removal is a crucial part in the validation process for many biopharmaceutical processes. Using SEB-YYWLHH system as an example, column design strategies are provided for a prescribed log removal of pathogens in Chapter 5. With the help from the general rate model developed in Chapter 4, the residence time in the column and the column dimension for prescribed log removal of SEB are obtained by either fixing the column length and varying the fluid velocity, or fixing the fluid velocity and varying the column length. General remarks of guidance and suggestions for column design are addressed according to these results. The effects of mass transfer and binding kinetics on protein purification in the adsorptive column have been well documented in the literature. But there is little information on how to design a column specifically to achieve several log removal of a pathogen. Chapter 5 also describes the influences of mass transfer and binding kinetics on SEB log removal. Finally, the effects of flow rate on the pressure drop in the column are considered.

Chapter 6 deals with the application of the peptide ligand for SEB detection. We use the peptide ligand in a solid-phase concentration step to prepare samples for ELISA. The affinity peptide column is used to concentrate trace SEB from very diluted samples that are hard to detect by ELISA. Using the affinity concentration step, the sensitivity of the ELISA was increased from ng/ml to pg/ml.

Chapter 7 provides a summary of conclusions of all the experimental and simulation results of this thesis and recommends future work.

1.4 References

Balint J, Totorica C, Stewart J, Cochran S. 1989. Detection, isolation and characterization of staphylococcal enterotoxin B in protein A preparations purified by immunoglobulin G affinity chromatography. J Immunol Methods 116:37-43.

Bastek PD, Land JM, Baumbach GA, Hammond DH, Carbonell RG. 2000. Discovery of Alpha-1-proteinase inhibitor binding peptides from the screening of a solid phase combinatorial peptide library. Separation Sci Technol 35:1681-1706.

Baumbach GA, Hammond DJ. 1992. Protein purification using affinity ligands deduced from peptide libraries. BioPharm May:24-35.

Bergdoll MS. 1983. Enterotoxins. In: Easman CS, Adlum C, editors. Staphylococcal and Staphylococcal Infections. London: Academic Press Inc. p 559-598.

Bhatti AR, Nadon LP, Micusan VV. 1994. Purification of superantigen staphylococcal enterotoxin B (SEB). IJBC 1:47-56.

Chase HA. 1983. Affinity separations utilizing immobilized monoclonal antibodies-A new tool for the biochemical engineer. Chem Eng Sci 39:1099-1125.

Enserink M, Malakoff D. 2001. Bioterrorism: Congress weighs select agent update. Science 294:1438-1438.

Franz DR, Jahrling PB, Friedlander AM, McClain DJ, Hoover DL, Bryne WR, Pavlin JA, Christopher CW, Eitzen EM. 1997. Clinical recognition and management of patients exposed to biological warfare agents. J Am Med Assoc 278:399-411.

Huang PY, Carbonell RG. 1995. Affinity purification of proteins using ligands derived from peptide libraries. Biotechnol Bioeng 47:288-297.

Johnson HM, Russell JK, Pontzer CH. 1991. Staphylococcal enterotoxin microbial superantigens. FASEB J 5:2706-2712.

Lam KS, Salmon SE, Hersh EM, Hruby VJ, Kazmierski WM, Knapp RJ. 1991. A new type of synthetic peptide library for identifying ligand-binding activity. Nature 354:82-84.

Lopes HR, Noleto ALS, Bergdoll MS. 1996. Purification of Staphylococcal enterotoxins B and C2 by dye ligand chromatography - production of antisera. Rev Microbiol 1:52-56.

Marrack P, Kappler J. 1990. The staphylococcal enterotoxins and their relatives. Science 248:705-711.

Sproule K, Morrill P, Pearson JC, Burton SJ, Hejnæs KR, Valore H, Ludvigsen S, Lowe CR. 2000. New strategy for the design of ligands for the purification of pharmaceutical proteins by affinity chromatography. J Chromatogr A 740:17-33.

Swaminathan S, Furey W, Pletcher J, Sax M. 1992. Crystal structure of staphylococcal enterotoxin B, a superantigen. Nature 359:801-806.

CHAPTER 2

LITERATURE REVIEW

2.1 Staphylococcal Enterotoxin B (SEB)

2.1.1 Staphylococcal Enterotoxins (SEs)

Staphylococcal enterotoxins (SEs) are a family of structurally related proteins produced by *Staphylococcus aureus*. They are monomeric proteins (25-30kDa) that contain one disulfide bond and are resistant to temperature and pH denaturation (Bergdoll, 1983). Staphylococcal enterotoxins are leading causes of food poisoning and are potent gastrointestinal toxins (Archer and Young, 1988). As little as 0.1μg of an enterotoxin is sufficient to cause symptoms of intoxication in humans (Evenson et al., 1988). SEs are also superantigens that bind to the major histocompatibility complex class II molecules (MHCII) and T cells bearing particular Vβ elements, triggering a massive release of T cell-derived cytokines followed by allergic and autoimmune symptoms (Balaban and Rasooly, 2000) and the eventual disappearance or inactivation of responding T cells (Li et al., 1999). To date, twelve SEs have been identified and differentiated based on serotyping: SEA (Casman et al., 1963), SEB (Casman et al., 1963), SEC (Bergdoll et al., 1965; Reiser et al., 1984), SED (Casman et al., 1967), SEE (Bergdoll et al., 1971), SEG (Munson et al., 1998), SEH (Su and Wong, 1995), SEI (Munson et al., 1998), SEJ (Zhang et al., 1998) and SEK (Orwin et al., 2001). Note that SEC is further divided into SEC1, SEC2 and SEC3 due to minor epitope

variations. The toxins may be grouped based on their degree of sequence homology. SEA, SED, SEE and SEJ form one group with an overall amino acid sequence homology of 51%-81%. SEB and the SECs form another group, with 42%-67% sequence homology. The homology between these two groups is around 22-33%. SEG, SHE, SEI and SEK each have poor or no homology with any other SE (Balaban and Rasooly, 2000; Marrack and Kappler, 1990). Another superantigen toxin produced by *Staphylococcus aureus*, originally designated as SEF, but renamed Toxic Shock Syndrome Toxin-1 (TSST1) (Bergdoll, 1985) has poor sequence homology to SEs but high structural homology with SEB (Prasad et al., 1993).

As gastrointestinal toxins, SEs are the second most common cause of reported food-borne illnesses. They usually contaminate some dairy food products, such as meat, poultry, fish, milk and their products (Balaban and Rasooly, 2000; Swaminathan et al., 1996). Patients with SE poisoning may present with emesis, diarrhea, nausea, dizziness and prostration. Little is known about the mechanism of this intoxication at present. It is possible that emesis occurs through stimulation of neural receptors in the abdomen by the toxins (Bayliss, 1940).

SEs have been extensively studied as superantigens. Superantigens cause immense T cell activation that can be several orders of magnitude greater than that evoked by routine antigens. This is due to their different modes of interaction with the major histocompatibility complex class II molecule (MHCII) and T cell receptor (TCR) from those of a routine antigen. Routine antigens have to be preprocessed by the antigen-presenting cells (APC) into small peptides (13 to 17 residues in length). These antigenic peptides bind to a cleft formed

by two α helices of the α and β chains of the MHCII molecule. The formed peptide-MHCII complex makes contact with all variable chains of TCR and the fraction of stimulated T cells is limited by these interactions (Goldsby et al., 2000; Swaminathan et al., 1992). Usually only 0.0001%~0.001% of T cells get activated this way (Marrack and Kappler, 1987). Superantigens need no such preprocessing. They bind as intact molecules but to a different part of the MHCII molecule than normal antigenic peptides. The superantigen-MHCII complexes make contact only with the Vβ chain of TCR. Different SEs have distinguishable specificities to TCR and MHC II even though they fall into the same group based on sequence homology (Swaminathan et al., 1996). The formation of MHCII-SE-TCR ternary complexes triggers the proliferation of all T cells bearing particular types of Vβ elements. Since there are only a limited number of Vβ elements in humans, a very large fraction (2~20%) of T cells get stimulated. The consequent release of T cell-derived lymphokines such as interleukin-2 or tumor necrosis factor may be involved in the mechanism of toxicity, causing fever, weight loss, and osmotic imbalances that could lead to death (Johnson et al., 1991; Marrack and Kappler, 1990; Swaminathan et al., 1992). Although it is well known that the emetic function is dissociable from that of T cell stimulation, both emesis and T cell stimulation are dependent upon distinct but overlapping regions on SEs (Harris et al., 1993).

2.1.2 Characteristics of SEB

SEB is a monomer protein with a MW of 28,366 Daltons and a pI of 8.6. The three-dimensional structure of SEB determined by X-ray crystallography reveals a molecule

containing two domains composed of residues 1-120 and 127-239 respectively (Figure 2.1) (Papageorgiou et al., 1998; Swaminathan et al., 1996). Domain 1 consists of two β sheets, one formed by β1, β4 and β5 and the other by β2, β3, β4 and β5. It also contains three α-helices, α1, α2 and α3. Domain 2 mainly consists of two α helices, α4 and α5 and a twisted β sheet formed by β6, β7, β9, β10 and β12; it also includes two very short β strands, β7 and β11. SEB binds to MHCII with high affinity (K_d ~10^{-6}) (Scholl et al., 1989) and to T cells bearing Vβ3, 7, 8.1, 8.2, 8.3 and 17 in mice (White et al., 1989). Based on the topology and mutational studies of SEB, the T-cell receptor-binding site on SEB encompasses a shallow cavity formed by domains 1 and 2. The MHCII molecule binds to an adjacent site, namely the α5 face of the SEB molecule. The active site for emesis is thought to be in the α4 groove (Swaminathan et al., 1992).

SEB is one of the most heat-stable proteins. The activity loss due to heat is fast initially and then levels off. Less than 50% activity is lost when the toxin is heated to 100°C at pH 7.3 for 5 mins (Schantz et al., 1965). Heat aggregation results in rapid loss of activity at 70 to 80°C. But heating to 100°C can recover 35 to 40% immunological activity because of the dissociation of aggregates at higher temperature. Therefore, heat treatment of SEB causes a more rapid loss of immunological activity at 70 to 80°C than at 90 to 100°C. After incubation at 25°C, some activity of toxins that have been inactivated by heat can be recovered (Fung et al., 1973; Jamlang et al., 1971; Satterlee and Kraft, 1969).

SEB is resistant to denaturation when it is exposed to denaturants, such as guanidine hydrochloride and urea. Isothermal denaturation experiments show that prolonged exposure

(hours to days, depending on denaturant conditions) of SEB in guanidine hydrochloride up to 6M and urea up to 9M is required for unfolding to reach equilibrium. Refolding the denatured toxin to native protein after dilution of denaturant is complete within minutes to a few hours. This indicates a very large activation energy for unfolding and a comparatively small activation energy for refolding of SEB. The stable structure of SEB is due to the disulfide loop that locks covalently two β sheets in a stable, anti-parallel configuration (Warren, 1977; Warren et al., 1974). However, SEB can be denatured rapidly and irreversibly when the pH is below 3.5. This is because SEB is a basic protein, and hence low pH results in protonation of carboxylate groups that are involved in maintaining the native SEB conformation. Such protonation leads to a conformational change of SEB so that the local positive electrostatic free energy resulting from protonation of the carboxylate groups can be reduced (Warren et al., 1974).

It is a challenge to deal with the microheterogeneity of SEB during its characterization. Different preparation and purification methods give different SEB-associated forms. It is generally agreed that only one component is synthesized within *Staphylococcus aureus* strains. The hydrolysis of labile amide groups of glutamine and asparagine residues in the protein by amidohydrolase in the fermentation broth converts the original component to less alkaline forms of SEB. Thus there are series of isomers of SEB that are different in pI, but serologically identical. This has been confirmed by the comparison between the amino acid sequence deduced from the DNA sequence, and the amino acid sequence analyzed from purified SEB by Edman degradation, where most of the differences involve aspartic acid and asparagines, and glutamic acid and glutamine (Huang

and Bergdoll, 1970; Jones and Khan, 1986). The distribution of the multi-charged SEB species is dependent on the operation conditions, especially temperature and pH, in the preparation process (Baird-Parker, 1971; Chang and Dickie, 1971; Metzger et al., 1972; Schantz et al., 1965; Spero et al., 1974). In addition, polymerization of SEB usually develops during storage, and low ionic strength can enhance that process (Jamlang et al., 1971). In the production of SEB, the native proteases in the fermentation broth are able to nick the SEB inside the disulfide loop yielding some low molecular weight (13~16 kDa), serologically related toxin materials (Spero et al., 1975; Spero et al., 1973).

2.1.3 Detection of SEB

The required detection level of enterotoxin in foods from outbreaks is 0.1~0.2μg/100g of food (Bergdoll, 1979). Most of the methods for detection of enterotoxins are based on the use of antibodies prepared against the enterotoxins. One of them is the gel diffusion method. Polyclonal antibodies prepared in rabbits using the individual purified enterotoxins react with the enterotoxins in gels to give precipitin reactions that are highly specific (Bergdoll, 1996). The used gels are generally Ouchterlony gel plates and microslides. The normal sensitivity of gel diffusion methods is around 0.1~0.5 μg/ml (Meyer and Palmieri, 1980; Robbins et al., 1974). The reversed passive latex agglutination method (RPLA) is more sensitive than gel diffusion. The antibody-coated latex particles agglutinate when brought in contact with the enterotoxins. RPLA is sensitive enough to detect enterotoxins in most foods that cause food poisoning (Wieneke and Gilbert, 1987).

However, enzyme-linked immunosorbent assay (ELISA) are usually employed instead of RPLA to detect small amounts of enterotoxins. Several kits are available commercially (Fey et al., 1984; Park et al., 1994). The antibody is treated with the sample and then the antibody-enterotoxin complex is incubated with the enzyme-antibody conjugate. The color developed from enzyme-substrate reaction is directly proportional to the amount of enterotoxin in the sample. Thus ELISA can be used directly on crude extracts from food or partially purified samples. Most of the sorbents used to attach antibodies are microtiter plates, others include polystyrene spheres, tubes, and dip sticks with wells. The sensitivity of an ELISA is usually less than 1 ng/g food (Bergdoll, 1996; Fey et al., 1984). However, occasional antibody cross-reactivity with unrelated antigens and the insensitivity with heat-treated foods prevent definitive identification of the enterotoxin with the use of an ELISA (Park et al., 1992; Rasooly and Rasooly, 1998). Western blotting can overcome these major problems because the Western procedure solubilizes denatured toxin, which may still be biological active, and allows characterization of antigen that reacts with the antibody (Rasooly and Rasooly, 1998). The most sensitive detection method (at pg level) is the T-cell proliferation assay which measures the ability of enterotoxins to act as superantigen. However, this assay is nonspecific since any enterotoxin in the sample can induce T-cell proliferation. Thus one more step such as an ELISA is subsequently needed to identify the enterotoxin (Rasooly et al., 1997). All these immunological methods share the same disadvantage. They are relatively time-consuming, ranging from several hours up to several days.

Biosensors based on immunological testing are an ideal alternative to the immunological methods mentioned above. The limits of detection and sensitivity of biosensors are comparable to ELISA, but the total assay time could be only a few minutes. The detection mechanism of biosensors is based on the interaction between a surface-immobilized receptor, mostly an antibody, and a solution-born analyte. The consequential biological response of the antigen-antibody interaction is then translated into an electronic output that can be analyzed (Nedelkov et al., 2000; Rasooly and Rasooly, 1999). There are two common detection methods used in biosensors. One is based on surface evanescent waves, which can be used to measure the changes in refractive index due to antigen-antibody interactions at the surface of optical waveguides; these changes can be recorded as a shift in resonance angle (Rasooly and Rasooly, 1999). The other is based on surface plasmon resonance (SPR), where the change in the refractive index at the surface results in a measured shift in the wavelength of light absorbed, or by light diffraction (Nedelkov et al., 2000). The major problems of ELISAs, such as antibody cross-reactivity with unrelated antigens and the insensitivity with heat-treated foods, can also occur with biosensors. As in ELISA, the use of sandwich format immunoassay that involves a secondary antibody could increase the specificity in a biosensor. A fiber-optic biosensor system that includes a secondary fluorescent-labeled antibody has been used to detect SEB with little cross-reactivity to SEA and SED (King et al., 1999; Tempelman et al., 1996). Recently, biomolecular interaction analysis mass spectrometry (BIA-MS) has been developed to differentiate specific antibody-enterotoxin binding from nonspecific antibody-antigen binding in SEB detection, following a second step, matrix-assisted laser desorption /ionization time-of-flight mass spectrometry, to

identify SEB (Nedelkov et al., 2000). These specific biosensor systems require complex instruments and are not as convenient as ELISAs.

2.1.4 Purification of SEB

The charaterization of the biological activity of SEs requires highly purified and homogeneous enterotoxins. Meanwhile, the methods of identification and quantification of SEs, such as ELISA and biosensors, also require highly purified enterotoxins as standards. Thus it is necessary to develop corresponding methods for the purification of SEs. SEs are produced within *Staphylococcus aureus* strains and are released in the fermentation growth medium. SEA, SED and SEE belonging to the same group based on sequence homology are synthesized and released into the growth medium near the beginning of the exponential growth phase, whereas SEB and SECs belonging to another group are produced during the late stationary phase (Baird-Parker, 1971; Spero et al., 1987). *Staphylococcus aureus* strains, which release one dominant enterotoxin, and the corresponding growth conditions, have been known for most of the SEs. For example, with a highly SEB-productive strain, *Staphylococcus aureus* S-6, the concentration of SEB can reach 270μg per ml culture supernant after 48-h fermentation (Donnelly et al., 1967; Lopes et al., 1996).

Challenges presented in the purification of SEs from fermentation broth include: 1) contaminants with similar molecular weights and charge to the enterotoxin of interest, such as other enterotoxins, protein A, proteases, staphylokinase, hemolysins or endotoxin (Bhatti et al., 1994); 2) microheterogeneity of SEs, which results from polymerization or hydrolysis

of labile amide groups. Different techniques have been used to purify SEs. Only minor variants are needed to apply these techniques to purify other enterotoxins because all SEs share a great structure homology and have similar properties. The degree of purity and percent recovery are the major criteria for characterizing SEB purification methods. Most of the methods developed to date seldom guarantee both (Table 2.1). Although multi-step procedures give high purity, they usually give low yield of SEB and take a long time, and cannot easily be adapted for large-scale purification. Chromatography methods give high recovery and purity compared to chemical methods, such as acid or ethanol precipitation (Table 2.1). Different chromatography methods, such as cation exchange, hydrophobic, reverse-phase or chromatofocusing, have been used successfully to recover SEB in large-scale. However, these methods are not specific enough to get highly purified and homogeneous SEB. Additional steps, such as gel filtration, electrophoresis or isoelectric focusing, are needed to polish the partially purified enterotoxin (Table 2.1). Dye ligand affinity chromatography is a kind of pseudo-affinity chromatography method, which is more specific than the chromatography methods mentioned above. The adsorption of enterotoxins to dye ligands results from a mixture of interactions consisting of electrostatic, hydrophobic and hydrogen bond interactions. Large-scale purification of SEA, SEB and SEC_2 with one-step dye ligand chromatography by using Red A as ligand has been demonstrated by (Brehm et al., 1990). But there are still some contaminants in the preparation of SEB after dye ligand chromatography. A pre-purification step, such as cation exchange, is recommended to remove a portion of the contaminants prior to Red A chromatography (Lopes et al., 1996).

Thus more specific ligands are needed to capture SEB in one-step so that better recovery and purity can be obtained.

2.2 Peptide Affinity Ligands

2.2.1 Advantages of Peptide Ligands (Bastek et al., 2000; Baumbach and Hammond, 1992; Huang et al., 1996; Huang and Carbonell, 1995; Huang and Carbonell, 1999)

Affinity chromatography is the most efficient way to purify biomolecules. Many biomolecules can be purified within one step using affinity chromatography with high recovery. The key in affinity chromatography is to find a proper affinity ligand corresponding to the molecules of interest. While monoclonal antibodies are the most common ligands for laboratory uses, it is difficult to scale up these columns because antibodies are quite costly and sensitive to operating conditions. Also, the leakage of the antibodies under harsh elution and cleaning conditions can result in serous contamination due to the immunogenicity of these proteins. Dye ligands and immobilized metal ions are more stable than antibodies so that they can stand harsh operation conditions, but both of them lack sufficient specificity. In addition, dye ligands may be toxic and there is severe leakage of immobilized metal ions. Prior experiences using peptides as ligands ranging from 3 to 25 amino acids have shown that peptides have affinities to molecules of interest that compare well with dyes and immobilized metal ions. As opposed to monoclonal antibodies, small peptide ligands are much more stable because they don't require a specific tertiary structure to maintain their biological activity. To prevent ligand decomposition by protease found in

the mixture, it is possible to use the D form of the terminal amino acid. Small peptides are also not likely to cause immune response in case of leakage into the products and it is easy to isolate small peptides from protein products downstream. Peptides can be manufactured aseptically in large scale under GMP (good manufacturing practices) conditions at relatively low cost. The interactions between peptides and proteins are moderate so that the protein can be eluted under mild conditions without damage to the protein activity. In addition to being good candidates as ligands in affinity chromatography, peptides are used widely to determine protein-protein interactions without a priori information on protein structure (for example in epitope mapping).

2.2.2 Combinatorial Peptide Libraries: Phage and Solid Phase Library

One of the challenges for use of peptide ligands is the identification of a sequence that shows affinity and specificity to the target protein. The design of specific complementary peptide sequence to the target protein has been demonstrated difficult even when the structure of the target protein is known (Lawrence and Davis, 1992; Saragovi et al., 1992). The development of combinatorial libraries has allowed screening millions of peptide sequences to discover specific peptides that bind to the target protein. Peptide libraries can be generated either biologically or synthetically. Several combinatorial library methods have been described in the literature (Lam et al., 1997). The most widely used biological libraries are phage-displayed libraries, while one-bead-one-peptide libraries are the dominant libraries obtained directly from chemical synthesis.

In phage-displayed peptide libraries, a random gene with a given length is synthesized and then inserted into bacterial phage gene III. The corresponding peptide coded by the inserted DNA is displayed at the N-terminal of the gene III protein (pIII) on the phage surface. Each phage displays one kind of peptide sequence that is different from other phages. Affinity peptides on phage that bind to the target protein are selected through several rounds of affinity purification. Millions of phage particles are incubated with the target protein that has already been immobilized on a Petri dish or ELISA plates. Non-binding phages are washed out extensively, and then the bound phages are eluted under harsh conditions. The eluted phages are then amplified on agar medium and subjected to the next round of affinity purification. The tight-binding phages are then cloned and propagated in *Escherichia coli.* The amino acid sequence of the peptide on the phage is deduced by sequencing the coded DNA in the phage gene III (Cwirla et al., 1990; Devlin et al., 1990; Scott and Smith, 1990).

Ligands identified from phage libraries frequently interact with natural binding sites on the target molecule and resemble the target's natural ligands. Thus phage-displayed random peptide libraries have been used to investigate protein-protein interactions in a variety of contexts. For example, phage-displayed random peptide libraries have been used to map the epitopes of monoclonal and polyclonal antibodies, and to identify peptide ligands for receptors, receptor ligands, and folded domains within larger proteins, such as several SH2, SH3 domains (Daniels and Lane, 1996; Zwick et al., 1998). Recently, peptide ligands for some superantigens, for example, SEB and TSST-1, have been determined with phage-

displayed random peptide libraries (Goldman et al., 2000; Sato et al., 1996). But biopanning with phage-displayed libraries is slow and subjected to non-specific binding.

The most important aspects in the determination of peptide ligands using phage display are the construction and maintenance of libraries with sufficient structural diversity and the efficient selection of specific binding phage from nonspecific binding phage. Phage-displayed random peptide libraries have been constructed to display peptides of variable length ranging from 6 to 38 amino acids (Daniels and Lane, 1996). Phage display libraries have the advantage of allowing exposure of very large peptide as potential ligands. Once it is created, a phage library can be regenerated continuously and re-used unlike a synthetic library. The problem in phage library construction is that the library may not be truly random due to genetic bias in the creation of these libraries. The efficiency of screening can be controlled by adjusting the washing conditions in the screening process (D'Mello and Howard, 2001). But it is also possible that the specific peptide on phage that is finally selected is not the original one from the library because of some biological bias in amplification and propagation of the phage. Care must be taken to maintain the diversity of the libraries. Usually the diversity of the original phage library is on the order of 10^8 peptides. Selection must be avoided during the library expansion and propagation for phages with selective growth advantage (Daniels and Lane, 1996). In addition, the resources of the peptide synthesis on phage are limited to the 20 natural amino acids so that D-amino acids or other molecules cannot be used to increase the diversity of the library.

Synthesized libraries can be created on solid supports through organic chemistry. There are several distinct combinatorial library methods (Lam et al., 1997). The one-bead-

one-peptide library method is used extensively in drug discovery processes due to its unique features (Lebl et al., 1995). Compared to other methods, the synthesis of a one-bead-one-peptide library is rapid with use of the "split synthesis" approach. Because one bead has one unique peptide sequence, all of the beads can be tested concurrently but independently. Once positive beads have been identified, the chemical structure of the peptides on the beads can be directly determined by sequencing or by an encoding strategy. In addition, the libraries can be used either in the solid phase (i.e. peptides attached on solid) or solution phase (i.e. peptides cleaved from solid support). As in phage-displayed libraries, the screening of peptide ligands from one-bead-one-peptide libraries involves three steps (Lam et al., 1997): (i) construction of the library, (ii) screening the library with the target molecule, (iii) determination of the peptide sequence.

Although peptide ligands from phage library have been presented on chromatographic support to purify proteins (Baumbach and Hammond, 1992; Huang et al., 1996; Huang and Carbonell, 1995), it is possible that the microenvironment and the orientation of the peptides on the chromatographic support could be very different from that on phage. This can affect adversely the interactions between the peptide ligands and the target (Buettner et al., 1996). It has been found that some peptides derived from phage library only work when the peptide is an integral part of the phage coat protein and not when isolated in free solution (Lowe, 2001). Chemically derived peptides are synthesized and screened on solid beads. They can be used directly to purify protein by chromatography. Thus one-bead-one-peptide libraries are widely used to discover peptide ligands for protein purification.

2.2.3 Construction of One-Bead-One-Peptide Libraries

The first one-bead-one–peptide library was synthesized by Lam et al. (Lam et al., 1991) using the "split synthesis" approach developed by Furka et al. (Furka and Sebetyen, 1991) (Figure 2.2). The resin beads are divided equally into separate reaction vessels each with a single amino acid. After the first amino acid is coupled to the resins, beads are repooled, mixed thoroughly, and redistributed into separate reaction vessels. The next coupling step is then performed. This divide-couple-recombine technique is repeated until the desired length of the peptide library is reached. There are X^n random sequences in the library, where X is the number of amino acids used for coupling, and n is the length of the library. Each resin bead displays only one peptide sequence. Thus libraries of this type are called "one-bead-one-peptide" libraries (Lam et al., 1991). Because other ligands besides naturally occurring amino acids, such as D-amino acids, oligonucleotides, synthetic oligomers, proteins and small molecules, also can be coupled to solid resins, the idea of a one-bead-one-peptide library has been extended to one-bead-one-compound library (Lam et al., 1997). The introduction of other compounds besides amino acids in combinatorial library construction increases the diversity of the library in comparison with a phage-displayed peptide library, in which phages only display peptides composed of natural amino acids. However, all synthetic methods have a practical limit on the size of the library as well as the length of the peptides on beads, while peptides on phage can be fairly large.

The choice of the solid support is critical for the library construction and the application of the library. The biological signal released from the peptides on a single bead depends quantitatively on the amount of the peptide on the bead. As a result, the size and

substitution homogeneity is of the utmost importance. Meanwhile, the resin should resist the formation of clusters because clusters would prevent the statistical distribution of resin beads and lower the number of structures created. In addition, resins should be compatible with various organic and aqueous media. Solid beads with porous structure are preferred. The high surface area that porous resins provide can attach more ligands, facilitating bead sequencing and providing high capacity for their use in chromatography. Moreover, the pores should be large enough to eliminate diffusion resistance especially when using large proteins as targets. In order to avoid nonspecific binding between the solid matrices and proteins, hydrophilic resins are preferred. If the peptide ligands will be used to purify protein in chromatography, the resins should have enough mechanical rigidity to withstand the high pressure used in liquid chromatography. A variety of polymer beads have been used to attach peptides in library construction, including polyhydroxylated methacrylate, polydimethylacrylamide, polyoxyethylene-grafted polystyrene, Tentagel and so on (Buettner et al., 1996; Lam et al., 1997).

2.2.4 Screening of One-Bead-One-Peptide Libraries

The identification of the specific peptide ligands to the target protein from a one-bead-one-peptide library depends on the screening methods used. Both solid-phase and solution phase methods have been developed for the one-bead-one-peptide combinatorial library method. The most widely adopted method of screening is the “on-bead” binding assay (Lam and Lebl, 1994; Lam et al., 1997). The target protein is incubated with the

library beads. The library beads with specific peptide sequence to the target protein bind the target protein. The binding of the target to the bead-bound ligands is usually detected by using a reporter group such as an enzyme, a radionuclide, a fluorescent probe, or a color dye covalently attached to the target molecules. Alternatively, antibodies can also be used in the detection scheme as in ELISA. The signals generated from these reporter groups are proportional to the amount and density of peptides on the bead. Nonspecific binding can result in high background resulting in some difficulty in determining the affinity ligands. This is usually eliminated by using a high ionic strength buffer (e.g. 0.2-0.4 M NaCl) to reduce purely electrostatic binding and blocking proteins (e.g. casein or bovine serum albumin) and nonionic detergents (e.g. 0.1% Tween 20).

One of the most convenient screening methods is the enzyme-linked colorimetric detection scheme. It has been used to discover the binding motifs for streptavidin (Lam and Lebl, 1992; Lam et al., 1991), avidin (Lam and Lebl, 1992), monoclonal antibodies (Lam et al., 1996), proteases (Lam et al., 1996), and MHC molecules (Smith et al., 1994). The alkaline phosphatase coupled target protein is used to bind to library beads, and then the substrate of alkaline phosphatase, 5-bromo-4-chloro-3-indolyl-phosphate (BCIP) is added. The reacting beads turn turquoise, while the majority of the beads in the library remain colorless. The positive turquoise beads are isolated and then sequenced by Edman degradation. The enzyme-linked colorimetric detection method is extremely rapid, taking a few hours to screen 10^7-10^8 beads. The problem with this method is that the enzyme molecule attached to the target can sterically affect the binding of the target to peptides on beads. Radionuclide-labeled targets can be used to screen library beads to avoid this

problem. The radionuclide probes, such as ^{3}H and ^{14}C, are particularly small compared to enzyme as reporter groups on the target, and it has been demonstrated that the labeled target shows almost same biological properties as the natural target (Jentoft and Dearborn, 1983). The library is incubated with the radiolabeled target protein, washed, and then suspended in agarose gel. The slurry is poured onto a gel bond to form a monolayer so that all beads are spatially separated. Exposure of the gel to autoradiography film can locate the positive beads that are then isolated and sequenced. Several researchers have screened peptide libraries using radiolabeled targets (Kassarjian et al., 1993; Mondorf et al., 1998; Nestler et al., 1996; Turck, 1994). The method developed by Mondorf et al. using ^{14}C offers high resolution and sensitivity (Mondorf et al., 1998). It has been used to identify affinity peptide ligands for s-protein (Mondorf et al., 1998), fibringen (Mondorf et al., 1998), Alpha-1-proteinase inhibitor (Bastek et al., 2000), α-lactalbumin (Gurgel et al., 2001b) and recombinant factor VIII (Chen et al., 2000). Immunostaining schemes similar to ELISA also can be used to target the protein on beads. There are no modifications of the target using this method, so the bead-bound ligands bind directly to the native protein, and not to any adducts. However, the antibodies used in the detection system could bind to bead-bound ligands besides the targets to bring the possibilities of interference and false positives. A two color PEptide Library Immunostaining Chromatographic ANanlysis (PELICAN) has been developed to determine beads specific for the target from those beads resulting from antibody cross reactivity (Buettner et al., 1996). It has been used to discover peptide leads for protease factor IX and fibrinogen (Buettner et al., 1997; Buettner et al., 1996). Other on-bead screening schemes involve dye-labeled targets or fluorescently labeled target (Chen et al., 1993; Needels et al.,

1993). However, dyes always complicate the screening process by binding directly to many peptide ligands, and the autofluorescence of library make the library unsuitable for this kind of screening process (Lam et al., 1997). In order to minimize the number of false positive beads and make the screening more selective, two different screening methods can be sequentially used for one target. For example, a dual-color detection scheme that uses two sequential orthogonal probes in enzyme-linked colorimetric detection methods (Lam et al., 1995), and a cross-screening scheme that combines an enzyme-linked colorimetric method and a radiolabeled assay (Liu and Lam, 2000) have been developed. In this way, many of the initially determined positive beads are eliminated by the second screening method, and the chances to get the true positive beads are greatly enhanced.

One of the disadvantages of on-bead screening is the high peptide density required for peptide sequencing on beads. This can lead to multiple-point attachment of the target to the peptides so that nonspecific interaction between target and peptides will be enhanced. Thus the selected peptide ligands may have less affinity and specificity to the target. Screening of soluble peptide libraries can make the affinity ligands more selective. The format of affinity chromatographic screening developed by Evans et al. and Huang & Carbonell is suitable for screening peptide libraries due to its rapidity (Evans et al., 1996; Huang and Carbonell, 1999). The targets are immobilized onto resins and then packed into a chromatographic column. The soluble peptide libraries are pumped into the column at a proper flow rate to ensure the peptides have enough time to bind to the immobilized targets. Then the column is washed thoroughly with binding buffer. The affinity peptide ligands bound to the targets are eluted and then isolated by reverse-phase chromatography. The fractions are then sequenced

by Edman degradation or mass spectrometry. Huang and Carbonell have demonstrated this technique by showing that the identified sequence consensus, NFVE, is the same as that found from the screening a phage displayed library for s-protein (Huang and Carbonell, 1999). Evans et al. used a similar system to recover the known epitope, YGGFL, for a monoclonal antibody (3E-7), and then determine the affinity ligands for bacterial lipopolysaccharide (LPS, endotoxin) (Evans et al., 1996). Although this technique is rapid and able to avoid false signals from nonspecific binding, some hydrophobic leads could be missed due to their minimal solubility. The slow binding kinetics and the orientation of the immobilized targets may limit the contact between the immobilized targets and free peptide ligands so that some potential leads could pass by the column. In addition, the methodologies used in this technique are more complex than those in on-bead screening (Huang and Carbonell, 1999).

False signals due to nonspecific binding cannot be absolutely excluded even though the forgoing screening process is carefully designed. A multi-tiered screening process has been developed to characterize the peptide beads in terms of affinity and selectivity of binding (Gurgel et al., 2001b). The forgoing screening process is called the primary screening. The secondary screening employs a batch format to confirm the binding of the target protein to the peptide ligands from the primary screening. Some peptides that bound weakly to the target protein are eliminated in the secondary screening. The tertiary screening employs a chromatographic column format to demonstrate the binding selectivity of the peptide ligands from the secondary screening. The consequential peptide ligands from this multi-tiered screening process show high affinity and are well suited for protein purification.

2.2.5 Protein Purification by Peptide Ligands

Baumbach and Hammond (1992) first demonstrated the principle of using peptide ligands from combinatorial libraries as affinity ligands in large-scale chromatography processes by using streptavidin as target. Since then, this technique has been successfully used to purify a variety of proteins, such as S-protein (Huang and Carbonell, 1995), Von Willebrand factor (Huang et al., 1996), Factor IX (Buettner et al., 1996), Factor VIII (Amatschek et al., 2000; Necina et al., 1998), Trypsin (Makriyannis and Clonis, 1997), anti-MUC1 antibodies (Murray et al., 1997; Murray et al., 1998), Alpha-1-proteinase inhibitor (Bastek et al., 2000), Monoclonal antibodies (IgG, IgA, IgE, IgM, IgY) (Fassina et al., 2001), α-lactalbumin (Gurgel et al., 2001a) and Fibrinogen (Kaufman et al., 2002).

2.2.6 Characterization of Peptide Ligands

Some peptide ligands identified by library screening are bioselective to their targets, while other peptide ligands are pseudo-affinity ligands behaving like dye ligands. Huang and Carbonell (1995) showed that the peptide ligand, YNFEVL, is so specific to s-protein that randomization of the peptide sequence destroys the binding. A similar study on the binding of von Willebrand Factor to the peptide RLRSFY showed that the randomization has little effect on the binding (Huang et al., 1996). These results suggest that there is a binding cleft on the s-protein molecule that leads to specific interactions with the responding peptide ligands, while no such specific clefts on the von Willebrand Factor. The pseudo-affinity

peptide ligands are better used to capture the target at the first step in purification (Bastek et al., 2000); other steps such as filtration are needed to polish the products. The bioselective peptide ligands can be efficient for purifying the protein in one step, but usually sample preparation prior to the affinity chromatography step is needed to protect the ligands and maximize the efficiency of the affinity column. Basically, the occurrence of affinity peptide ligands depends on the screening of the peptide library. A more selective ligand could be found if more stringent screening conditions are used, but also make the screening process more complicated and laborious.

Ligand density can affect the interactions between the peptide ligands and the target protein. If the protein has a cleft and thereby the binding is attributed to monovalent interactions, the capacity increases when increasing the ligand density, while the association constant may remain constant at low ligand density and decrease at high ligand density due to steric effects. Thus there is an optimal density at which the peptide ligands have high capacity and an acceptable extent of steric hindrance. If the binding is attributed to multivalent interactions, increasing the ligand density typically increases the capacity and association constant. For highly specific ligands, increasing the ligand density may increase the steric hindrance at the surface and make the binding less efficient, namely, decreasing the association constant and the utilization of the ligands. Small protein molecules are expected to have monovalent interactions with the adsorbent. The binding of s-protein to a peptide sequence, YNFEVL, has been shown to be 1:1 specific (Smith et al., 1993). Further adsorption isotherm measurements in a batch system have shown that the binding capacity increases from 0.0466μmol/ml to 1.1650μmol/ml, while the peptide utilization decreases

from 96% to 40%, and the binding constant decreases from 1.2×10^5 to 5.6×10^4 M^{-1} when the peptide density increases from 0.05 to 3.0μmol/ml (Huang and Carbonell, 1995). It is more likely that the binding of large protein molecules to peptide ligands is multivalent because there may have several interaction sites at their surfaces. The results of binding of von Willebrand Factor (vWF) to a small peptide ligand, Ac-RVRSFYK, immobilized on Toyopearl resin, shows that the association constant increases from 8.82×10^5 to 2.06×10^6 M^{-1}, and the maximum capacity from 2.32 to 10.33 mg/ml when the peptide density increases from 32 to 60 mg/ml (Huang et al., 1996).

The driving force for binding of the peptide ligand and the target protein molecule depends on the composition and orientation of the amino acids in the peptide ligand. Typically, charged amino acids in the peptide ligand tend to form ionic interactions with the target molecule, while hydrophobic leads potentially contact hydrophobic patches on the target molecule driven by hydrophobic interactions. For example, the specific binding of fibrinogen to ligand FLLVPL is dominated by hydrophobic interactions and ionic interactions with the N-terminal free amino group (Kaufman et al., 2002). Gurgel et al. found that the binding of α-lactalbumin to peptide ligand WHWRKR is mainly electrostatic at low temperatures, but hydrophobic at high temperatures (Gurgel et al., 2001c).

The immobilization of peptides on chromatography beads also substantially affects the interactions between the peptide and its target protein. The association constant of s-protein is lower when the peptide YNFEVL is immobilized on the resin than in solution (Huang and Carbonell, 1995). Thus soluble peptides can be used in the elution of s-protein

from immobilized peptide ligands. For other proteins, i.e. α-1-proteinase inhibitor and fibrinogen, it is necessary to present the corresponding peptides on the resin because soluble peptides show weak binding (Bastek, 2000; Kaufman et al., 2002).

2.3 References

Amatschek K, Necina R, Hahn R, Schallaun E, Schwinn H, Josic D, Jungbauer A. 2000. Affinity chromatography of human blood coagulation factor VIII on monoliths with peptides from a combinatorial library. J High Resol Chromatogr 23:47-58.

Archer DL, Young EE. 1988. Contemporary issues: diseases with food vector. Clin Microbiol Rev 1:377-398.

Baird-Parker AC. 1971. Factors affecting the production of bacterial food poisoning toxins. J Appl Bacteriol 34:181-197.

Balaban N, Rasooly A. 2000. Review: Staphylococcal enterotoxins. Int J Food Microbiol 61:1-10.

Bastek PD. 2000. Purification of alpha-1-proteinase inhibitor using ligands from combinatorial peptide libraries [Doctoral dissertation]. Raleigh, NC: North Carolina State University.

Bastek PD, Land JM, Baumbach GA, Hammond DH, Carbonell RG. 2000. Discovery of Alpha-1-proteinase inhibitor binding peptides from the screening of a solid phase combinatorial peptide library. Separation Sci Technol 35:1681-1706.

Baumbach GA, Hammond DJ. 1992. Protein purification using affinity ligands deduced from peptide libraries. BioPharm May:24-35.

Bayliss M. 1940. Studies on the mechanism of vomiting produced by Staphylococal enterotoxin. J Exp Med 72:669-684.

Bergdoll MS. 1979. Staphylococcal intoxications. In: Riemann H, Bryan FL, editors. Food-borne infections and intoxications. 2 ed. New York: Academic Press. p 443-494.

Bergdoll MS. 1983. Enterotoxins. In: Easman CS, Adlum C, editors. Staphylococcal and Staphylococcal Infections. London: Academic Press Inc. p 559-598.

Bergdoll MS. 1985. The staphylococcal enterotoxins: an update. In: Jelijaszewicz J, editor. The Staphylococci. New York: gustav Fischer Verlag. p 247-254.

Bergdoll MS. 1996. Detection of the staphylococcal toxins. Adv Exp Med Biol 391(Natural Toxins 2):465-479.

Bergdoll MS, Borja CR, Avena RM. 1965. Identification of a new enterotoxin as enterotoxin C. J Bacteriol 90:1481-1485.

Bergdoll MS, Borja CR, Robbins RN, Weiss KF. 1971. Identification of enterotoxin E. Infect Immun 4:593-595.

Bergdoll MS, Sugiyama H, Dack GM. 1959. Staphylococcal enterotoxin. I. Purification. Arch Biochem Biophys 85:62-69.

Bergdoll MS, Sugiyama H, Dack GM. 1961. The recovery of staphylococcal enterotoxin from bacterial culture supernatants by ion exchange. J Biochem Microbiol Technol Eng 3:41-50.

Bhatti AR, Nadon LP, Micusan VV. 1994. Purification of superantigen staphylococcal enterotoxin B (SEB). IJBC 1:47-56.

Brehm RD, Tranter HS, Hambleton P, Melling J. 1990. Large-scale purification of staphylococcal enterotoxins A, B, and C2 by dye ligand affinity chromatography. Appl Environ Microbiol 56:1067-1072.

Buettner JA, Dadd CA, Baumbach GA, Hammond DJ; 1997. Fibrinogen binding peptides. U.S. patent 5,723,579.

Buettner JA, Dadd CA, Baumbach GA, Masecar BL, Hammond DJ. 1996. Chemically derived peptide libraries: A new resin and methodology for lead identification. Int J Peptide Protein Res 47:70-83.

Casman EP, Bennett RW, Dorsey AE, Issa JA. 1967. Identification of a fourth staphylococcal enterotoxin, enterotoxin D. J Bacteriol 94:1875-1882.

Casman EP, Bergdoll MS, Robinson J. 1963. Designation of staphylococcal enterotoxins. J Bacteriol 85:715-716.

Chang PC, Dickie N. 1971. Fractionation of staphylococcal enterotoxin B by isoelectric focusing. Biochim Biophys Acta 236:367-375.

Chen JK, Lane WS, Brauer AW, Tanaka A, Schreiber SL. 1993. Biased combinatorial libraries: novel ligands for the SH3 domain of phosphatidylinositol 3-kinase. J Am Chem Soc 115:12591-12592.

Chen LA, Buettner JA, Carbonell RG; 2000. Peptides binding factor VIII for use in affinity purification of the protein. U. S. patent WO 2000031121.

Cwirla SE, Peters EA, Barrett RW, Dower WJ. 1990. Peptides on phage: A vast library of peptides for identifying ligands. Proc Natl Acad Sci USA 87:6378-6382.

Daniels DA, Lane DP. 1996. Phage peptide libraries. Methods 9:494-507.

Devlin JJ, Panganiban LC, Delvin PE. 1990. Random peptide libraries: A source of specific protein binding molecules. Science 249:404-406.

D'Mello F, Howard CR. 2001. An improved selection procedure for the screening of phage display peptide libraries. J Immunol Methods 247:191-203.

Donnelly CB, Leslie JE, Black LA, Lewis KH. 1967. Serological identification of entreotoxigenic staphylococci from cheese. Appl Microbiol 15:1382-1387.

Ende IA, Terplan G, Kickhofen B, Hammer DK. 1983. Chromatofocusing: A new method for purification of staphylococcal enterotoxins B and C1. Appl Environ Microbiol 46:1323-1330.

Evans DM, Williams KP, McGuinness B, Tarr G, Regnier F, Afeyan N, Jindal S. 1996. Affinity-based screening of combinatorial libraries using automated, serial-column chromatography. Nat Biotechnol 14:504-507.

Evenson ML, Hinds MW, Bernstein RS, Bergdoll MS. 1988. Estimation of human dose of staphylococcal enterotoxin A from a large outbreak of staphylococcal food poisoning involving chocolate milk. Int J Food Microbiol 7:311-316.

Fassina G, Ruvo M, Palombo G, Verdoliva A, Marino M. 2001. Novel ligands for the affinity-chromatographic purification of antibodies. J Biochem Biophys Methods 49:481-490.

Fey H, Pfister H, Ruegg O. 1984. Comparative evaluation of different enzyme-linked immunosorbent assay systems for the detection of staphylococcal enterotoxins A, B, C, and D. J Clin Microbiol 19:34-38.

Frea JI, McCoy E, Strong FM. 1963. Purification of type B staphylococcal enterotoxin. J Bacteriol 86:1308-1313.

Fung DYC, Steinberg DH, Miller RD, Kurantnick MJ, Murphy TF. 1973. Thermal inactivation of staphylococcal enterotoxins B and C1. Appl Microbiol 26:938-942.

Furka A, Sebetyen F. 1991. General method for rapid synthesis of multicomponent peptide mixtures. Int J Peptide Protein Res 37:487-493.

Goldman ER, Pazirandeh MP, Mauro JM, King KD, Frey JC, Anderson GP. 2000. Phage-displayed peptides as biosensor reagents. J Mol Recognit 13:382-387.

Goldsby AG, Kindt TJ, Osborne BA. 2000. Kuby Immunology. New York: W. H. Freeman and Company. 201-268 p.

Gurgel PV, Carbonell RG, Swaisgood HE. 2001a. Fractionation of whey proteins with a hexapeptide ligand affinity resin. Bioseparation 9:385-392.

Gurgel PV, Carbonell RG, Swaisgood HE. 2001b. Identification of peptide ligands generated by combinatorial chemistry that bind alpha-Lactalbumin. Separation Sci Technol 36:2411-2431.

Gurgel PV, Carbonell RG, Swaisgood HE. 2001c. Studies of the Binding of a-Lactalbumin to Immobilized Peptide Ligands. J Agric Food Chem 49:5765-5770.

Harris TO, grossman D, Kappler JW, Marrack P, Rich RR, Betley MJ. 1993. Lack of complete correlation between emetic and T-cell-stimulatory activities of staphylococcal enterotoxins. Infect Immun 61:3175-3183.

Huang IY, Bergdoll MS. 1970. The primary structure of staphylococcal enterotoxin B. J Biol Chem 245:3518-3525.

Huang PY, Baumbach GA, Dadd CA, Buettner JA, Masecar BL, Hentsch M, Hammond DJ, Carbonell RG. 1996. Affinity purification of von Willebrand Factor using ligands derived from peptide libraries. Bioorg Med Chem 4:699-708.

Huang PY, Carbonell RG. 1995. Affinity purification of proteins using ligands derived from peptide libraries. Biotechnol Bioeng 47:288-297.

Huang PY, Carbonell RG. 1999. Affinity chromatographic screening of soluble combinatorial peptide libraries. Biotechnol Bioeng 63:633-641.

Jamlang EM, Bartlett ML, Snyder HE. 1971. Effect of pH, protein concentration, and ionic strength on heat inactivation of staphylococcal enterotoxin B. Appl Microbiol 22:1034-1040.

Jentoft N, Dearborn DG. 1983. Protein labeling by reductive alkylation. Method Enzymol 91:570-579.

Johansson HJ, Pettersson TN, Berglof JH. 1990. Development of a chromatographic process for large-scale purification of staphylococcal enterotoxin B. J Chem Tech Biotechnol 49:233-241.

Johnson HM, Russell JK, Pontzer CH. 1991. Staphylococcal enterotoxin microbial superantigens. FASEB J 5:2706-2712.

Jones CL, Khan SA. 1986. Nucleotide sequence of the enterotoxin B gene from Staphylococcus aureus. J Bacteriol 166:29-33.

Kassarjian A, Schellenberger V, Turck CW. 1993. Screening of synthetic peptide libraries with radiolabeled acceptor molecules. Peptide Res 6:129-133.

Kaufman DB, Hentsch ME, Baumbach GA, Buettner JA, Dadd CA, Huang PY, Hammond DJ, Carbonell RG. 2002. Affinity purification of fibrinogen using a ligand from a peptide library. Biotechnol Bioeng 77:278-289.

King KD, Anderson GP, Bullock KE, Regina MJ, Saaski EW, Ligler FS. 1999. Detecting staphylococcal enterotoxin B using an automated fiber optic biosensor. Biosens Bioelectron 14:163-170.

Lam KS, Lake D, Salmon SE, Smith J, Chen ML, Wade S, Abdul-Latif F, Knapp RJ, Leblova Z, Ferguson RD and others. 1996. A one-bead one-peptide combinatorial library method for B-cell epitope mapping. Method Enzymol 9:482-493.

Lam KS, Lebl M. 1992. Streptavidin and avidin recognize peptide ligands with different motifs. Immunol Methods 1:11-15.

Lam KS, Lebl M. 1994. Selectide technology: bead-binding screening. Methods 6:372-380.

Lam KS, Lebl M, Krchnak V. 1997. The "one-bead-one-compound" combinatorial library method. Chem Rev 97:411-448.

Lam KS, Salmon SE, Hersh EM, Hruby VJ, Kazmierski WM, Knapp RJ. 1991. A new type of synthetic peptide library for identifying ligand-binding activity. Nature 354:82-84.

Lam KS, Wade S, Abdul-Latif F, Lebl M. 1995. Application of a dual color detection scheme in the screening of a random combinatorial peptide library. J Immunol Methods 180:219-223.

Lawrence MC, Davis PC. 1992. CLIX: a search algorithm for finding novel ligands capable of binding proteins of known three-dimensional structure. Proteins 12:31-41.

Lebl M, Krchnak V, Sepetov NF, Seligmann B, Strop P, Felder S, Lam KS. 1995. One-bead-one-structure combinatorail libraries. Biopolymers (Peptide Science) 37:177-198.

Li H, Llera A, Malchiodi EL, Mariuzza RA. 1999. The structural basis of T cell activation by superantigens. Annu Rev Immunol 17:435-466.

Liu G, Lam KS. 2000. One-bead one compound combinatorial library method. In: Fenniri H, editor. Combinatorial chemistry: Oxford University Express. p 33-49.

Lopes HR, Noleto ALS, Bergdoll MS. 1996. Purification of Staphylococcal enterotoxins B and C2 by dye ligand chromatography - production of antisera. Rev Microbiol 1:52-56.

Lowe CR. 2001. Combinatorial approaches to affinity chromatography. Curr Opin Chem Biol 5:248-256.

Makriyannis T, Clonis YD. 1997. Design and study of peptide-ligand affinity chromatography adsorbents: application to the case of trypsin purification from bovine pancreas. Biotechnol Bioeng 53:49-57.

Marrack P, Kappler J. 1987. The T cell receptor. Science 238:1073-1079.

Marrack P, Kappler J. 1990. The staphylococcal enterotoxins and their relatives. Science 248:705-711.

Melconian AK, Flandrois J, Fleurette J. 1983. Modified Method for production and purification of Staphylococcus aureus enterotoxin B. Appl Environ Microbiol 45:1140-1143.

Metzger JF, Johnson AD, Collins IWS. 1972. Fractionation and purification of Staphylococcus aureus enterotoxin B by electrofocusing. Biochim Biophys Acta 257:183-186.

Meyer RF, Palmieri MJ. 1980. Single radial immunodiffusion method for screening staphylococcal isolates for enterotoxin. Appl Environ Microbiol 40:1080-1085.

Mondorf K, Kaufman DB, Carbonell RG. 1998. Screening of combinatorial peptide libraries: Identification of ligands for affinity purification of proteins using a radiological approach. J Pept Res 52:526-536.

Munson SH, Tremaine MT, Betley MJ, Welch RA. 1998. Identification and characterization of staphylococcal enterotoxin types G and I from Staphylococcus aureus. Infect Immun 66:3337-3348.

Murray A, Sekowski M, Spencer DIR, Denton G, Price MR. 1997. Purification of monoclonal antibodies by epitope and mimotope affinity chromatography. J Chromatogr A 782:49-54.

Murray A, Spencer DIR, Missailidis S, Denton G, Price MR. 1998. Design of ligands for the purification of anti-MUC1 antibodies by peptide epitope affinity chromatography. J Pept Res 52:375-383.

Necina R, Amatschek K, Schallaun E, Schwinn H, Josic D, Jungbauer A. 1998. Peptide affinity chromatography of human clotting factor VIII: Screening of the vWF-binding domain. J Chromatogr B 715:191-201.

Nedelkov D, Rasooly A, Nelson RW. 2000. Multitoxin biosensor-mas spectrometry analysis: a new approach for rapid, real time, sensitive analysis of staphylococcal toxins in food. Int J Food Microbiol 60:1-13.

Needels MC, Jones DG, Tate EH, Heinkel GL, Kochersperger LM, Dower WJ, Barrett RW, Gallop MA. 1993. Generation and screening of an oligonucleotide-encoded synthetic peptide library. Proc Natl Acad Sci USA 90:10700-107054.

Nestler HP, Wennemers H, Sherlock R, Dong DL-Y. 1996. Microautoradiographic identification of receptor-ligand interactions in bead-supported combinatorial libaries. Bioorg Med Chem Lett 6:1327-1330.

Orwin PM, Leung DYM, Donahue HL, Novick RP, Schlievert PM. 2001. Biochemical and biological properties of staphylococcal enterotoxin K. Infect Immun 69:360-366.

Papageorgiou AC, Tranter HS, Acharya KR. 1998. Crystal structure of microbial superantigen staphylococcal enterotoxin B at 1.5Å resolution: Implications for superantigen recognition by MHC class II molecules and T -cell receptors. J Mol Biol 277:61-79.

Park CE, Akhtar M, Rayman MK. 1992. Nonspecific reactions of a commercial enzyme-linked immunosorbent assay kit (TECRA) for detection of staphylococcal enterotoxins in foods. Appl Environ Microbiol 58:2509-2512.

Park CE, Akhtar M, Rayman MK. 1994. Evaluation of a commercial enzyme immunoassay kit (RIDASCREEN) for detection of staphylococcal enterotoxins A, B, C, D, and E in foods. Appl Environ Microbiol 60:677-681.

Prasad GS, Earhart CA, Murray DL, Novick RP, Schlievert PM, Ohlendorf DH. 1993. Structure of toxic shock syndrome toxin 1. Biochemistry 32:13761-13766.

Rasooly A, Rasooly RS. 1998. Detection and analysis of staphylococcal enterotoxin A in food by Western immunoblotting. Int J Food Microbiol 41:205-212.

Rasooly L, Rasooly RS. 1999. Real time biosensor analysis of staphylococcal enterotoxin A in food. Int J Food Microbiol 49:119-127.

Rasooly L, Rose NR, Shah DB, Rasooly A. 1997. In vitro assay of Staphylococcus aureus enterotoxin A activity in food. Appl Environ Microbiol 63:2361-2365.

Reiser RF, Robbins RN, Noleto AL, Khoe GP, Bergdoll MS. 1984. Identification, purification, and some physicochemical properties of staphylococcal enterotoxin C3. Infect Immun 45:625-630.

Robbins R, Gould S, Bergdoll M. 1974. Detecting the enterotoxigenicity of Staphylococcus aureus strains. Appl Microbiol 28:946-950.

Saragovi HU, Greene MI, Chrusciel RA, Kahn M. 1992. Loops and secondary structure mimetics: development and applications in basic science and rational design. Biotechnology 10:773-778.

Sato A, Ida N, Fukuyama M, Miwa K, Kazami J, Nakamura H. 1996. Identification from a phage display library of peptides that bind to toxic shock syndrome toxin-1 and that inhibit its binding to major histocompatibility complex (MHC) class II molecules. Biochemistry 35:10441-10447.

Satterlee LD, Kraft AA. 1969. Effect of meat and isolated meat proteins on the thermal inactivation of staphylococcal enterotoxin B. Appl Microbiol 17:906-909.

Schantz EJ, Roessler WG, Wagman J, Spero L, Dunnery DA, Bergdoll MS. 1965. Purification of staphylococcal enterotoxin B. Biochemistry 4:1011-1016.

Scholl PR, Diez A, Geha RS. 1989. Staphylococcal enterotoxin B and toxic shock syndrome toxin-1 bind to distinct sites on HLA-DR and HLA-DQ molecules. J Immunol Methods 143:2583-2588.

Scott JK, Smith GP. 1990. Searching for peptide ligands with an epitope library. Science 249:386-390.

Smith GP, Schultz DA, Ladbury JE. 1993. A ribonuclease s-protein antagonist discovered with a bacteriophage display library. Gene 128:37.

Smith MH, Lam KS, Hersh EM, Lebl M, Grimes WJ. 1994. Peptide sequences binding to MHC class I proteins. Mol Immunol 31(1431-1437).

Spero L, Johnson-Winegar A, Schmidt JJ. 1987. In: Hardegree, Tu AT, editors. Handbook of natural toxins. New York: Marcel Dekker Inc. p 131-163.

Spero L, Metzger JF, Warren JR, Griffin BY. 1975. Biological activity and complementation of the two peptides of staphylococcal enterotoxin B formed by limited tryptic hydrolysis. J Biol Chem 250:5026-5032.

Spero L, Warren JR, Metzger JF. 1973. Effect of single peptide bond scission by trpsin on the structure and activity of staphylococcal enterotoxin B. J Biol Chem 248:7289-7294.

Spero L, Warren JR, Metzger JF. 1974. Microheterodeneity of staphylococcal enterotoxin B. Biochim Biophys Acta 336:79-85.

Strickler MP, Neill RJ, Stone MJ, Hunt RE, Brinkley W, Gemski P. 1989. Rapid purification of staphylococcal enterotoxin B by high-pressure liquid chromatography. J Clin Microbiol 27:1031-1035.

Su YC, Wong AC. 1995. Identification and purification of a new staphylococcal enterotoxin, H. Appl Environ Microbiol 61:1438-1443.

Swaminathan S, Furey W, Pletcher J, Sax M. 1992. Crystal structure of staphylococcal enterotoxin B, a superantigen. Nature 359:801-806.

Swaminathan S, Furey W, Sax M. 1996. Structure of the staphylococcal enterotoxins. In: Parker MW, editor. Protein toxin structure. Austin: Landes Company. p 231-245.

Tempelman LA, King KD, Anderson GP, Ligler FS. 1996. Quantitating staphylococcal enterotoxin B in diverse media using a potable fiber-optic biosensor. Anal Biochem 233:50-57.

Turck CW. 1994. Radioactive screening of synthetic peptide libraries. Methods 6:394-400.

Warren JR. 1977. Comparative kinetic stabilities of staphylococcal enterotoxin types A, B, and C1. J Biol Chem 252:6831-6834.

Warren JR, Spero L, Metzger JF. 1974. Isothermal denaturation of aqueous staphylococcal enterotoxin B by guanidine hydrochloride, urea and acid pH. Biochemistry 13:1678-1683.

White J, Herman A, Pullen AM, Kubo R, Kappler JW, Marrick P. 1989. The V beta-specific superantigen staphylococcal enterotoxin B: stimulation of mature T cells and clonal deletion in neonatal mice. Cell 56:27-35.

Wieneke AA, Gilbert RJ. 1987. Comparison of four methods for the detection of staphylococcal enterotoxin in foods from outbreaks of food poisoning. Int J Food Microbiol 4:135-143.

Williams RR, Wehr CT, Bennett RW. 1983. High-performance liquid chromatography of staphylococcal enterotoxin B. J Chromatogr A 266:179-186.

Zhang S, Iandolo JJ, Stewart GC. 1998. The enterotoxin D plasmid of Staphylococcus aureus encodes a second enterotoxin determinant (sej). FEMS Microbiol Lett 168:227-233.

Zwick MB, Shen J, Scott JK. 1998. Phage-displayed peptide libraries. Curr Opin Biotechnol 9:427-436.

Table 2.1 Methods used in the purification of SEB.

Source	Procedure	Recovery (%)	Purity (%)	Homogeneity
(Bergdoll et al., 1959; Bergdoll et al., 1961)	Acid precipitation; Adsorption on Amberlite IRC-50; Ethanol precipitation; Starch-bed electrophoresis	~0.04 Only mg quantities obtained	Highly purified	Nearly homogeneous
(Frea et al., 1963)	Ethanol precipitation; Gel filtration using Sephadex G-100; Electrophoresis on Sephadex	~0.08% Only mg quantities obtained	Partial purified	Nearly homogeneous
(Schantz et al., 1965)	2× Cation-exchange using CG-50 resin; Cation-exchange using CM-cellulose;	50-60	~99	Homogeneous in size; Microheterogeneity in charge
(Ende et al., 1983)	Cation-exchange using CG-50 resin; Chromatofocusing; Sephadex G-50	60	100; No contaminants detected	Homogeneous in size; Microheterogeneity in charge
(Melconian et al., 1983)	Cation-exchange using Biorex 70 resin; Isoelectric focusing; Sephadex G-100	9	99	Homogeneous in size and charge

Table 2.1 (continued)

Source	Procedure	Recovery (%)	Purity (%)	Homogeneity
(Williams et al., 1983)	Size-exclusion chromatography using MicroPak TSK 3000SW	N/A	Poor resolution of SEB	N/A
	Cation-exchange chromatography using MicroPak TSK IEX 530CM	N/A	Contaminated with low-molecular-weight species	N/A
	Reversed phase chromatography using MicroPak Protein-C_{18}	N/A	Contaminated with low-molecular-weight species	N/A
(Strickler et al., 1989)	Reverse-phase chromatography using DeltaPak C_{18}; Cation-exchange chromatography using Protein Pak SP-5PW	45	Contaminated with low-molecule-weight toxin material	Homogeneous in Gel filtration HPLC analysis
(Brehm et al., 1990)	Cross-flow filtration; Dye ligand Chromatography using Red A	44	99	Homogeneous in size; Microheterogeneity in charge
(Johansson et al., 1990)	Cation exchange using S Sepharose; Cation exchange using S Sepharose conducted on BioPilot; Gel filtration using Superdex 75 conducted on BioPilot	74	~99	Homogeneous in size;

Table 2.1 (continued)

Source	Procedure	Recovery (%)	Purity (%)	Homogeneity
(Bhatti et al., 1994)	$(NH_4)_2SO_4$ precipitation; Hydrophobic chromatography using Phenyl-Sepharose; Chromatofocusing; SephadexG-25	56	100; No contaminates detected	Homogeneous in size; Microheterogeneity in charge
(Lopes et al., 1996)	Cation-exchange using CG-50 resin; Dye ligand Chromatography using Red A	59	~99	Homogeneous in size

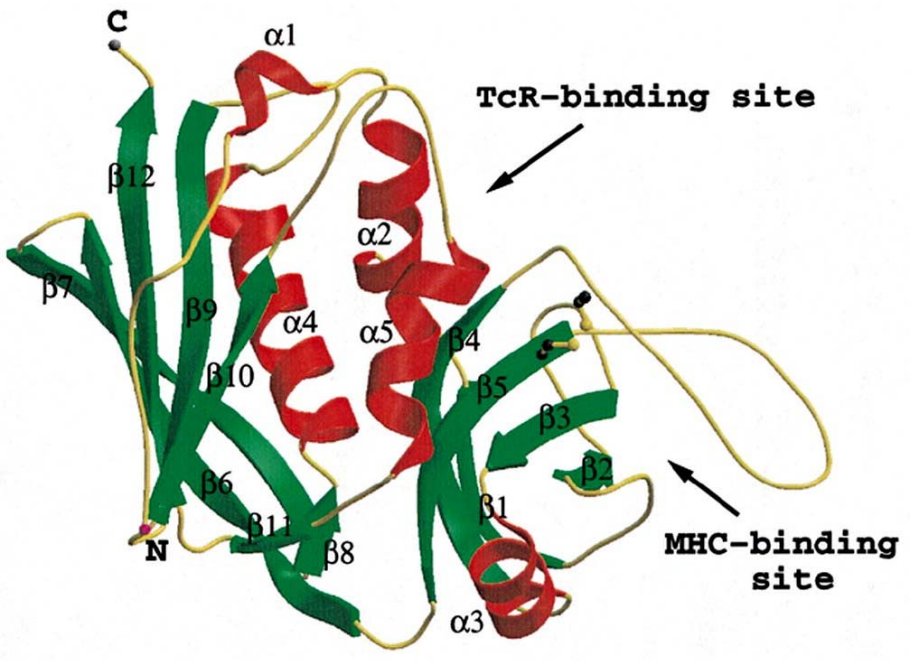

Figure 2.1 Schematic diagram of the structure of SEB (Papageorgiou et al., 1998)

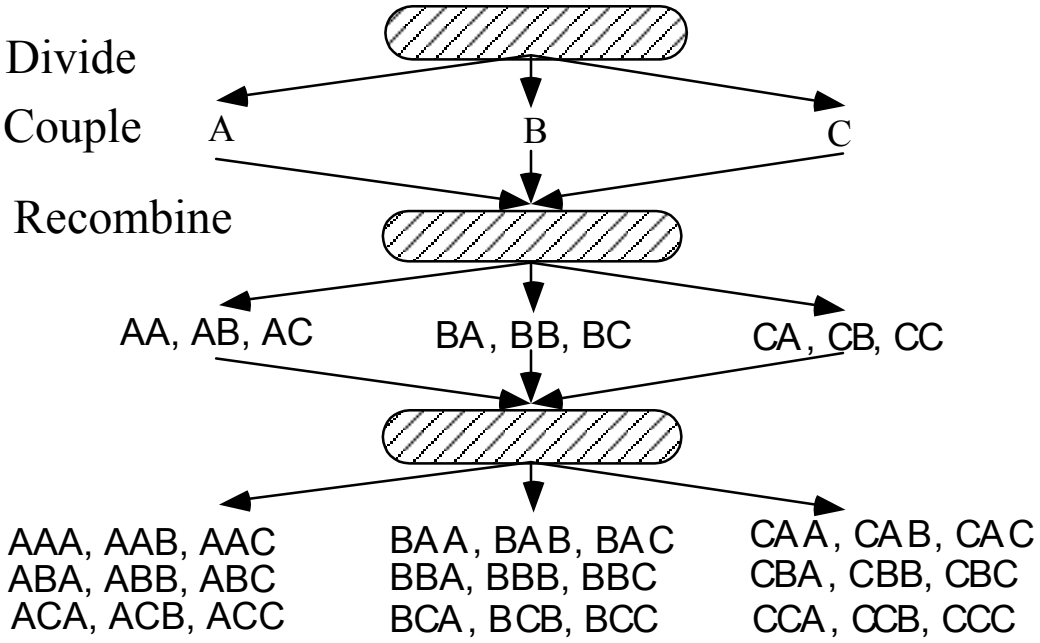

Figure 2.2 Split synthesis of the one-bead-one-peptide library

CHAPTER 3

A HEXAMER PEPTIDE LIGAND THAT BINDS SELECTIVELY TO STAPHYLOCOCCAL ENTEROTOXIN B (SEB): ISOLATION FROM A SOLID PHASE COMBINATORIAL LIBRARY

Guangquan Wang, Jitakshi De, Ruben G. Carbonell

Department of Chemical Engineering, North Carolina State University

1017 Main Campus Drive, Centennial Campus, Partner's Building I, Suite 3200

Raleigh, NC 27695-7006

Joseph S. Schoeniger, Diana C. Roe

Sandia National Laboratories

Livermore, CA 94551-9951

Except for the Appendix, this is a manuscript submitted for publication in

***Journal of Peptide Research**, December 2003*

Abstract

By screening a solid-phase combinatorial peptide library, a short peptide ligand, YYWLHH, has been discovered that binds with high affinity and selectivity to Staphylococcal Enterotoxin B (SEB), but only weakly to other staphylococcal enterotoxins that share sequence and structural homology with SEB. Using column affinity chromatography with an immobilized YYWLHH stationary phase, it was possible to separate SEB quantitatively from *Staphylococcus aureus* fermentation broth, a complex mixture of proteins, carbohydrates and other biomolecules. The immobilized peptide was also used to purify native SEB from a mixture containing denatured and hydrolyzed SEB, and showed little cross reactivity with other SEs. To our knowledge this is the first report of a highly specific short peptide ligand for SEB. Such a ligand is a potential candidate to replace antibodies for detection, removal and purification strategies for SEB.

Keywords: affinity adsorption; combinatorial peptide library; peptide ligands; staphylococcal enterotoxin B

3.1 Introduction

Staphylococcal enterotoxins (SEs) are a family of structurally related proteins produced by *Staphylococcus aureus*. They are monomeric proteins (25-30kDa) that contain one disulfide bond and are resistant to temperature and pH denaturation (Bergdoll, 1983). Staphylococcal enterotoxins are leading causes of food poisoning and are potent gastrointestinal toxins (Archer and Young, 1988). As little as 0.1μg of an enterotoxin is sufficient to cause symptoms of intoxication in humans (Evenson et al., 1988). SEs are also superantigens that bind to the major histocompatibility complex class II molecules (MHCII) and T cells bearing particular Vβ elements, triggering a massive release of T cell-derived cytokines followed by allergic and autoimmune symptoms (Balaban and Rasooly, 2000) and the eventual disappearance or inactivation of responding T cells (Li et al., 1999). To date, twelve SEs, have been identified and differentiated based on serotyping: SEA (Casman et al., 1963), SEB (Casman et al., 1963), SEC (Bergdoll et al., 1965; Reiser et al., 1984), SED (Casman et al., 1967), SEE (Bergdoll et al., 1971), SEG (Munson et al., 1998), SEH (Su and Wong, 1995), SEI (Munson et al., 1998), SEJ (Zhang et al., 1998) and SEK (Orwin et al., 2001). Note that SEC is further divided into SEC1, SEC2 and SEC3 due to minor epitope variations. The toxins may be grouped based on their degree of sequence homology. SEA, SED, SEE and SEJ form one group with an overall amino acid sequence homology of 51%-81%. SEB and the SECs form another group, with 42%-67% sequence homology. The homology between these two groups is around 22-33%. SEG, SHE, SEI and SEK have poor or no homology to any other SE (Balaban and Rasooly, 2000; Marrack and Kappler, 1990).

Another superantigen toxin produced by *Staphylococcus aureus*, originally designated as SEF, but renamed Toxic Shock Syndrome Toxin-1 (TSST1) (Bergdoll, 1985) has poor sequence homology to SEs but high structural homology to SEB (Prasad et al., 1993).

SEB is the most widely studied member of the SEs (Swaminathan et al., 1992). The SEB monomer has a molecular weight of 28,366 Daltons and an isoelectric point (pI) of 8.6. It is heat-stable and resistant to denaturation by 6 M of guanidine hydrochloride or 9 M of urea (Warren et al., 1974). Trace SEB is usually detected by immunodiffusion assay (Meyer and Palmieri, 1980), enzyme-linked immunosorbent assay (ELISA) (Fey et al., 1984; Park et al., 1994), or biosensors based on immunoaffinity techniques (Rowe et al., 1999). Due to the extreme toxicity of SEs, and their inherent stability, they are considered a significant bioterrorism threat as either an aerosol or food and water contaminant (Franz et al., 1997), and are listed by the CDC as select agents (Enserink and Malakoff, 2001). All existing assays for SEB use antibodies for binding and detection. Small ligands that are more robust and inexpensive than antibodies and can specifically capture SEB from complex sources may have widespread potential in field applications for detecting and removing small quantities of SEB from food, water and aerosol sources.

The development of cost-effective and highly stable affinity ligands that bind to specific SEs would also allow improved purification of these important proteins. Homogeneous and highly purified preparations of SEs are required in studies of the biological activity of SEs and the development of methods for identification and quantification of SEs (Bhatti et al., 1994; Lopes et al., 1996). It is therefore of interest to develop more efficient and convenient purification methods to recover enterotoxins from

fermentation broths and cell culture. Furthermore, SEs can contaminate other proteins produced from Staphylococcal bacteria, such as protein A, which plays an important role in purification and therapeutic removal of IgG and IgG-containing immune complexes in the treatment of certain cancers and autoimmune diseases (Balint et al., 1989). Although recombinant protein A is commercially available to purify IgG, the native form of protein A has a higher affinity and selectivity for antibody purification. The extra steps needed to remove trace SEs may reduce the activity and yield of protein A, and could be streamlined using affinity methods to remove SEs.

Small peptide ligands are much more stable than monoclonal antibodies because they do not require a specific tertiary structure to maintain their biological activity and they are not as likely to cause an immune response in case of leakage into the products. Small peptides can be manufactured aseptically in large scale under GMP (good manufacturing practices) conditions at relatively low cost. The interactions between small peptides and proteins tend to be moderate so that the target protein can be eluted under mild conditions without damage to protein activity. Baumbach and Hammond first demonstrated the applicability of peptide ligands found from combinatorial peptide libraries as affinity ligands in large-scale chromatography processes using streptavidin as the target molecule (Baumbach and Hammond, 1992). Since then, combinatorial libraries have been used to find peptides that purify a variety of proteins, such as S-protein (Huang and Carbonell, 1995), Von Willebrand factor (Huang et al., 1996), Factor IX (Buettner et al., 1996), Factor VIII (Amatschek et al., 2000; Necina et al., 1998), Trypsin (Makriyannis and Clonis, 1997), anti-MUC1 antibodies (Murray et al., 1997; Murray et al., 1998), Alpha-1-proteinase inhibitor

(Bastek et al., 2000), Monoclonal antibodies (IgG, IgA, IgE, IgM, IgY) (Fassina et al., 2001), α-lactalbumin (Gurgel et al., 2001) and Fibrinogen (Kaufman et al., 2002). In addition to being good candidates as ligands in affinity chromatography, peptides are used widely to determine protein-protein interactions without a priori information on protein structure (for example in epitope mapping) (Lam et al., 1996).

Peptide ligands are usually identified from either biological combinatorial peptide libraries, such as phage-displayed libraries (Cwirla et al., 1990; Devlin et al., 1990; Scott and Smith, 1990), or solid phase combinatorial peptide libraries, such as one-bead-one-peptide libraries (Lam et al., 1991). Because biopanning with phage-displayed libraries is slow and subject to non-specific binding (Huang and Carbonell, 1999), one-bead-one-peptide libraries are a more efficient choice for identifying affinity peptide ligands (Lam et al., 1997). One-bead-one-peptide libraries are created on chromatography resins so that each bead contains only one peptide sequence (Lam et al., 1991). The peptide ligands found to bind to the target protein from these one-bead-one-peptide libraries can be directly used in chromatography to purify the target protein, or in an on-bead assay to detect the target protein.

The present study describes the identification of an affinity peptide ligand that binds SEB from a one-bead-one-peptide library of hexamers. Recently, peptide ligands for SEB have been determined from a phage-displayed random peptide library (Goldman et al., 2000). However, to date this study is the first demonstration of the identification of a small affinity ligand for SEB from a solid phase combinatorial peptide library.

Three stages of screening (hereafter referred to as primary, secondary and tertiary screening) were sequentially used to identify the peptide ligand. For primary screening, a

radiological technique was used to find approximately 12 beads that bound positively for SEB out of approximately 1.7 million lead compounds. The secondary screening employed a batch format to confirm the binding of SEB to the peptide ligands from the primary screening. This batch format was used in both a competitive and non-competitive mode. The non-competitive mode involved screening using only pure SEB in buffer. For the competitive mode, SEB was spiked into mixtures of casein and bovine serum albumin (BSA). Elimination of peptides that bound weakly to SEB or bound to other proteins reduced the number of lead candidates from 12 down to only one (YYWLHH). The tertiary screening employed a chromatographic column format to demonstrate the binding selectivity of YYWLHH for different SEs or related proteins. The ligand that resulted from this multi-tiered screening is well characterized in terms of affinity and selectivity of binding, and can be a potential replacement for antibodies for detection, removal, analysis and purification of SEB.

3.2 Materials and Methods

3.2.1 Peptide Synthesis

The hexamer peptide library was synthesized directly onto 120 μm beads of Toyopearl AF-Amino-650M (TA650M) resin (TOSOH Biosep, Montgomeryville, PA) with 18 of the 20 natural amino acids (excepting cysteine and methionine) using standard fluorenylmethyloxycarbonyl (Fmoc) chemistry (Buettner et al., 1996). The base resin from

Tosoh Biosciences was a hydroxylated polymethacrylate amino resin with 1000 Å pores, making it suitable for capturing proteins up to 5 M Da in size. Briefly, a 1:1 mixture of Fmoc-L-alanine to tBoc (tert.butyloxycarbonyl)-L-alanine was coupled to the amino functionality on the resin. The tBoc group was released with TFA and the free amino functionality was acetylated with acetic anhydride. No further peptide synthesis occurred at these acetylated sites. Subsequently, the Fmoc protecting groups were released with piperidine. Fmoc-protected amino acids were used to synthesize peptides onto resin by using "split synthesis" until the last cycle was finished (Lam et al., 1991). The final substitution density based on total amino acid analysis was 100 μmol/g.

Individual peptide sequences were synthesized directly onto TA650M resin with a mean particle diameter of 65 μm at a substitution density of 100 μmol/g at Peptides International, Louisville, KY. All the remaining amino groups used to couple peptides on the base resin were acetylated. The peptide composition and density was confirmed by quantitative amino acid analysis at Protein Technologies Laboratories, Texas A&M University, TX.

3.2.2 Radiolabeling of SEB

Highly purified SEB of at least 95% purity (Toxin Technology, Sarasota, FL) was labeled at 4°C with ^{14}C by reductive methylation utilizing sodium cyanoborohydride and ^{14}C-formaldehyde (NEN Life Science Products, Boston, MA) as described by Jentoft and Dearborn (1983). The sodium cyanoborohydride was recrystallized prior to use due to

hydrate formation during storage. SEB was dissolved into 0.1 M sodium phosphate buffer, pH 7.0. Sodium cyanoborohydride and ^{14}C-formaldehyde were then added sequentially. The ^{14}C-formaldehyde was added at a 2-fold molar excess over 5% of the total methylation sites (34 total, 33 lysines + N-terminus) to achieve around 5% methylation of the amino groups in SEB. Sodium cyanoborohydride was added at 10X the molarity of ^{14}C-formaldehyde. The reaction was performed at 4°C overnight. The labeled SEB was separated from ^{14}C-formaldehyde by using an EconoPac 10DG Desalting Column (Biorad, Hercules, CA) equilibrated with 0.1 M sodium phosphate buffer, pH 7.0. The radioactivity of each fraction collected during the separation was determined using a 1500 Tri-Carb Liquid Scintillation Analyzer (Packard, Meridian, CT) and CytoScint ES scintillation liquid (ICN, Mesa, CA). The radioactivity yield after labeling was around 10^{14}~10^{15} dpm/mole SEB.

3.2.3 Primary Screening

A radiological detection approach was used to deduce the peptides that bind SEB (Mondorf et al., 1998). 20 mg of peptide library beads were washed with 20% methanol for one hour, and then washed thoroughly with the binding buffer, phosphate buffered saline (PBS) (Sigma, St. Louis, MO) containing 10mM phosphate buffer, 2.7 mM KCl, and 137 mM NaCl, pH 7.4. The blocking reagent was 1% casein (Pierce, Rockford, IL) or 0.5% casein plus 0.5% BSA (Pierce, Rockford, IL). The beads were first blocked with 1ml of blocking reagent in PBS in a 1.7 ml centrifuge tube for 2 hours on a rotating plate to minimize nonspecific interactions between the beads and ^{14}C-labeled SEB. Concentrated

^{14}C-labeled SEB was added directly into the reaction slurries to reach a concentration of 0.5 μM and then incubated for 2 hours at room temperature (20°C). Following the incubation, the beads were transferred to a Poly-Prep chromatography column (Biorad, Hercules, CA) and washed thoroughly with PBS with 0.05% Tween (Sigma, St. Louis, MO) until the radioactivity of the flowthrough reached background levels. The washed beads were suspended into 0.8% low melting agarose (Biorad, Hercules, CA) at 35°C and divided equally into two aliquots in 50 ml containers. Each of these slurries was poured onto a 160×180 mm gelbond film (BioWhittaker Molecular Applications, Rockland, ME) to form a monolayer of beads. The gelbond was air-dried overnight in a hood and subsequently exposed to Kodak Biomax MR autoradiography film (Fisher, Atlanta, GA) for 5 days. Positive signals on the film were confirmed by reexposure of the gelbond to a new film. Beads corresponding to the positive signals were identified by careful alignment of the films and gels, and isolated with a scalpel under a microscope. The isolated beads were each placed in a centrifuge tube with water and incubated for 10 minutes at 75°C in a water bath, followed by sonication for 10 minutes to remove the agarose from the beads. The clean beads were suspended in methanol and sent to Protein Technologies Laboratories, Texas A&M University, TX, for sequencing by Edman degradation using a Hewlett-Packard G1005A.

3.2.4 Secondary Screening: binding confirmation in a batch format

Individual peptide sequences determined to bind SEB in the primary screening were synthesized directly onto TA650M resins (65 μ diameter) at a substitution of 100 μmol/g resin (Peptides International, Louisville, KY). All remaining amino groups were acetylated as described previously. Beads were washed with 20% methanol for one hour, and then washed thoroughly with PBS buffer. Two different secondary screenings were done with a noncompetitive format and a competitive format. In the noncompetitive format, beads (20 mg) were incubated with 400 μl of 1 μM ^{14}C-SEB in PBS buffer in a 0.5 ml centrifugal filter with 0.45 μm Durapore membrane (Millipore, Milford, MA) on a rotating plate for two hours, washed with PBS buffer for 15 min, and then sequentially washed for one hour each with 400 μl of: 1 M NaCl in PBS buffer (to remove non-specifically bound SEB), 2% acetic acid and 6 M GdnHCl. After centrifugation each solution was collected into scintillation fluid for radioactivity counting. The total unbound ^{14}C-SEB was determined by combining the counts of unbound ^{14}C-SEB and the wash of PBS. Finally, resins were suspended in scintillation liquid and counted for radioactivity in the same manner, allowing a total radioactivity balance. Aliquots of acetylated and unacetylated TA650M resins were treated the same as above as controls. All experiments were conducted at room temperature.

In the competitive format, SEB-binding peptide resins identified from the non-competitive format studies were incubated with a mixture of labeled SEB and a blocking protein to test the selective affinity of the peptides for SEB. The procedure was similar to that of non-competitive format except using a mixture of SEB and blocking proteins. Two

blockers including 1 mg/ml BSA and 1 mg/ml casein were tested for their effects on SEB binding. Acetylated and unacetylated TA650M amino resins were used as controls.

3.2.5 Tertiary Screening: binding confirmation in a column format

To test the selectivity of the peptides that showed positive binding in the secondary screening, the performance of the peptide ligands was investigated in a chromatography column format. In order to minimize usage of SEB due to its high cost and toxicity, ~32 mg of peptide beads were packed into a microbore column (2.1 mm ID×30 mm) from Alltech (Deerfield, IL) and tested on a Waters 616 LC system (Millipore, Milford, MA) with a UV detector (Knauer, Germany) at 280 nm. The column was pre-equilibrated with ~50 column volumes binding buffer (PBS + 0.5 M NaCl) at 0.15 ml/min (260 cm/hr). Each sample was injected through a 100 µl loop (Thomson, Springfield, VA) at a flow rate of 20 µl/min for 10 minutes to allow sufficient residence time for binding. The flow rate was increased to 0.15 ml/min for the remainder of the run. The column was washed sequentially with the binding buffer for 10 minutes, 1 M NaCl in PBS for 20 minutes, and then 2% acetic acid in water for another 20 minutes. To investigate the effect of salt in the binding buffer on the separation of SEB from *E. coli* lysate (see below), the elution time of the 1 M NaCl wash was increased from 20 minutes to 35 minutes. All experiments were conducted at room temperature.

As in the secondary screening, a noncompetitive format was used first in the tertiary screening. A solution of 0.5 mg/ml SEB in PBS buffer was injected into the column to verify the binding ability of selected resins. In the competitive tertiary screenings, dilutions of *E.*

coli lysate (Promega, Medison, WI), BSA, and *Staphylococcus aureus* fermentation broth (Toxin Technology, Sarasota, FL) with the binding buffer were added to the injected samples containing SEB. *E. coli* lysate is a complex mixture of biomolecules with large numbers of hydrophobic intracellular proteins and lipids, and highly charged species such as DNA, and RNA. Attempting a one-step purification using affinity chromatography from such a mixture is an extremely difficult challenge due to the potential competition from nonspecific binding of other species. Since BSA is a fairly hydrophobic protein, a separation of SEB from BSA provides an additional example to help confirm the selectivity of the peptide ligand. The *Staphylococcus aureus* fermentation broth is the normal starting solution for SEB purification and can be used to demonstrate the affinity and selectivity of the peptide ligand in real applications. The broth used for these studies contained small amounts of SEE, a protein with a structure that is homologous to SEB. The protein concentrations of the *E. coli* lysate, BSA, and *Staphylococcus aureus* fermentation broth loaded into the columns in these experiments were 1, 5 and 5 mg/ml, respectively. The effects of the salt concentration and mass ratio of SEB to competitive reagents on the purification of SEB from the mixture were investigated.

In addition to using the pulse injection mode in the tertiary screening experiments described above, the selectivity of the selected peptide ligand and its potential to purify SEB were further checked using breakthrough curves. 5 ml of *Staphylococcus aureus* fermentation broth spiked with trace SEB were loaded on the column at a flow rate of 0.10 ml/min. The column was then washed sequentially with the binding buffer for 20 minutes

and 2% acetic acid for 20 minutes. The column was re-equilibrated with 50 column volumes of binding buffer before the next run.

3.2.6 Cross Reactivity with Other Toxins

To investigate possible cross reactivity of the selected peptide ligands for SEB with other staphylococcal toxins, highly purified SEA, SEC1, and staphylococcal toxic shock syndrome toxin-1 (TSST1) (Toxin Technology, Sarasota, FL) at a concentration of 0.5 mg/ml in PBS were applied to the column packed with the selected peptide ligands in the same way as the noncompetitive tertiary screening for SEB described above.

3.2.7 Binding of Nicked vs. Native Protein

To show the potential of the selected peptide ligands to separate native SEB from the "nicked protein", which is a common contaminant in pure SEB preparations, partially purified SEB (Toxin Technology, Sarasota, FL) was applied to the selected resin in a column format. The packing, pre-equilibration, and loading procedures of the column were the same as in the tertiary screening experiments described above. A sample of 1.5 mg/ml of partially purified SEB was loaded into the column. The column was washed with the binding buffer for 10 minutes to remove unbound materials. The bound protein was released by using 2% acetic acid in water.

3.2.8 Analytical Methods

The Micro-BCA Assay (Pierce, Rockford, IL) was used to quantify total protein concentrations. The gel electrophoresis runs were performed on an XCell *SuperLock*™ Mini-Cell system from Invitrogen, Carlsbad, CA. Fractions collected from 2% acetic acid eluates were neutralized with 2 M Tris, pH 10.5, to bring the pH to 7. The protein compositions of the collected samples were determined by SDS-PAGE under reducing conditions using NuPAGE Novex 4-12% Bis-Tris gels (Invitrogen, Carlsbad, CA), while the nucleic acids were detected using Novex 4-20% TBE gels (Invitrogen, Carlsbad, CA).

3.3 Results and Discussion

3.3.1 Primary Screening

In order to keep the biological properties of labeled SEB almost the same as the natural target, only 5% of the amino groups on SEB molecule were methylated in our study. Also, a peptide library with a low degree of substitution of 100 μmol/g of peptide was used to minimize nonspecific interactions with the resin. Although these factors lowered the signal strength, the radiological technique used in the primary screening is sensitive to radiation levels as low as 70 dpm/bead (Mondorf et al., 1998). Casein or BSA was first used to block the nonspecific binding sites for SEB on library beads. Optimization of the experimental conditions in the primary screening showed that the usage of 1 μM of ^{14}C-

labeled SEB and five-day exposures yielded a relative low background and the highest signal-to-background ratio.

From the 1 gram of library beads that were screened (1g represents ~5% of the whole hexapeptide library containing roughly 34 x 10^6 peptides) twelve positive beads showed signals well above the background. The sequences of the peptides from each of these beads are listed from the N to the C terminus in Table 3.1. Aromatic amino acids dominate the first three positions at the N terminus in peptides No.7 to No.12. There is an N-terminal consensus, YYW, in sequences No. 7, 8, and 9. In addition, there is another consensus, WHH, near the C terminus in sequences No.9 to No.12, and a similar sequence to WHH (WLH) in sequence No.8. The consensus WHH is similar to WHK, the consensus in the peptide sequences determined by Goldman et al. from a 12-mer phage-displayed library (Goldman et al., 2000). These sequences indicate that aromatic amino acids and histidine may play an important role in peptide binding to SEB.

3.3.2 Secondary Screening

The secondary screening was used to confirm the ability of the peptide ligands from the primary screening to bind SEB efficiently and determine whether they bound SEB in preference to non-specific blocking proteins. Eleven of the peptide sequences determined from the primary screening were synthesized directly onto TA650M resins through their C termini. Because it was difficult to call the first cycle of No.8 in Table 3.1, both PYWLHH and YYWLHH were synthesized for the secondary screening. Care was taken to ensure

binding equilibrium was reached and non-specifically adsorbed proteins were removed prior to elution of SEB that bound specifically under denaturing conditions (see Materials and Methods). Results are shown in Table 3.2 with blank TA650M resin and its acetylated form as controls. This table indicates the percentage of protein bound that did not bind to the resin, as well as the percentage of the applied protein that eluted with 1 M NaCl, 2% acetic acid and 6 M Guanidine HCl, as well as percentage of the protein that remained bound on the beads.

Only two peptide sequences, YYWFYY and YYWLHH, were able to bind most of the added SEB (more than 90%) strongly enough so that it was not eluted by only 1 M NaCl. It is interesting to note the large difference in performance between these two peptides and other peptides such as FYYLPE, PYWLHH, YWHHHD and YIWHHI that have great similarities in the type and hydrophobicity of residues in their sequences. These other peptides were essentially unable to bind any SEB, and gave results that are very similar to the binding observed with the control resins. It is also important to note that all of these peptides are positively charged due to the terminal amino group and since the pI of the protein is 8.6, SEB itself will be positively charged in the binding buffer. As a result, it is not surprising that there is no binding of SEB to either the amino resin or to the acetylated amino resin controls. However, the best peptides for binding (YYWFYY and YYWLHH) are also positively charged and very hydrophobic as are the peptides with similar structures that did not bind SEB. As a result, we are led to conclude that there might be something specific about the three amino acids at the N-terminal (YYW) consensus sequence from these two peptides that may be responsible for SEB recognition.

We compared the binding characteristics of the combinatorial hexapeptides above with those of a peptide modeled on the 12-mer phage-display peptides developed by Goldman et al. (Goldman et al., 2000). One peptide from those sequences, WHKAPRAPAPLL, contains the WHK consensus found in these experiments at its N terminus. We synthesized the hexapeptide, WHKAPR, onto TA650M resin to test its ability to bind SEB. As shown in Table 3.2, it performed no better than the control resins. Apparently, either other amino acids than the N-terminal consensus are essential for SEB binding, or SEB adsorption is sensitive to the change of the solid support from a phage surface to Toyopearl resin. Murray et al. found that in the purification of anti-MUC1 antibody, the hexamer peptide KSKAGV from a phage library could not capture the target antibody when the sequence was linked to a Sepharose matrix (Murray et al., 1997).

To determine the selectivity of the positive peptide ligands, YYWFYY and YYWLHH, a competitive secondary screening was performed. Two proteins, casein and BSA, the blockers used in the primary screening, were used as competitive binders in these studies. The results are presented in Table 3.3 with TA650M resin and its acetylated form as controls. The binding capacities of both YYWFYY and YYWLHH decreased in the presence of either competitive protein. Casein was a stronger inhibitor of SEB binding than BSA. The SEB concentration in these experiments was approximately 0.028 mg/ml while the BSA and Casein concentrations were 1 mg/ml. Even though this was a very large excess (35 times higher mass concentration) of contaminant proteins, the % of SEB bound to the surface in these batch experiments was still quite significant – over 60% of the SEB loaded in the case of YYWLHH. The overall binding performance of YYWLHH was somewhat better

than that of YYWFYY. This indicates that there is a significant contribution to the binding strength and selectivity from the amino acids that are close to the resin surface, even though, as we saw from the results of the primary screening, the residues near the N terminus (YYW) seem to play an important role in binding as well. It is also interesting to note from the data in Table 3.3 that most of the loss of SEB binding capacity as a result of competition with BSA and Casein occurred in the fraction of bound SEB that was eluted by 6 M Guanidine HCl. There was also some reduction in the SEB fraction eluted by 2% acetic acid but this was not as large. This suggests that there might be two different populations of bound SEB on these resins, a fraction that requires elution with the chaotropic solvent 6 M Guanidine HCl, and a second fraction that elutes with 2% acetic acid. These two different fractions could result from protein denaturation after binding, or from two populations of peptide density on the surface or two different mechanisms of binding SEB to the same sites.

Table 3.4 shows that there is a significant reduction in binding of SEB to both peptide resins as a result of adding 0.05% Tween to the binding buffer. This is a strong indication that hydrophobic interactions are playing a major role in binding to the peptide. The results in Table 3.4 also show that addition of 1 M NaCl in the binding buffer also increased somewhat the amount of SEB bound to both YYWLHH and YYWFYY. Since these peptides are both positively charged at the pH of the binding buffer and the protein is also positively charged, adding salt at this concentration tends to decrease electrostatic repulsion and enhance hydrophobic interactions with the residues on the peptide. However, it needs to be pointed out that the hydrophobic interactions between SEB and these positive peptide

ligands are apparently specific since other peptides chosen from the primary screening with similar hydrophobicity did not bind SEB even in the presence of 1 M NaCl (data not shown).

3.3.3 Tertiary Screening

Because YYWLHH was more specific for SEB adsorption than YYWFYY in competitive secondary screening, YYWLHH was chosen as the affinity ligand for additional chromatography tests. TA650M resin, acetylated TA650M resin, and two hydrophobic peptide ligands from the primary screening (FYYLPE and YIWHHI) were used as controls. In the first experiments performed, only pure SEB was used in the binding buffer at a concentration of 0.5 mg/mL. As shown in Figure 3.1, the bound SEB on the YYWLHH column did not elute in 1 M NaCl but was eluted by 2% acetic acid. On the other hand, most of the pure SEB injected in control columns remained in the flow-through with very minute fractions found in the salt and acid elutions. Because SEB did not bind to the base resin (TA650M resin) in its acetylated form, the binding of SEB to the affinity column was clearly due to the presence of the immobilized YYWLHH peptide. The binding of SEB to YYWLHH was not due to nonspecific electrostatic interactions because nothing came out when the column was rinsed with 1 M NaCl. The performance of the hydrophobic peptides FYYLPE and YIWHHI in the control study was similar to amino resins and acetylated resins (Figure 3.1) further supporting the contention that adsorption of SEB onto YYWLHH was not due to nonspecific hydrophobic interactions.

To further characterize the binding of YYWLHH to SEB, 1 mg/ml of *E. coli* lysate, a complex mixture of proteins, lipids, RNA, DNA, polysaccharides and other biomolecules, was used as an extreme challenge to test the selectivity of the ligand for SEB in the presence of large numbers of species with a broad range of sizes, charges and hydrophobicities. Even though this is not the natural source for SEB and under normal circumstances one would not carry out affinity separations from such a crude mixture, it was thought that the attempt would provide some insight as to the selective nature of the resin. Because the peptide ligand YYWLHH is positively charged in the binding buffer and has three hydrophobic residues in its sequence, negatively charged species such as DNA and RNA as well as all hydrophobic proteins and lipids in *E. coli* lysate have the potential to bind to YYWLHH.

Figure 3.2(a) shows the effect of salt concentration on the retention of fractions of biomolecules from *E. coli* lysate on the YYWLHH column. It is clear that the addition of at least 0.5 M NaCl to the binding buffer greatly reduced the amount of material bound to the resin due to electrostatic interactions. This material was subsequently eluted upon addition of 1 M NaCl in the form of a sharp initial peak followed by a broader peak at about 40 minutes. Figure 3.2(b) shows a series of identical experiments, except in the presence of 0.5 mg/ml of SEB. With PBS only in the binding buffer, it is clear that the material from *E. coli* lysate bound to the column by electrostatic interactions interferes with SEB binding. As the salt concentration in the buffer increases the recovery of SEB increases significantly. Note that the SEB is not eluted from the column by the salt wash, but it elutes with the 2% acetic acid wash. Subsequent gel electrophoresis analysis of the *E. coli* lysate fraction bound in PBS only, and eluted from the column with 1 M NaCl, showed that it consisted primarily of

DNA (results not shown). Apparently the DNA can bind to the surface of the resin by electrostatic interactions via the positive charges on the peptide and can block the binding of SEB. Control experiments with acetylated amino resin and the base amino resin showed conclusively that the *E. coli* lysate material only bound by electrostatic interactions to the amino resin and there was essentially no binding at salt concentrations of 0.5 M NaCl or higher (Figure 3.3). It is remarkable that the small peptide YYWLHH is able to recognize and separate SEB from such a complex mixture as *E. coli* lysate under conditions where electrostatic interactions are minimized in order to prevent adsorption of DNA and RNA to the surface. Given the vast number of other proteins, lipids and other biomolecules in the system, the essentially complete capture of SEB in the presence of these other contaminants is an impressive feat and suggests that the binding of the peptide to the resin is indeed highly specific.

The results above confirmed the potential competition between negatively charged species such as DNA and RNA and surface sites for SEB binding. It was decided to take a more detailed look at the competition between a negatively charged, but hydrophobic, protein such as BSA and SEB for binding to YYWLHH. Figure 3.4(a) shows the results of adding increasing amounts of SEB to the injected sample in the presence of 5 mg/ml of BSA as the competitive protein. Because BSA, with an isoelectric point (pI) of 4.9, carries a net negative charge at pH 7.4, there is a possibility of electrostatic interactions between the negatively charged BSA and positively charged YYWLHH. To eliminate this effect, 0.5 M NaCl was added to the binding buffer, and as can be seen in Figure 3.4(a), BSA alone exhibits little binding to the column under these conditions. Over 80% of the BSA peak area

is in the flow through. The remaining fraction of the injected BSA is bound strongly to the resin, probably by hydrophobic interactions, and this is released by elution with 2% acetic acid. Figure 3.4(a) shows that increasing amounts of SEB results in increasingly large peaks of SEB being eluted from the column by the acid wash, with the area of these peaks being proportional to the amount of applied SEB. The SEB is eluted first as a result of the addition of the 2% acetic acid and any residual BSA comes out in the second acid peak. There was a quantitative recovery of all of the applied SEB to the resin. The SDS-PAGE analysis shown in Figure 3.4(b) indicates that there is a very clean separation between these two proteins under these conditions. Control experiments with acetylated amino resin and the base amino resin showed conclusively that the BSA couldn't be retained without the functional peptide YYWLHH (Figure 3.5). The observation that a fraction of the BSA binds to the resin and is eluted with 2% acetic acid might be due to some denaturation of the protein upon adsorption to the surface or to a population of high peptide density sites on the resin. A similar effect was also seen when using the peptide ligand AcWHWRKR for the purification of α-Lactalbumin from whey protein in which BSA is one of the major contaminants (Gurgel et al., 2001). In addition, some dye columns also show this characteristic adsorption behavior for human albumin with multiple elution peaks (Gianazza and Arnaud, 1982; Miribel and Arnaud, 1987).

SEB is an exoprotein, produced inside *Staphylococcus aureus* cells and released into the fermentation broth, which is the starting material for SEB purification. A series of chromatography runs was performed using similar methods as those used in Figure 3.4, except using 5 mg/ml of fermentation broth instead of 5 mg/ml of BSA as the competitive

protein. The fermentation broth used in these experiments contained some trace amounts (< 5 μg/ml) of SEE as well as some SEB. These trace concentrations of toxin are much lower than the SEB amounts injected into the column in combination with the *Staphylococcus aureus* fermentation broth. As shown in Figure 3.6(a), nearly 100% proteins in the fermentation broth passed through the column according to BCA total protein assay. As in Figure 3.4, nothing appeared to come out in 1M NaCl, and the area under the 2% acetic acid peak increased by the same proportion as the increase in SEB concentration in the injected mixture. Electrophoresis analysis showed that SEB was concentrated in the peak after 2% acetic acid elution (Figure 3.6(b)). The composition of the toxin peak was uniform and the recovery of SEB from the fermentation broth was complete.

Preparative chromatography for protein purification is generally operated under nonlinear conditions, namely the column is overloaded. The affinity of the peptide ligand YYWLHH to SEB and its potential for SEB purification was further investigated when the column was continuously loaded with 5 mg/ml fermentation broth spiked with trace SEB. The protein concentration ratio of the fermentation broth to SEB in the loading mixture was 100 and the loading volume (5 ml) was as large as nearly 50 times the column volume. As shown in Figure 3.7(a), there was a sharp peak and a shoulder peak after 2% acetic acid elution when only fermentation broth was loaded on the column, indicating that the peptide column captured some proteins from the fermentation broth during the loading. SDS-PAGE analysis showed that the sharp peak represents the background toxin captured by the column (potentially SEE and some SEB) and the shoulder peak corresponds to nonspecific binding of other proteins in the fermentation broth (Figure 3.7(c)). Even though a portion of the surface

sites were occupied by background toxin and other nonspecifically bound proteins, the peptide column was far from saturation. When the fermentation broth spiked with SEB was applied to the column, more than 70% of the spiked SEB was captured and eluted during the continuous loading (Figure 3.7(a)). As shown in Figure 3.7(b), electrophoresis analysis showed that the sharp peak was the SEB standard and the shoulder peak contained the nonspecifically bound proteins in the fermentation broth. The sample taken at half of the loading time (25 minutes) showed a visible SEB band indicating some SEB passed through the column due to the interference from the fermentation broth. The resolution between the toxin peak and the shoulder peak could be improved if a linear gradient of the acetic acid from 0 to 2% was used. It has been reported that the concentration of SEB could reach to 0.27 mg per ml culture supernant after 48-hour fermentation with the use of a highly SEB-productive strain, *Staphylococcus aureus* S-6 (Lopes et al., 1996). The high capacity and selectivity of the resins with the peptide ligand YYWLHH indicate that this resin would indeed be suitable for a nearly one-step SEB affinity purification directly from the broth.

3.3.4 Cross Reactivity with Other Bacterial Superantigens

Having established that this peptide can recognize SEB in the presence of other proteins in a complex mixture, it was decided to find out to what degree it might be able to distinguish SEB from other Staphylococcal enterotoxins that have close similarities in sequence and tertiary structure. Three other toxins from *Staphylococcal aureus*, SEA, SEC1 and TSST1, were injected into a column with YYWLHH resin and the elution results

compared to binding of SEB. Figure 3.8 shows that SEB had the smallest elution flow-through and sharpest elution peak with 2% acetic acid of all of the toxins tested. SEC1 seemed to be pretty much spread out during the injection, indicating weak reversible binding to the resin. SEA had a very well defined flow-through peak and a much smaller peak upon acid elution. TSST1 exhibited a broader peak upon elution but a relatively small flow-through peak. The interaction of this protein with the resin was the most similar to the SEB case. SEB shares a high degree of homology and a similar three-dimensional structure to other SEs (Li et al., 1999). Probably as a result, certain pseudo-affinity ligands (for example, dye ligands) used to purify SEB may also bind other SEs (Brehm et al., 1990). SEB shows 31%, 67%, and 16% sequence homology with SEA, SEC1 and TSST1 respectively (Balaban and Rasooly, 2000; Kim et al., 1994).

The significant cross reactivity of YYWLHH with TSST1, despite the fact it has less sequence homology to SEB than SEA and SEC1 may indicate that the adsorption of SEs to this short peptide may depend more on the tertiary than the primary structure of the proteins. TSST1 and SEB have very similar three-dimensional structures (Prasad et al., 1993). Peptide ligands for TSST1 deduced from a 15-amino-acid phage library showed a significant enrichment of aromatic amino acids and one of them contained YYW (Sato et al., 1996). Also, the binding sites of TSST1 and SEB on a human class II major histocompatibility molecule (DR1) overlap substantially, although there are also significant differences in binding (Kim et al., 1994).

3.3.5 Binding of Native vs. Nicked SEB

Possible contaminants in partially purified SEB include staphylococcal proteases, hemolysins and protein A as well as other minor staphylococcal proteins and a small amount of SEA. The dominant contaminants, based on electrophoresis, are nicked proteins of SEB. The native proteases in the crude toxins are able to nick the SEB inside the disulfide loop yielding some low molecular weight (13~16 kDa), serologically related toxin materials. These nicked proteins remain associated through disulfide bonds under native conditions, so that they show the same molecular weight as the native SEB under non-reducing conditions in SDS-PAGE, while they separate from the native SEB under reducing conditions in SDS-PAGE, due to destruction of this disulfide loop. It is difficult to obtain homogeneous SEB due to the presence of nicked proteins even after multi-step high-pressure liquid chromatography in SEB purification (Strickler et al., 1989; Williams et al., 1983). As shown in Figure 3.9(a), injection of a partially purified SEB sample through the YYWLHH column resulted in two peaks, a flow-through peak and a strongly bound the peak that eluted with 2% acetic acid. The SDS-PAGE analysis under reducing and non-reducing conditions in Figure 3.9(b) and 3.9(c) shows that it was the nicked proteins did not bind to the YYWLHH column and the native SEB was retained and eluted in the acid wash. The SEB peak gave a single homogeneous band of 28 kDa after SDS-PAGE under both reducing and non-reducing conditions. The loss of native SEB in the flow-through was minimal (Figure 7(b), lane 3). The results in Figure 3.9 indicate that YYWLHH seems to recognize native SEB and the interactions between the peptide ligand and SEB might be through the disulfide bridge.

3.4 Conclusions

A short peptide ligand that can bind SEB selectively, YYWLHH, has been identified from a solid phase combinatorial hexamer peptide library using a multi-tiered screening process. It has been demonstrated that this peptide can be used as an affinity ligand for detection and purification of SEB from complex mixtures. Although it shows cross reactivity with TSST1, peptide YYWLHH shows little cross reactivity with SEA and SEC1. The YYWLHH column was able to capture SEB efficiently even at low concentrations. The affinity of YYWLHH has been demonstrated to be sufficiently high for purification of SEB from a mixture of SEB with *E. coli* lysate, BSA, or *Staphylococcus aureus* fermentation broth in one step. It was also possible to obtain highly purified native SEB from a heterogeneous SEB preparation containing nicked or denatured protein. Because it is relatively inexpensive to produce in large quantities and it is chemically robust, this ligand might find use in the development of field detection, removal and purification methods for SEB.

3.5 Reference

Amatschek K, Necina R, Hahn R, Schallaun E, Schwinn H, Josic D, Jungbauer A. 2000. Affinity chromatography of human blood coagulation factor VIII on monoliths with peptides from a combinatorial library. J High Resol Chromatogr 23:47-58.

Archer DL, Young EE. 1988. Contemporary issues: diseases with food vector. Clin Microbiol Rev 1:377-398.

Balaban N, Rasooly A. 2000. Review: Staphylococcal enterotoxins. Int J Food Microbiol 61:1-10.

Balaban N, Rasooly A. 2001. Analytical chromatography for recovery of small amounts of staphylococcal enterotoxins from food. Int J Food Microbiol 64:33-40.

Balint J, Totorica C, Stewart J, Cochran S. 1989. Detection, isolation and characterization of staphylococcal enterotoxin B in protein A preparations purified by immunoglobulin G affinity chromatography. J Immunol Methods 116:37-43.

Bastek PD, Land JM, Baumbach GA, Hammond DH, Carbonell RG. 2000. Discovery of Alpha-1-proteinase inhibitor binding peptides from the screening of a solid phase combinatorial peptide library. Separation Sci Technol 35:1681-1706.

Baumbach GA, Hammond DJ. 1992. Protein purification using affinity ligands deduced from peptide libraries. BioPharm May:24-35.

Bergdoll MS. 1983. Enterotoxins. In: Easman CS, Adlum C, editors. Staphylococcal and Staphylococcal Infections. London: Academic Press Inc. p 559-598.

Bergdoll MS. 1985. The staphylococcal enterotoxins: an update. In: Jelijaszewicz J, editor. The Staphylococci. New York: gustav Fischer Verlag. p 247-254.

Bergdoll MS, Borja CR, Avena RM. 1965. Identification of a new enterotoxin as enterotoxin C. J Bacteriol 90:1481-1485.

Bergdoll MS, Borja CR, Robbins RN, Weiss KF. 1971. Identification of enterotoxin E. Infect Immun 4:593-595.

Bhatti AR, Nadon LP, Micusan VV. 1994. Purification of superantigen staphylococcal enterotoxin B (SEB). IJBC 1:47-56.

Brehm RD, Tranter HS, Hambleton P, Melling J. 1990. Large-scale purification of staphylococcal enterotoxins A, B, and C2 by dye ligand affinity chromatography. Appl Environ Microbiol 56:1067-1072.

Buettner JA, Dadd CA, Baumbach GA, Masecar BL, Hammond DJ. 1996. Chemically derived peptide libraries: A new resin and methodology for lead identification. Int J Peptide Protein Res 47:70-83.

Casman EP, Bennett RW, Dorsey AE, Issa JA. 1967. Identification of a fourth staphylococcal enterotoxin, enterotoxin D. J Bacteriol 94:1875-1882.

Casman EP, Bergdoll MS, Robinson J. 1963. Designation of staphylococcal enterotoxins. J Bacteriol 85:715-716.

Cwirla SE, Peters EA, Barrett RW, Dower WJ. 1990. Peptides on phage: A vast library of peptides for identifying ligands. Proc Natl Acad Sci USA 87:6378-6382.

Devlin JJ, Panganiban LC, Delvin PE. 1990. Random peptide libraries: A source of specific protein binding molecules. Science 249:404-406.

Enserink M, Malakoff D. 2001. Bioterrorism: Congress weighs select agent update. Science 294:1438-1438.

Evenson ML, Hinds MW, Bernstein RS, Bergdoll MS. 1988. Estimation of human dose of staphylococcal enterotoxin A from a large outbreak of staphylococcal food poisoning involving chocolate milk. Int J Food Microbiol 7:311-316.

Fassina G, Ruvo M, Palombo G, Verdoliva A, Marino M. 2001. Novel ligands for the affinity-chromatographic purification of antibodies. J Biochem Biophys Methods 49:481-490.

Fey H, Pfister H, Ruegg O. 1984. Comparative evaluation of different enzyme-linked immunosorbent assay systems for the detection of staphylococcal enterotoxins A, B, C, and D. J Clin Microbiol 19:34-38.

Franz DR, Jahrling PB, Friedlander AM, McClain DJ, Hoover DL, Bryne WR, Pavlin JA, Christopher CW, Eitzen EM. 1997. Clinical recognition and management of patients exposed to biological warfare agents. J Am Med Assoc 278:399-411.

Gianazza E, Arnaud P. 1982. A general method for fractionation of plasma proteins. Dye-ligand affinity chromatography on immobilized Cibacron blue F3-GA. Biochem J 201:129-136.

Goldman ER, Pazirandeh MP, Mauro JM, King KD, Frey JC, Anderson GP. 2000. Phage-displayed peptides as biosensor reagents. J Mol Recognit 13:382-387.

Gurgel PV, Carbonell RG, Swaisgood HE. 2001. Fractionation of whey proteins with a hexapeptide ligand affinity resin. Bioseparation 9:385-392.

Huang PY, Baumbach GA, Dadd CA, Buettner JA, Masecar BL, Hentsch M, Hammond DJ, Carbonell RG. 1996. Affinity purification of von Willebrand Factor using ligands derived from peptide libraries. Bioorg Med Chem 4:699-708.

Huang PY, Carbonell RG. 1995. Affinity purification of proteins using ligands derived from peptide libraries. Biotechnol Bioeng 47:288-297.

Huang PY, Carbonell RG. 1999. Affinity chromatographic screening of soluble combinatorial peptide libraries. Biotechnol Bioeng 63:633-641.

Jentoft N, Dearborn DG. 1983. Protein labeling by reductive alkylation. Method Enzymol 91:570-579.

Kaufman DB, Hentsch ME, Baumbach GA, Buettner JA, Dadd CA, Huang PY, Hammond DJ, Carbonell RG. 2002. Affinity purification of fibrinogen using a ligand from a peptide library. Biotechnol Bioeng 77:278-289.

Kim J, Urban RG, Strominger JL, Wiley DC. 1994. Toxic shock syndrome toxin-1 complexes with a class II major histocompatibility molecule HLA-DR1. Science 266:1870-1874.

Lam KS, Lake D, Salmon SE, Smith J, Chen ML, Wade S, Abdul-Latif F, Knapp RJ, Leblova Z, Ferguson RD and others. 1996. A one-bead one-peptide combinatorial library method for B-cell epitope mapping. Method Enzymol 9:482-493.

Lam KS, Lebl M, Krchnak V. 1997. The "one-bead-one-compound" combinatorial library method. Chem Rev 97:411-448.

Lam KS, Salmon SE, Hersh EM, Hruby VJ, Kazmierski WM, Knapp RJ. 1991. A new type of synthetic peptide library for identifying ligand-binding activity. Nature 354:82-84.

Lapeyre C, Maire T, Messio S, Dragacci S. 2001. Enzyme immunoassay of staphylococcal enterotoxins in dairy products with cleanup and concentration by immunoaffinity column. J AOAC Int 84:1587-1592.

Li H, Llera A, Malchiodi EL, Mariuzza RA. 1999. The structural basis of T cell activation by superantigens. Annu Rev Immunol 17:435-466.

Lopes HR, Noleto ALS, Bergdoll MS. 1996. Purification of Staphylococcal enterotoxins B and C2 by dye ligand chromatography - production of antisera. Rev Microbiol 1:52-56.

Makriyannis T, Clonis YD. 1997. Design and study of peptide-ligand affinity chromatography adsorbents: application to the case of trypsin purification from bovine pancreas. Biotechnol Bioeng 53:49-57.

Marrack P, Kappler J. 1990. The staphylococcal enterotoxins and their relatives. Science 248:705-711.

Meyer RF, Palmieri MJ. 1980. Single radial immunodiffusion method for screening staphylococcal isolates for enterotoxin. Appl Environ Microbiol 40:1080-1085.

Miribel L, Arnaud P. 1987. Fractionation of plasma proteins using dye-ligand chromatography: elution profiles on immobilized Green TSK-AF. J Biochem Biophys Methods 14:291-302.

Mondorf K, Kaufman DB, Carbonell RG. 1998. Screening of combinatorial peptide libraries: Identification of ligands for affinity purification of proteins using a radiological approach. J Pept Res 52:526-536.

Munson SH, Tremaine MT, Betley MJ, Welch RA. 1998. Identification and characterization of staphylococcal enterotoxin types G and I from Staphylococcus aureus. Infect Immun 66:3337-3348.

Murray A, Sekowski M, Spencer DIR, Denton G, Price MR. 1997. Purification of monoclonal antibodies by epitope and mimotope affinity chromatography. J Chromatogr A 782:49-54.

Murray A, Spencer DIR, Missailidis S, Denton G, Price MR. 1998. Design of ligands for the purification of anti-MUC1 antibodies by peptide epitope affinity chromatography. J Pept Res 52:375-383.

Necina R, Amatschek K, Schallaun E, Schwinn H, Josic D, Jungbauer A. 1998. Peptide affinity chromatography of human clotting factor VIII: Screening of the vWF-binding domain. J Chromatogr B 715:191-201.

Orwin PM, Leung DYM, Donahue HL, Novick RP, Schlievert PM. 2001. Biochemical and biological properties of staphylococcal enterotoxin K. Infect Immun 69:360-366.

Park CE, Akhtar M, Rayman MK. 1994. Evaluation of a commercial enzyme immunoassay kit (RIDASCREEN) for detection of staphylococcal enterotoxins A, B, C, D, and E in foods. Appl Environ Microbiol 60:677-681.

Prasad GS, Earhart CA, Murray DL, Novick RP, Schlievert PM, Ohlendorf DH. 1993. Structure of toxic shock syndrome toxin 1. Biochemistry 32:13761-13766.

Reiser RF, Robbins RN, Noleto AL, Khoe GP, Bergdoll MS. 1984. Identification, purification, and some physicochemical properties of staphylococcal enterotoxin C3. Infect Immun 45:625-630.

Rowe CA, Tender LM, Feldstein MJ, Golden JP, Scruggs SB, MacCraith BD, Cras JJ, Ligler FS. 1999. Array biosensor for simultaneous identification of bacterial, viral, and protein analytes. Anal Chem 71:3846-3852.

Sato A, Ida N, Fukuyama M, Miwa K, Kazami J, Nakamura H. 1996. Identification from a phage display library of peptides that bind to toxic shock syndrome toxin-1 and that inhibit its binding to major histocompatibility complex (MHC) class II molecules. Biochemistry 35:10441-10447.

Scott JK, Smith GP. 1990. Searching for peptide ligands with an epitope library. Science 249:386-390.

Strickler MP, Neill RJ, Stone MJ, Hunt RE, Brinkley W, Gemski P. 1989. Rapid purification of staphylococcal enterotoxin B by high-pressure liquid chromatography. J Clin Microbiol 27:1031-1035.

Su YC, Wong AC. 1995. Identification and purification of a new staphylococcal enterotoxin, H. Appl Environ Microbiol 61:1438-1443.

Swaminathan S, Furey W, Pletcher J, Sax M. 1992. Crystal structure of staphylococcal enterotoxin B, a superantigen. Nature 359:801-806.

Warren JR, Spero L, Metzger JF. 1974. Isothermal denaturation of aqueous staphylococcal enterotoxin B by guanidine hydrochloride, urea and acid pH. Biochemistry 13:1678-1683.

Williams RR, Wehr CT, Bennett RW. 1983. High-performance liquid chromatography of staphylococcal enterotoxin B. J Chromatogr A 266:179-186.

Zhang S, Iandolo JJ, Stewart GC. 1998. The enterotoxin D plasmid of Staphylococcus aureus encodes a second enterotoxin determinant (sej). FEMS Microbiol Lett 168:227-233.

3.6 Appendix

3.6.1 Purification of SEB from E. coli Lysate

Figure 3.10 shows the results of adding increasing amounts of SEB to the injected sample in the presence of *E. coli* lysate. The results shown indicate that SEB can be quantitatively purified from 1 mg/ml *E. coli* lysate using immobilized YYWLHH. The area under the 2% acetic acid peak increased by the same proportion as the increase in SEB concentration in the injected mixture, indicating that all of the injected SEB was released by 2% acetic acid, as shown in Figure 3.10(a). There was an extremely small tail peak after the toxin peak (almost invisible) and electrophoresis showed that it represented some components in *E. coli* lysate that adsorbed to the column more strongly. SDS-PAGE analysis was done on the fractions collected during the chromatography separation (Figure 3.10(b)). SEB was concentrated in the first peak after 2% acetic acid elution. The remaining fractions collected unbound proteins (flow-through peak), proteins bound with electrostatic interactions (1 M NaCl peak), and tightly bound proteins (the peak after SEB peak). The composition of the toxin peak was uniform and the recovery of SEB from *E. coli* lysate was almost the same as that in noncompetitive chromatography runs. The band corresponding to proteins in 1 M NaCl fraction was undetectable in electrophoresis even after 10X concentration, indicating that the protein concentration might be very low or the peak might result from DNA or RNA in *E. coli* lysate. Another run of all the fractions in gels for nucleic acids detection did find several clear bands in both flow through and 1M salt fractions (Figure 3.10(c)).

The results in Figure 3.11 indicate that even relatively high concentrations of non-specific interferents had minimal effect of the binding of SEB to YYWLHH. The addition of *E. coli* lysate up to 2.5 mg/ml to 0.5 mg/ml of SEB had little effect on the results. The area of the toxin peak dropped to 70% and 50% of the injected sample when the concentration of *E. coli* lysate increased to 5 mg/ml and 10 mg/ml, respectively (Figure 3.11(a)). Some of the SEB came out in the flow-through and 1 M salt fractions as demonstrated in SDS-PAGE gels (Figure 3.11(b)).

According to Figures 3.10 and 3.11, some nonspecifically bound proteins came out after SEB, suggesting their binding energies are larger than that of SEB. If the column is overloaded under nonlinear conditions, those nonspecific bond proteins could displace the SEB molecules in the column, and experimental studies confirmed that (data not shown). Therefore, although the YYWLHH column can purify SEB from *E. coli* lysate in one step for small volume samples, *E. coli* lysate is not a suitable background matrix for the purification of SEB especially in a large-scale. Because of its complexity, *E. coli* lysate has been a commercial universal blocking reagent (Promega, Madison, WI) to lower the background in various immunological assays.

3.6.2 Detection of SEB

The application of HPLC for SEB detection in food safety analysis is currently limited because relatively pure material is required. Using the peptide ligand YYWLHH, which has been shown to bind SEB specifically, as the adsorbent in HPLC could eliminate

the limiting factor in sample preparation. To test its applicability, both noncompetitive and competitive formats were conducted. *E. coli* lysate was used as the competitive reagent. The detection of 12.5 μg of SEB with/without 250 μg of *E. coli* lysate in a 500μl solution is shown in Figure 3.12(a). SEB was released in the first peak in 2% acetic acid and the composition of the toxin peak is uniform based on SDS-PAGE (Figure 3.12(b)). The band corresponding to proteins in 1 M NaCl fraction was undetectable in electrophoresis even after 10X concentration, indicating that the protein concentration might be very low or the peak might result from DNA or RNA in *E. coli* lysate. Another run of all the fractions in gels for nucleic acids detection did find several clear bands in both flow through and 1M salt fractions (results not shown). Both formats recovered almost all the injected SEB based on Micro-BCA assay (Table 3.5). Thus *E. coli* lysate has minimal interference to SEB detection although some trace material in *E. coli* lysate was released together with SEB. This experiment was repeated with a much lower concentration of 1.25 μg in 500 μl of solution. The interference of *E. coli* lysate became significant because the amount of released material was comparable to the eluted toxin in the first acid peak (results not shown). However, it was still possible to detect the injected SEB by comparing the peak height and peak area of the first eluted peak after the 2% acetic acid wash (data not shown). Therefore, the limit of sensitivity of the column for SEB detection is approximately 10 μg/ml (3.5×10^{-7} M) provided that the interference of *E. coli* lysate can be neglected. The most important index for analytical chromatography is the peak resolution in protein detection and analysis. Although the peptide column showed a significant nonspecific binding to nucleic acids and some

proteins in the *E. coli* lysate, the SEB peak showed a high resolution relative to other peaks due to the nonspecific binding.

ELISA is the most commonly used method to detect SEB. Although it doesn't require highly purified protein, ELISA needs an extraction-concentration method to help in elimination of other proteins that might lead to false positive results and concentration of toxins in food extracts. Cation exchange and immunoaffinity chromatography has been used to recover small amounts of SEs from food before ELISA or western blotting is used for their detection (Balaban and Rasooly, 2001; Lapeyre et al., 2001). The peptide ligand YYWLHH is more specific than a cation exchanger and more stable than antibodies. Therefore, the column capture step by using YYWLHH may become a part of an ELISA with a robust ligand.

Table 3.1 Sequences deduced from the primary screening.

No.	Peptide Sequences					
1	K	L	Q	A	T	I
2	I	Q	I	R	F	G
3	A	Y	F	K	V	P
4	A	F	G	W	W	H
5	V	P	T	Y	S	E
6	F	Y	Y	L	P	E
7	Y	Y	W	F	Y	Y
8	Y/P	Y	W	L	H	H
9	Y	Y	W	H	H	X*
10	Y	W	H	H	H	D
11	Y	I	W	H	H	I
12	R	W	W	H	H	H

*: Symbol for amino acids that cannot be sequenced.

Table 3.2 Noncompetitive secondary screening.

Peptides	Unbound (% of total)	1 M NaCl (% of total)	2% acetic acid (% of total)	6 M GdnHCl (% of total)	Beads (% of total)
Control resins					
Amino[1]	91.85	0.19	1.74	0.37	5.85
Acetylated[2]	91.78	0.42	0.06	1.49	6.25
Peptide sequences from the one-bead-one-peptide library					
KLQATI	82.49	1.43	0.75	12.51	2.82
IQIRFG	85.93	1.25	0.52	9.77	2.53
AYFKVP	75.71	0.62	0.89	6.65	16.13
AFGWWH	94.43	0.54	1.17	1.94	1.92
VPTYSE	96.59	1.68	0.90	0.31	0.52
FYYLPE	95.25	0.60	0.79	1.66	1.70
YYWFYY	6.39	0.65	**59.93**	**26.14**	6.89
YYWLHH	6.58	0.61	**74.12**	**15.24**	3.45
PYWLHH	74.45	0.55	7.06	14.94	3.00
YWHHHD	76.10	5.01	1.62	8.09	9.18
YIWHHI	87.91	1.34	1.36	4.36	5.03
Peptide sequence from a phage library (Goldman et al., 2000)					
WHKAPR	88.36	2.83	1.26	4.85	2.70

1: Toyopearl AF-Amino-650M resins
2: acetylated Toyopearl AF-Amino-650M resins

Table 3.3 Competitive secondary screening.

Peptides	Blocker	Unbound (% of total)	1 M NaCl (% of total)	2% acetic acid (% of total)	6 M GdnHCl (% of total)	Beads (% of total)
Amino[1]	No blocker	92.63	0.37	1.89	3.37	1.74
	Casein	93.54	3.26	2.13	0.61	0.46
	BSA	95.31	1.40	2.07	0.74	0.48
Acetylated[2]	No blocker	95.24	0.17	0.06	0.33	4.20
	Casein	98.59	1.07	0.07	0.16	0.11
	BSA	98.57	0.86	0.06	0.26	0.25
YYWFYY	No blocker	5.00	0.85	**57.95**	30.00	6.20
	Casein	47.09	4.49	**39.63**	6.22	2.57
	BSA	35.35	3.11	**44.95**	13.03	3.56
YYWLHH	No blocker	4.88	0.51	**74.72**	15.70	4.19
	Casein	32.06	2.68	**56.47**	6.36	2.43
	BSA	25.28	2.45	**59.03**	10.17	3.07

1: Toyopearl AF-Amino-650M resins
2: acetylated Toyopearl AF-Amino-650M resins

Table 3.4 Effect of salt and detergent on the binding of SEB to YYWFYY and YYWLHH in a noncompetitive secondary screening.

Peptide ligand	Binding buffer	% bound
YYWFYY	PBS	93.58
	PBS + 1 M NaCl	97.35
	PBS + 0.05% Tween	24.84
YYWLHH	PBS	91.92
	PBS + 1 M NaCl	97.54
	PBS + 0.05% Tween	28.06

Table 3.5 Recovery of SEB analyzed by Micro-BCA in Figure 3.12.

Sample	Recovered SEB (μg)
250 μg *E. coli* lysate + 12.5 μg SEB	11.82
12.5 μg SEB	11.63

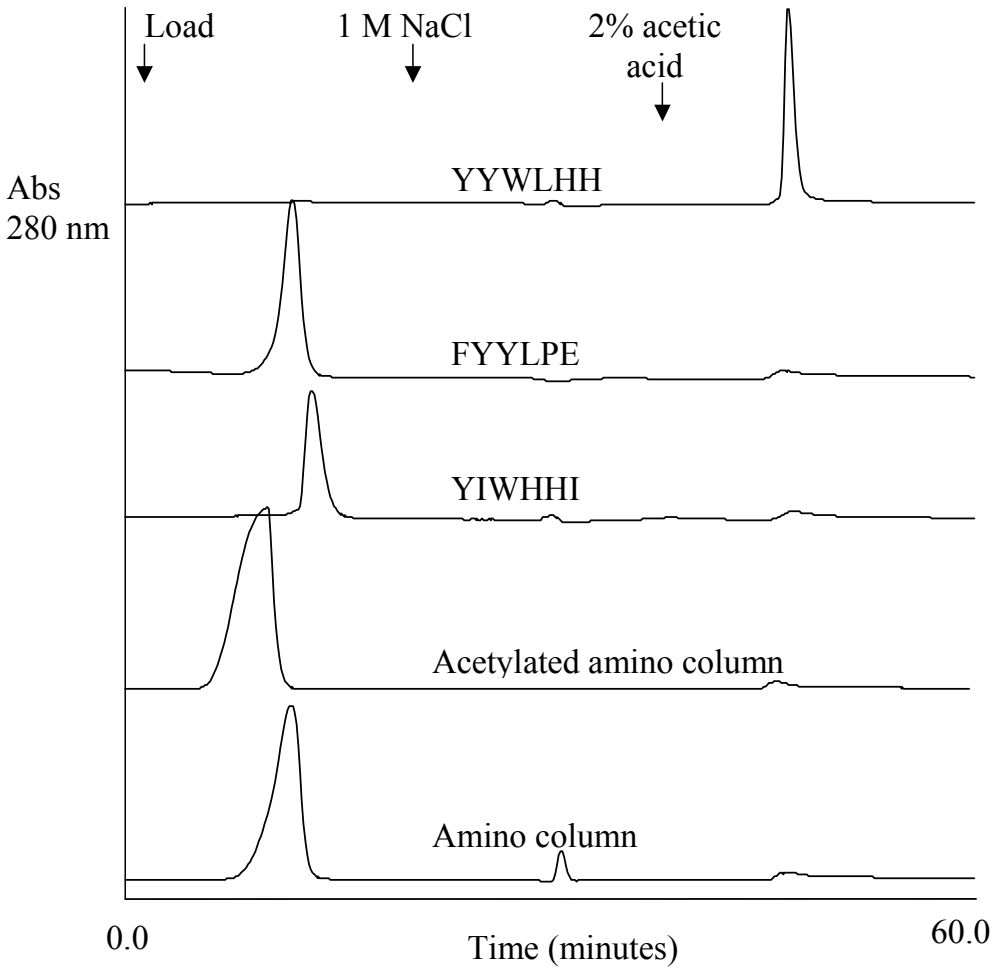

Figure 3.1 Binding of 0.5 mg/ml SEB on different columns. Amino column packed with Toyopearl AF-Amino-650M resins; acetylated amino column packed with acetylated Toyopearl AF-Amino-650M resins.

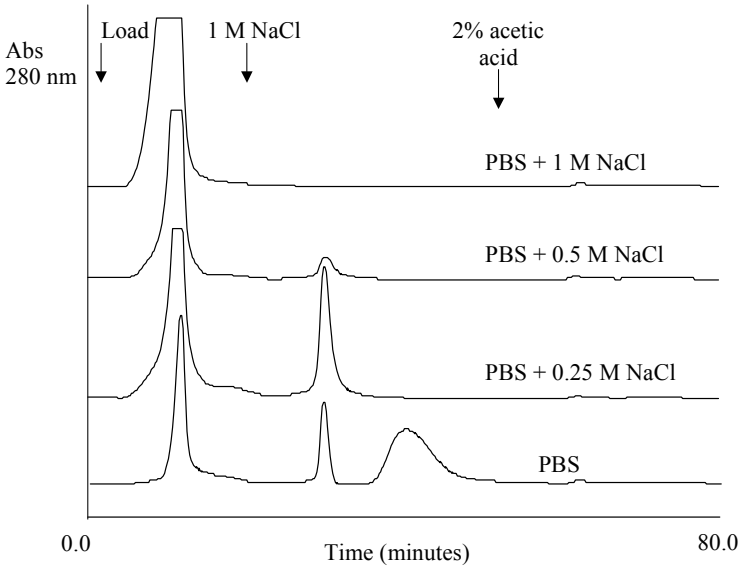

(a)

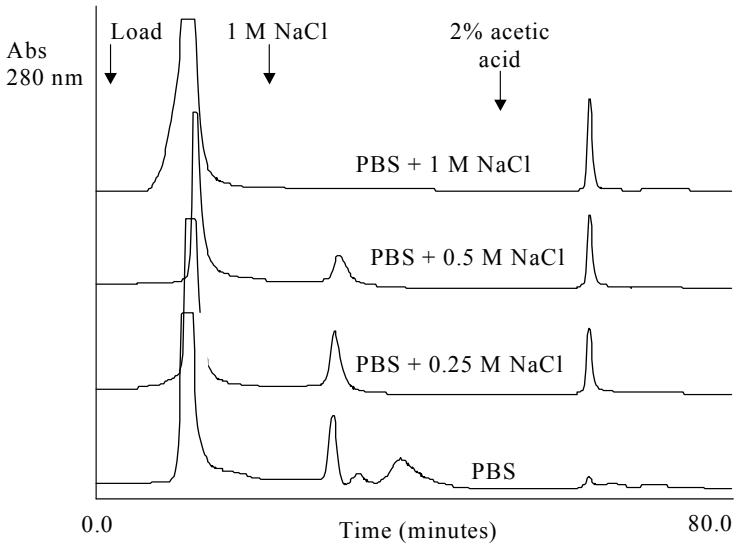

(b)

Figure 3.2 Effect of salt in the binding buffer on the separation of SEB from *E. coli* lysate using a YYWLHH column. **(a)** Injection of 1mg/ml *E. coli* lysate. **(b)** Injection of 0.5mg/ml SEB combined with 1mg/ml *E. coli* lysate.

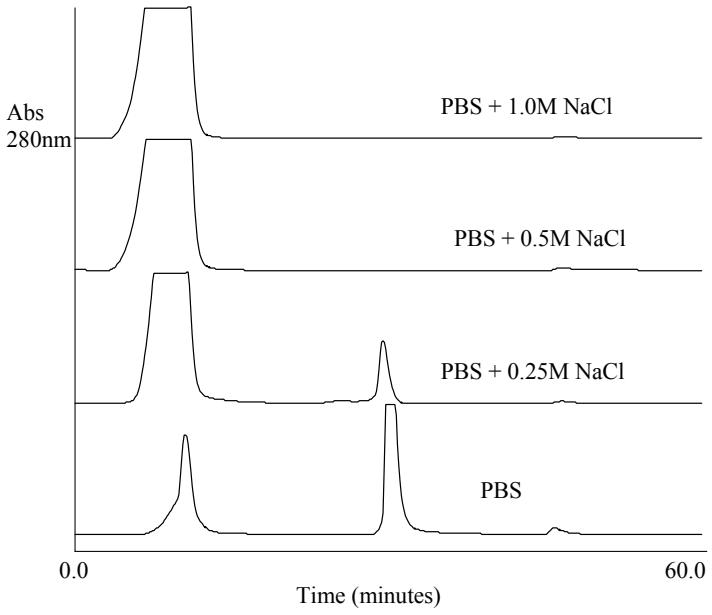

(a)

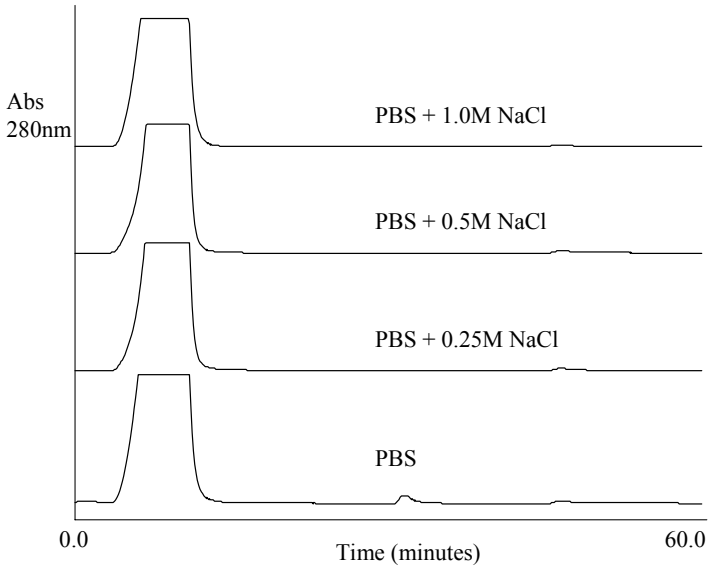

(b)

Figure 3.3 Effect of salt on the binding of *E. coli* lysate to control columns. **(a)** an amino column packed with Toyopearl AF-Amino-650M resins; **(b)** an acetylated amino column packed with acetylated Toyopearl AF-Amino-650M resins.

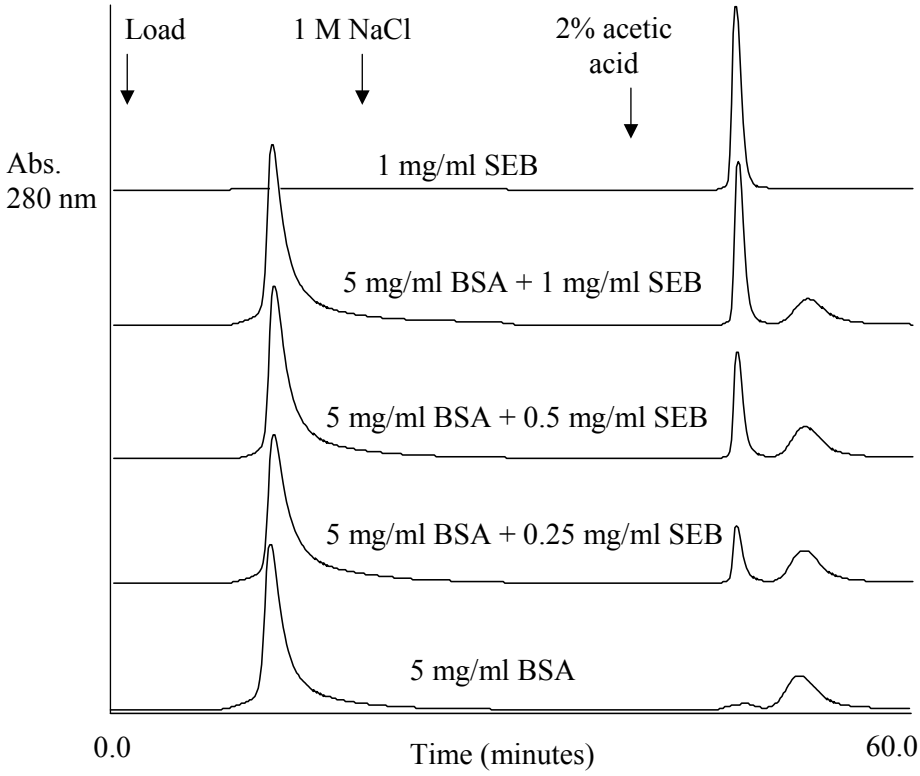
Load
1 M NaCl
2% acetic acid
Abs. 280 nm
1 mg/ml SEB
5 mg/ml BSA + 1 mg/ml SEB
5 mg/ml BSA + 0.5 mg/ml SEB
5 mg/ml BSA + 0.25 mg/ml SEB
5 mg/ml BSA
0.0
Time (minutes)
60.0

(a)

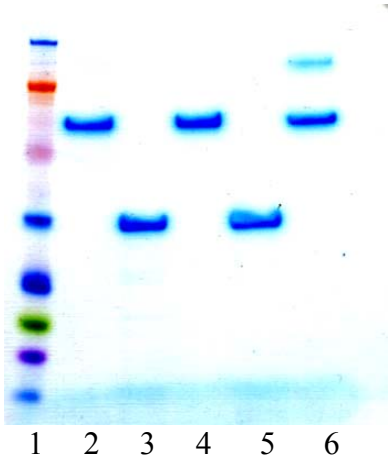
1 2 3 4 5 6

(b)

Figure 3.4 **(a)** Purification of various amount of SEB from 5 mg/ml BSA using a YYWLHH column. **(b)** SDS-PAGE of the chromatographic separation of 0.5 mg/ml SEB from 5 mg/ml BSA using a YYWLHH column. Lane 1, 2 and 3 contain the molecular weight markers, BSA, and SEB standard, respectively; lane 4 is the flow through peak; lane 5 and 6 correspond to eluates in the first and second peaks of the 2% acetic acid, respectively.

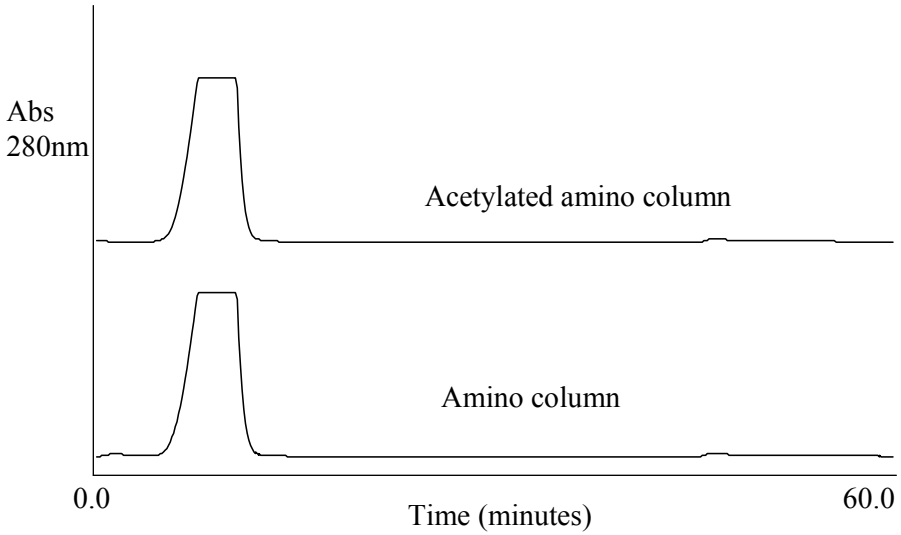

Figure 3.5 Binding of BSA to control columns. Amino column packed with Toyopearl AF-Amino-650M resins; acetylated amino column packed with acetylated Toyopearl AF-Amino-650M resins.

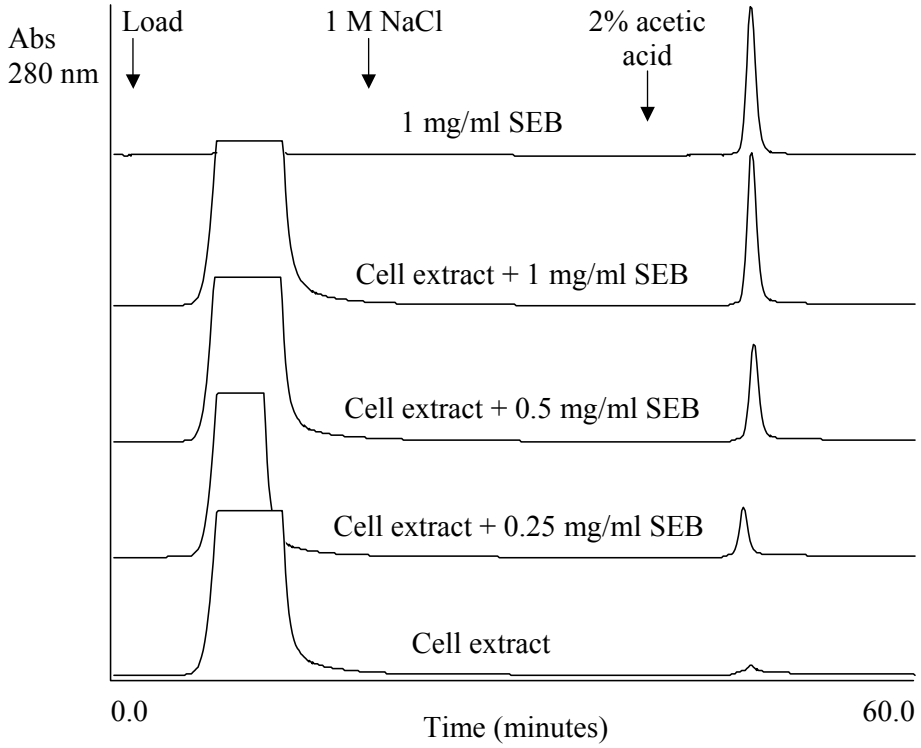
Abs
280 nm
Load
1 M NaCl
2% acetic
acid
1 mg/ml SEB
Cell extract + 1 mg/ml SEB
Cell extract + 0.5 mg/ml SEB
Cell extract + 0.25 mg/ml SEB
Cell extract
0.0
Time (minutes)
60.0

(a)

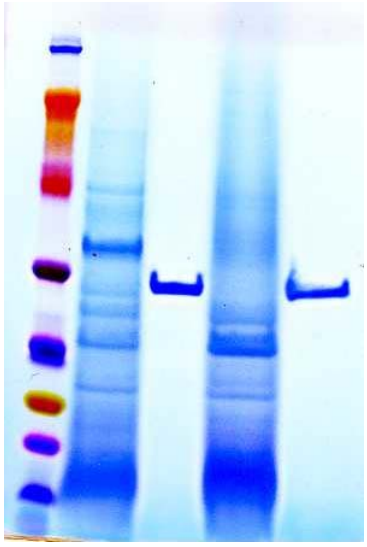
1
2
3
4
5

(b)

Figure 3.6 **(a)** Purification of various amount of SEB from 5 mg/ml *Staphylococcus aureus* fermentation broth using a YYWLHH column. **(b)** SDS-PAGE of the chromatographic separation of 0.5 mg/ml SEB from 5 mg/ml *Staphylococcus aureus* fermentation broth using a YYWLHH column. Lane 1, 2 and 3 contain the molecular weight markers, fermentation broth, and SEB standard, respectively; lane 4 is the flow through; lane 5 corresponds to the eluate in the peak of 2% acetic acid elution.

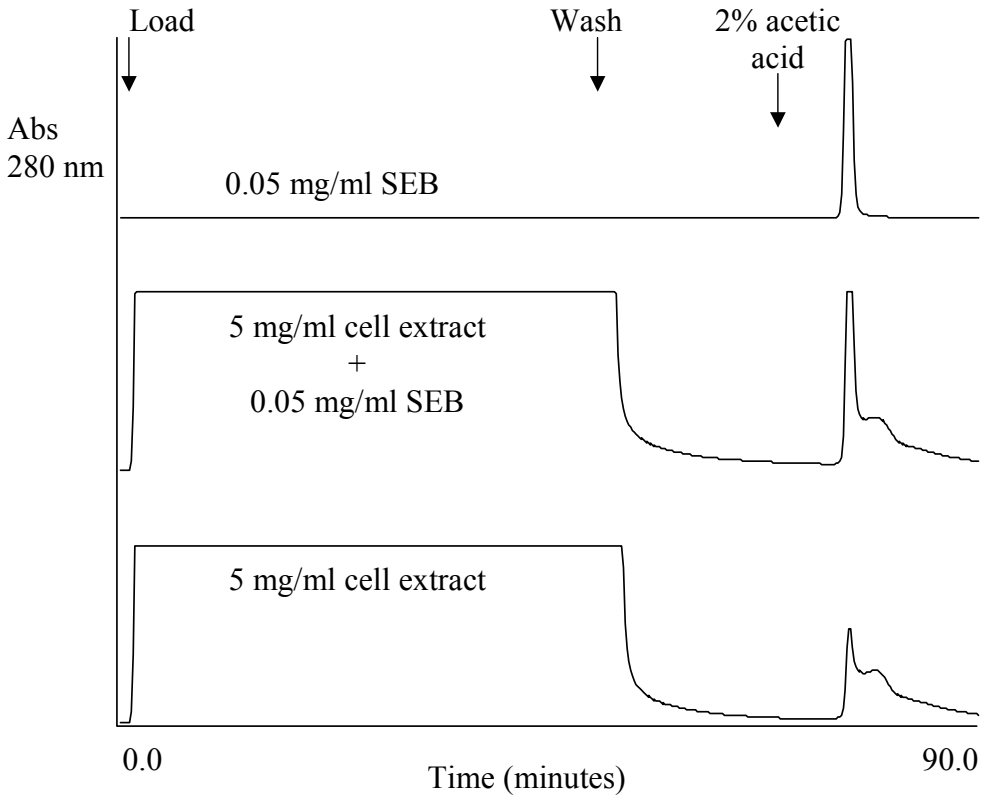
Load
Wash
2% acetic acid
Abs 280 nm
0.05 mg/ml SEB
5 mg/ml cell extract
+
0.05 mg/ml SEB
5 mg/ml cell extract
0.0
Time (minutes)
90.0

(a)

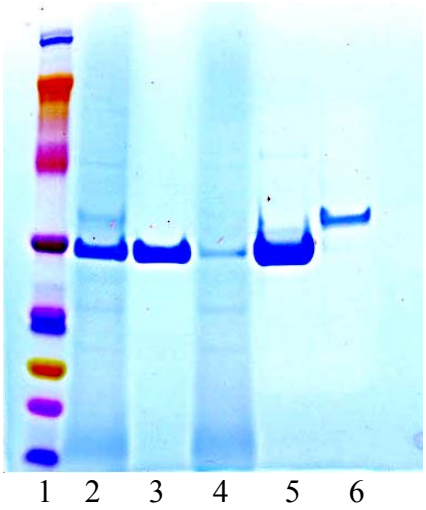
1 2 3 4 5 6

(b)

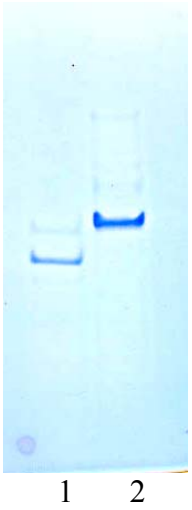
1 2

(c)

Figure 3.7 **(a)** Purification of 0.05 mg/ml SEB from 5 mg/ml *Staphylococcus aureus* fermentation broth in a 5 ml loading sample on a YYWLHH column. **(b)** SDS-PAGE of the chromatographic separation of 0.05 mg/ml SEB from 5 mg/ml fermentation broth in a 5 ml loading sample using a YYWLHH column. Lane 1 and 3 contain the molecular weight markers and SEB standard, respectively; lane 2 is the injected sample; lane 4 is the flow through sample taken midway (25 minutes) through the loading time; lane 5 and 6 correspond to eluates in the sharp and shoulder peaks of 2% acetic acid elution, respectively. **(c)** SDS-PAGE of the elution peaks after loading 5 ml of 5 mg/ml fermentation broth. Lane 1 represents the eluate in the sharp peak of the 2% acetic acid elution, and lane 2 corresponds to the shoulder peak after the same elution.

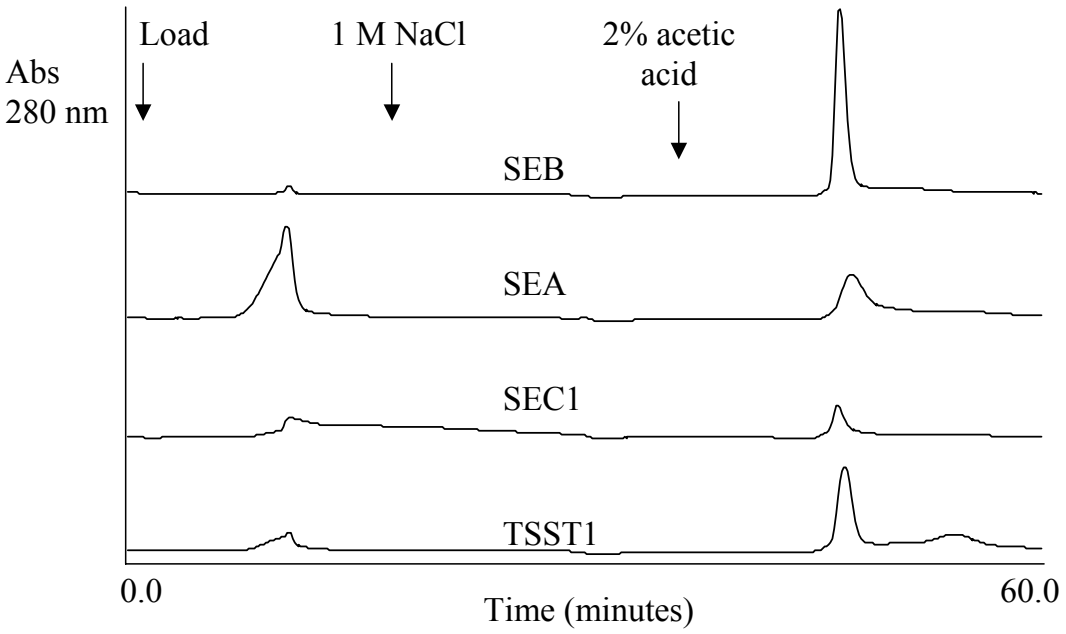

Figure 3.8 Binding of different SEs at a concentration of 0.5 mg/ml on a YYWLHH column.

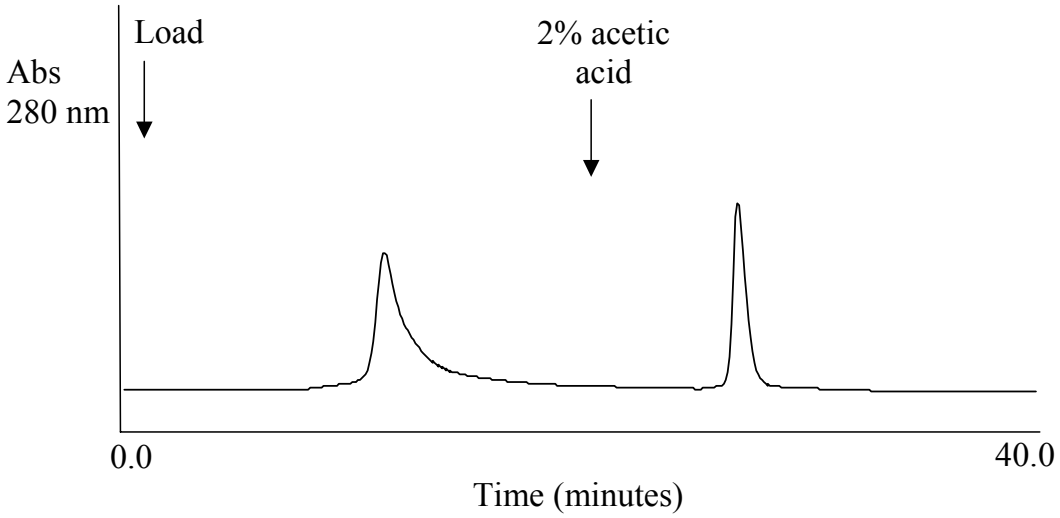
Load
2% acetic
acid
Abs
280 nm
0.0
40.0
Time (minutes)

(a)

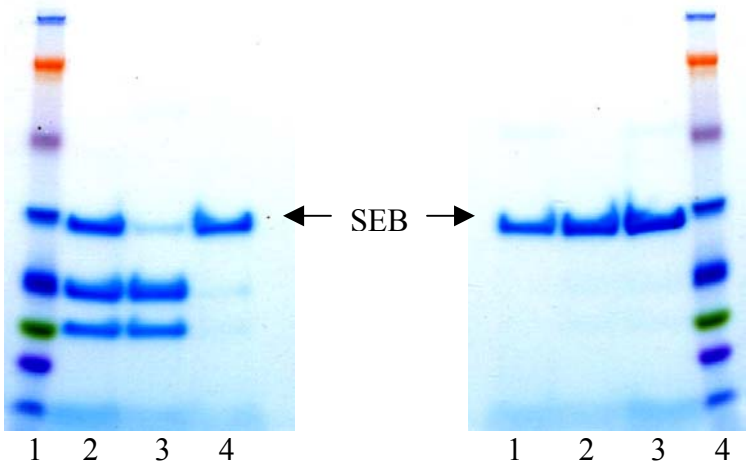
SEB
1 2 3 4
1 2 3 4

(b) **(c)**

Figure 3.9 **(a)** Separation of nicked and native SEB proteins using a YYWLHH column. **(b)** SDS-PAGE of the chromatographic separation of SEB from partially purified SEB on YYWLHH-immobilized resin with reduced samples. Lane 1 contains the molecular weight standards; lane 2 is the partially purified SEB; lane 3 is the flow through; and lane 4 is the 2% acetic acid elute. **(c)** SDS-PAGE of the chromatographic separation of SEB from partially purified SEB on YYWLHH-immobilized resin with non-reduced samples. Lane 1 is the 2% acetic acid eluate; lane 2 is the flow through; lane 3 is the partially purified SEB; and lane 4 contains the molecular weight standards.

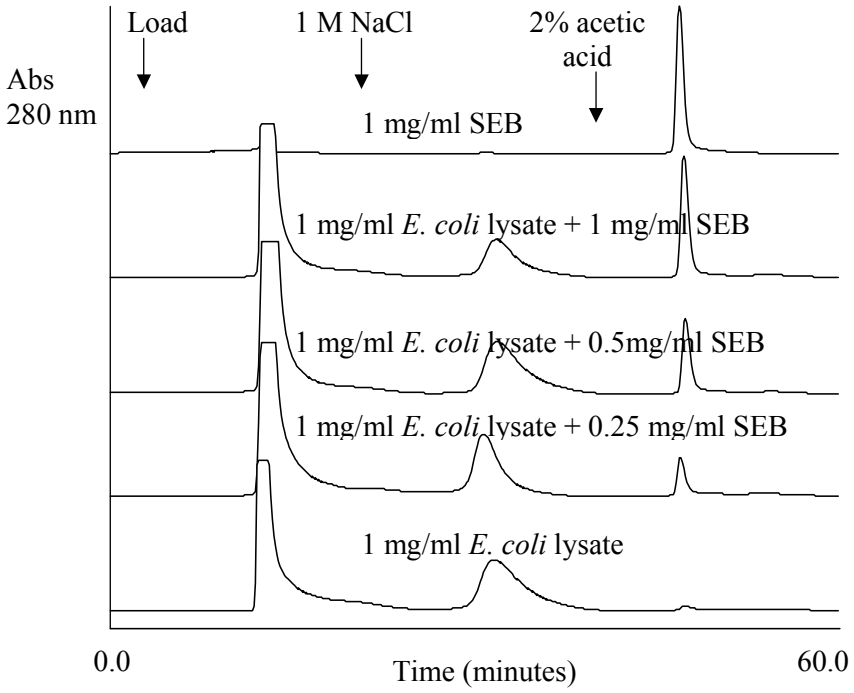

(a)

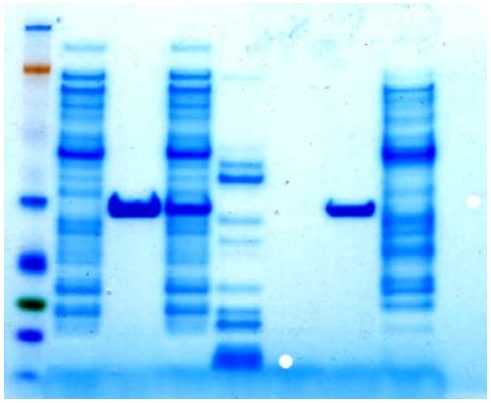

1 2 3 4 5 6 7 8

(b)

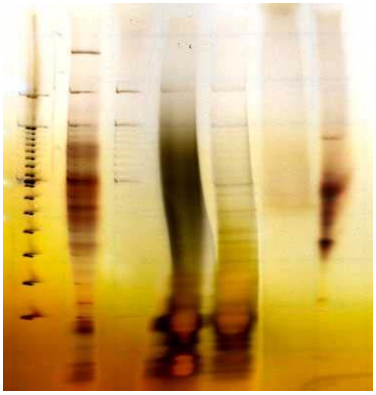

1 2 3 4 5 6 7

(c)

Figure 3.10 **(a)** Purification of various amount of SEB from 1 mg/ml *E. coli* lysate using a YYWLHH column. **(b)** SDS-PAGE of the chromatographic separation of 0.5 mg/ml SEB from 1 mg/ml *E. coli* lysate using a YYWLHH column. Lane 1, 2 and 3 contain the molecular weight markers, *E. coli* lysate, SEB standard, respectively; lane 4 is the injected sample; lane 5 is the flow through peak; lane 6 is the 1 M NaCl eluate; lane 7 and 8 correspond to eluates in the first and second peaks of 2% acetic acid elution, respectively. **(c)** Electrophoresis analysis of nucleic acids in the fractions as the same as in (b). Lanes 1 to 7 correspond to the DNA ladder, *E. coli* lysate standard, SEB standard, flow through peak, 1 M NaCl eluate, first and second peaks in 2% acetic acid elution, respectively.

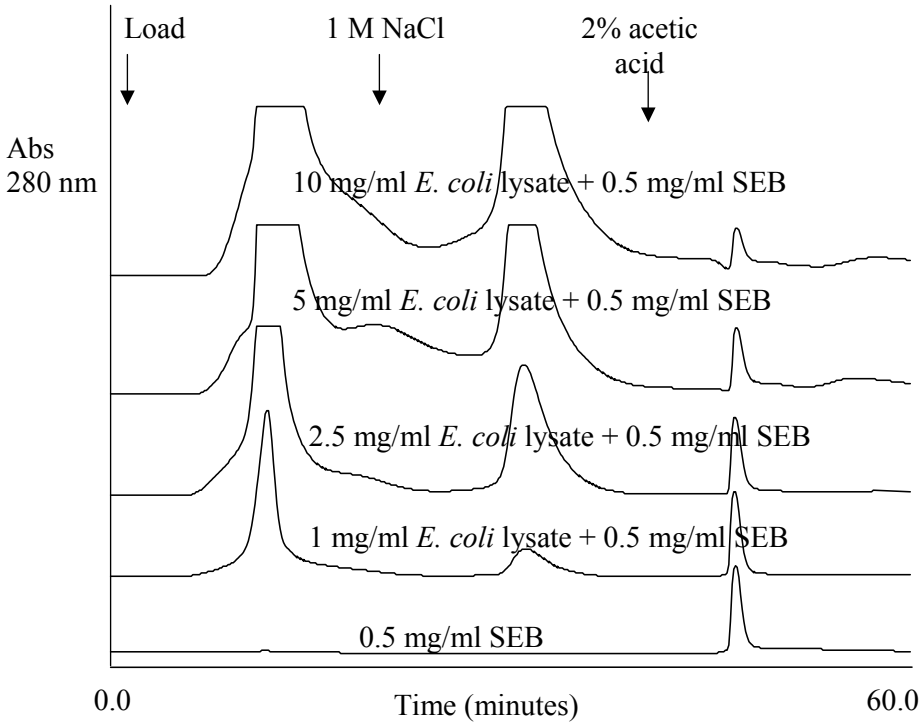
Load
1 M NaCl
2% acetic acid
Abs 280 nm
10 mg/ml E. coli lysate + 0.5 mg/ml SEB
5 mg/ml E. coli lysate + 0.5 mg/ml SEB
2.5 mg/ml E. coli lysate + 0.5 mg/ml SEB
1 mg/ml E. coli lysate + 0.5 mg/ml SEB
0.5 mg/ml SEB
0.0
Time (minutes)
60.0

(a)

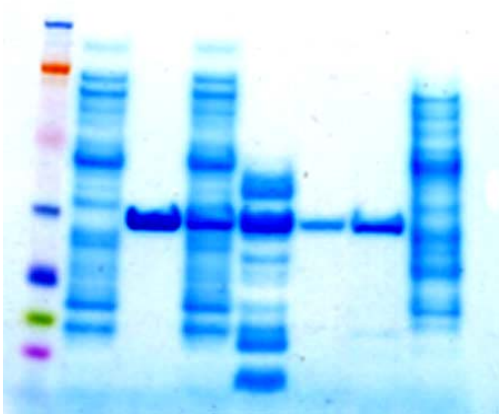
1 2 3 4 5 6 7 8

(b)

Figure 3.11 **(a)** Purification of 0.5 mg/ml SEB from various amount of *E. coli* lysate using a YYWLHH column. **(b)** SDS-PAGE of the chromatographic separation of 0.5 mg/ml SEB from 5 mg/ml *E. coli* lysate using a YYWLHH column. Lane 1, 2 and 3 contain the molecular weight markers, *E. coli* lysate, SEB standard, respectively; lane 4 is the injected sample; lane 5 is the flow through peak; lane 6 is the 1 M NaCl eluate; lane 7 and 8 correspond to eluates in the first and second peaks of 2% acetic acid elution, respectively.

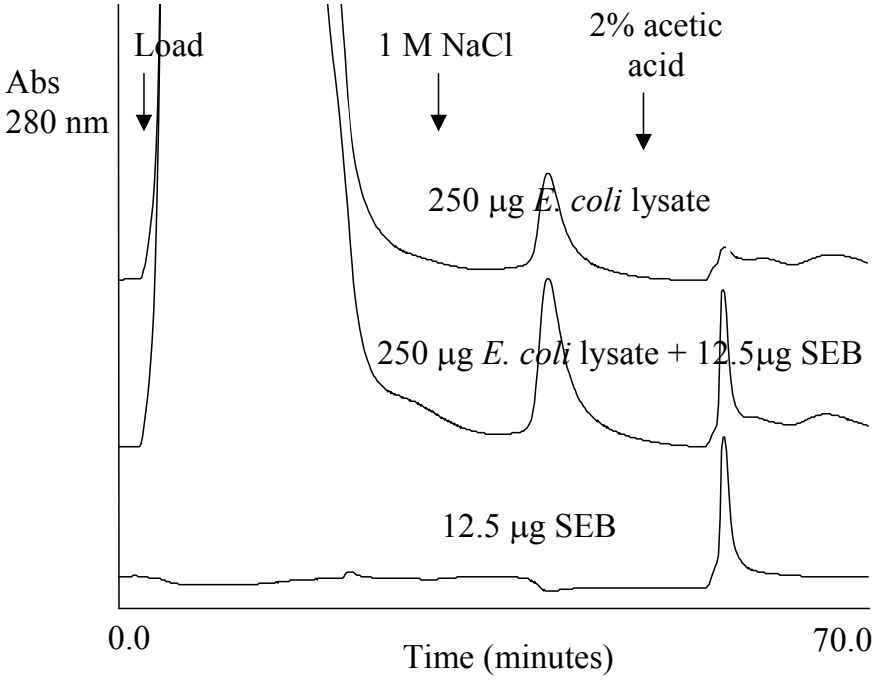
Load
1 M NaCl
2% acetic acid
Abs 280 nm
250 µg E. coli lysate
250 µg E. coli lysate + 12.5µg SEB
12.5 µg SEB
0.0
Time (minutes)
70.0

(a)

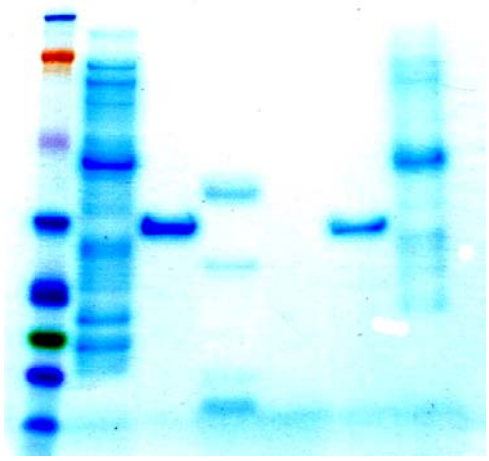
1 2 3 4 5 6 7

(b)

Figure 3.12 **(a)** Detection of SEB with/without *E. coli* lysate using a YYWLHH column. **(b)** SDS-PAGE of the chromatographic detection of SEB from the *E. coli* lysate using a YYWLHH column. Lane 1 contains the molecular weight standards; lane 2 is the *E. coli* lysate standard; lane 3 is the SEB standard; lane 4 is the flow through peak; lane 5 is the 1 M NaCl eluate; lane 6 and 7 correspond to eluates in the first and second peaks of 2% acetic acid elution, respectively.

CHAPTER 4

CHARACTERIZATION OF A PEPTIDE AFFINITY SURPPORT THAT BINDS SELECTIVELY TO STAPHYLOCOCCAL ENTEROTOXIN B (SEB)

Guangquan Wang, Ruben G. Carbonell

Department of Chemical Engineering, North Carolina State University

1017 Main Campus Drive, Centennial Campus

Partner's Building I, Suite 3200, Box 7006

Raleigh, NC 27695-7006

This is a manuscript in preparation for submission to

Journal of Chromatography A

Abstract

Peptide ligands used in affinity chromatography have shown competitive advantages over monoclonal antibodies and pseudo affinity ligands due to their high stability and selectivity for protein purification and detection. A good understanding of mass transfer kinetics and adsorption properties in peptide affinity chromatography can facilitate column design and optimization. In this article, the influences of mass transfer and adsorption-desorption kinetics on the binding of SEB to a peptide ligand, Tyr-Tyr-Trp-Leu-His-His (YYWLHH) have been studied. The mass transfer parameters for SEB adsorption were measured using pulse experiments. The adsorption isotherms of SEB on YYWLHH resin with different peptide densities were measured and described using the bi-Langmuir equation. The general rate model was used to fit experimental breakthrough curves to obtain the intrinsic rate constants of the adsorption-desorption process on the peptide ligands. An analysis on the number of transfer units found both intraparticle mass transfer and the kinetics of adsorption are rate-limiting steps. The effect of peptide density on both equilibrium (batch format) and dynamic adsorption (column format) was also investigated. The variations in dissociation constants with peptide density indicate that the binding mechanism changes from monovalent to multivalent adsorption of protein to ligand with increasing peptide density.

Keywords: mathematical modeling, peptide affinity chromatography, peptide density, Staphylococcal enterotoxin B

4.1 Introduction

Short peptides have been used as affinity ligands to purify various proteins (Amatschek et al., 2000; Bastek et al., 2000; Gurgel et al., 2001; Huang et al., 1996; Huang and Carbonell, 1995; Kaufman et al., 2002). It has been shown that short peptides are more specific than pseudo affinity ligands such as dye ligands and metal ions, and more stable than bioaffinity ligands such as antibodies (Bastek et al., 2000; Huang and Carbonell, 1995). Peptide ligands used in affinity chromatography to isolate or concentrate a target protein are generally screened from solid phase combinatorial or parallel peptide libraries, which are created on a suitable chromatographic support (Pflegerl et al., 2002). The relatively high selectivity, stability, and low cost of small peptides make them suitable as affinity ligands to purify proteins in large-scale purification processes (Huang and Carbonell, 1995). Little information is available in the literature on the role of mass transfer and adsorption-desorption kinetics in peptide affinity chromatography. Such information is important for column design and optimization. A lumped kinetic model has been employed to fit the breakthrough curves of fibrinogen that binds to a short peptide FLLVPL (Kaufman et al., 2002). However, the capacity and association constant derived from the fitting of the experimental breakthrough data with this model are inconsistent with equilibrium experiments. The use of too simple a mass transfer model might lead to erroneous descriptions of the experimental data and to misunderstandings of the fundamentals of the process involved (Kaczmarski et al., 2001). A more complete model that accounts for all

mass transfer resistances and adsorption-desorption kinetics should be used to model the breakthrough curves or zone profiles.

Another factor that is crucial for column design and optimization is the peptide density on the adsorbent. Ligand density has significant influences on the interactions between the peptide ligands and the target protein. A better understanding of these effects can help to optimize the affinity adsorption of the target protein to increase the binding efficiency. If the binding is attributed to monovalent interactions, the capacity increases with increase in ligand density, while the association constant may remain constant at low ligand density and decrease at high ligand density due to steric effects. Such an effect was seen on the binding of s-protein to YNFEVL. Thus there is an optimal density at which the peptide ligands have high capacity and an acceptable extent of steric hindrance. Small protein molecules, such as s-protein, have monovalent interactions with peptide ligands and typically show the phenomena mentioned above (Huang and Carbonell, 1995). If the binding is attributed to multivalent interactions, increasing the ligand density typically increases the capacity and association constant. This was seen in the adsorption of a large protein molecule, von Willebrand Factor (vWF), to peptide ligands on a resin surface (Huang et al., 1996). But for highly specific ligands, increasing the ligand density tends to increase the steric hindrance at the surface and makes the binding less efficient, decreasing the association constant and the ligand utilization.

Staphylococcal enterotoxin B (SEB) is a primary toxin in food poisoning, which can cause emesis as a gastrointestinal toxin. In addition, it functions as a superantigen to interact with the major histocompatibility complex class II molecules (MHCII) and T cells bearing

particular Vβ elements, triggering a massive release of T cell-derived cytokines followed by allergic and autoimmune symptoms (Balaban and Rasooly, 2000; Li et al., 1999). A short peptide ligand that selectively binds to SEB, YYWLHH, has been identified from a solid phase combinatorial peptide library (Wang et al., 2003). Mass transfer parameters and intrinsic rate constants are required for the design of a peptide affinity column that can be used to either detect or remove SEB. In this article, a description of the mass transfer and adsorption-desorption kinetics in peptide affinity chromatography is presented using SEB as a model protein. The apparent heterogeneous nature of the binding of SEB to YYWLHH resin is described by a bi-Langmuir isotherm. A complete model, the general rate (GR) model, is employed to model the breakthrough curves of SEB with mass transfer parameters determined from pulse experiments. The rate-limiting steps are determined from an analysis of the number of transfer units. Results of the GR model are compared to those of several simpler models, such as the lumped pore diffusion model (POR), the transport-dispersive model (TD), and the reaction-dispersive model (RD), helping to understand the role of each process involved in the peptide affinity chromatography. The effect of peptide density on the dissociation constant, maximum capacity, and rate constant for adsorption provides information on the mechanism of SEB adsorption to the YYWLHH support.

4.2 Theory

4.2.1 Isotherm Models

The Langmuir model has been used to fit adsorption isotherm data of proteins on peptide resins (Huang et al., 1996; Huang and Carbonell, 1995; Kaufman et al., 2002). It assumes a set of equivalent, distinguishable and independent binding sites (Guiochon et al., 1994). However, the adsorption of protein molecules onto peptide ligands might involve multi-point binding, and can be affected by non-homogeneous local peptide density distributions. As a result, a more complex isotherm equation may need to be used to provide a more accurate fit to the experimental data. For example, Bastek (2000) found that a bi-Langmuir model improved the fit of isotherms for binding α_1-proteinase inhibitor (α_1PI) to peptide resins. The bi-Langmuir model postulates two noncompetitive binding sites, a high-energy binding site and a low-energy binding site. The Langmuir and bi-Langmuir equations are written in the form,

$$Q^* = \frac{Q_m^* C}{K_d + C} \tag{4.1}$$

$$Q^* = \frac{Q_{m,1}^* C}{K_{d,1} + C} + \frac{Q_{m,2}^* C}{K_{d,2} + C} \tag{4.2}$$

where K_d and Q_m^* are the dissociation constant and the maximum capacity, respectively.

4.2.2 General Rate (GR) Model

The GR model (Gu, 1995; Guiochon et al., 1994; Kaczmarski et al., 2001) takes into account all mass transfer processes in packed bed chromatography, namely, (1) axial dispersion of the solute molecules in the bulk phase; (2) film mass transfer of the solute molecules from the bulk phase to the external surface of the adsorbent particles; (3) diffusion of the solute molecules inside the pores of these particles; and (4) rates of adsorption and desorption on the pore surface. One of the challenging tasks of the GR model is the independent determination of a relatively large number of mass transfer parameters. Due to the mathematical complexity of the GR model, only numerical solutions are available.

Although the GR model is the most realistic model, it still requires a number of assumptions: 1) the chromatographic process is isothermal; 2) the column is packed homogeneously with porous particles that are spherical and uniform in size; 3) the mobile phase velocity is constant, and there is no convection inside the pores; 4) the compressibility of the mobile phase is negligible; 5) the radial concentration gradient in the column is negligible; 6) convection and axial dispersion are the only mass transfer mechanisms in the axial direction, and the dispersion coefficient is independent of the concentration; 7) the surface of each particle is assumed to be uniform and surface diffusion within the particles is neglected. The GR model consists of the following differential equations in dimensionless form,

$$\frac{\partial c_b}{\partial \tau} - \frac{1}{Pe}\frac{\partial^2 c_b}{\partial z^2} + \frac{\partial c_b}{\partial z} + \xi\left(c_b - c_p\big|_{r=1}\right) = 0 \tag{4.3}$$

$$\left(1-\varepsilon_p\right)\frac{\partial q}{\partial \tau}+\varepsilon_p\frac{\partial c_p}{\partial \tau}-\eta\left(\frac{1}{r^2}\frac{\partial}{\partial r}\left(r^2\frac{\partial c_p}{\partial r}\right)\right)=0 \tag{4.4}$$

All dimensionless groups are defined in the nomenclature section. As demonstrated later, the isotherm data of SEB on short peptide ligands (YYWLHH) fits very well to the bi-Langmuir isotherm. Thus we assume there are two types of noncompetitive binding sites, type I and type II, and that the adsorption rate of SEB is of second order while the desorption rate is first order on each site,

$$q=q_1+q_2 \tag{4.5}$$

$$\frac{\partial q_1}{\partial \tau}=Da_1^a c_p\left(q_{m,1}-q_1\right)-Da_1^d q_1 \tag{4.6}$$

$$\frac{\partial q_2}{\partial \tau}=Da_2^a c_p\left(q_{m,2}^*-q_2\right)-Da_2^d q_2 \tag{4.7}$$

If local equilibrium holds, setting the time derivatives in equations (4.6) and (4.7) to zero results in the bi-Langmuir isotherm,

$$q_1^*=\frac{a_1 c_p}{1+b_1 c_p} \tag{4.8}$$

$$q_2^*=\frac{a_2 c_p}{1+b_2 c_p} \tag{4.9}$$

The initial conditions are

$$\tau=0,\ c_b=0;\ c_p=0;\ q=0;\ q_1=0;\ q_2=0 \tag{4.10-4.14}$$

At the entrance and exit of the column the boundary conditions are,

$$z=0,\ \frac{\partial c_b}{\partial z}=Pe_b(c_b-c_f);\ z=1,\ \frac{\partial c_b}{\partial z}=0 \tag{4.15, 4.16}$$

The boundary conditions at the particle surface are,

$$r = 0,\ \frac{\partial c_p}{\partial r} = 0;\ r = 1,\ \frac{\partial c_p}{\partial r} = Bi\left(c_b - c_p\big|_{r=1}\right) \qquad (4.17, 4.18)$$

A Matlab code was written to solve the GR model. The finite element method was used to discretize the bulk phase partial differential equation (Gu, 1995) while the orthogonal collocation method was used to discretize the pore phase partial differential equation (Finlayson, 1980; Villadsen and Michelsen, 1978). The resulting ordinary partial differential equations were solved using the built-in function *ode15s* in Matlab. The intrinsic rate constants were estimated by fitting the breakthrough curve using the built-in function lsqcurvefit in Matlab.

4.2.3 Estimation of Mass Transfer Parameters

Both the interstitial porosity (ε_b) of the column and the particle porosity (ε_p) should be determined before the estimation of mass transfer parameters. For a pulse of solute that is not retained in the column and can access all the pores in the chromatographic support, the total porosity (ε_t) is related to the first moment (μ_1) of the outlet pulse profiles (Arnold et al., 1985; Boyer and Hsu, 1992b; Natarajan and Cramer, 2000),

$$\mu_1 = \frac{\int_0^\infty C(L,t)tdt}{\int_0^\infty C(L,t)dt} = \frac{L}{u_0}\varepsilon_t \qquad (4.19)$$

where the total porosity includes contributions from both the bed and particle porosities,

$$\varepsilon_t = \varepsilon_b + (1-\varepsilon_b)\varepsilon_p \qquad (4.20)$$

A plot of μ_1 versus L/u_0 should give a straight line. The total porosity is equal to the slope of this line. If a big solute that is excluded from particle pores is used in the pulse injections, the total porosity measured in this case is only the interstitial porosity of the column (ε_b). The particle porosity can be then calculated using Eqn. (4.20).

The film mass transfer coefficient (k_f) can be estimated using the correlation of Wakao et al. (1958).

$$Sh = 2 + 1.45\,\mathrm{Re}^{1/2}\,Sc^{1/3} \tag{4.21}$$

The axial dispersion coefficient (D_b) and the intraparticle diffusion coefficient (D_p) can be determined from the height equivalent to a theoretical plate (*HETP*) under unretained conditions if the outlet pulse profile is a Gaussian peak in a pulse experiment (Arnold et al., 1985; Boyer and Hsu, 1992b; Natarajan and Cramer, 2000). In the GR model, the HETP equation for an unretained solute is related to the moments of the pulse response and the column length,

$$\begin{aligned} HETP &= \frac{\mu_2^* L}{\mu_1^2} \\ &= \frac{2\varepsilon_b D_b}{u_0} + \frac{2\varepsilon_p^2(1-\varepsilon_b)R_p^2}{15\left[\varepsilon_b + (1-\varepsilon_b)\varepsilon_p\right]^2}\left(\frac{1}{\varepsilon_p D_p} + \frac{5}{k_f R_p}\right)u_0 \end{aligned} \tag{4.22}$$

The contribution of film mass transfer to the *HETP* is calculated using the estimated film mass transfer coefficient from Eqn. (4.21),

$$HETP_f = \frac{2\varepsilon_p^2(1-\varepsilon_b)R_p u_0}{3k_f\left[\varepsilon_b + (1-\varepsilon_b)\varepsilon_p\right]^2} \tag{4.23}$$

Thus the contribution of axial dispersion and pore diffusion to the *HETP* can be found by subtracting Eqn. (4.23) from Eqn. (4.22),

$$HETP^{\#} = HETP - HETP_f$$
$$= \frac{2\varepsilon_b D_b}{u_0} + \frac{2\varepsilon_p^2 (1-\varepsilon_b) R_p^2 u_0}{15\varepsilon_p D_p \left[\varepsilon_b + (1-\varepsilon_b)\varepsilon_p\right]^2} \tag{4.24}$$

Axial dispersion involves molecular diffusion and eddy diffusion. But the contribution of molecular diffusion to axial dispersion is negligible. Thus $\frac{D_b}{u_0}$ is weakly dependent on flow velocity at low Reynolds numbers. A plot of ($HETP^{\#}$) versus u_0 in this case should give a straight line. Under these conditions, the intraparticle diffusion coefficient can be determined from the slope of this line, while the axial dispersion coefficient can be estimated from the intercept. One can compare measured values of the axial dispersion coefficient to those estimated from a widely used correlation given by (Gunn, 1987),

$$\frac{D_b}{2R_p u} = \left\{ \frac{\mathrm{Re}\, Sc}{4\alpha_1^2 (1-\varepsilon_b)} (1-p)^2 + \frac{\mathrm{Re}^2\, Sc^2}{16\alpha_1^4 (1-\varepsilon_b)^2} p(1-p)^3 \times \left[\exp\left(\frac{-4\alpha_1^2 (1-\varepsilon_b)}{p(1-p)\,\mathrm{Re}\, Sc} \right) - 1 \right] \right\}$$
$$+ \frac{\varepsilon_b}{\tau_b\, \mathrm{Re}\, Sc} \tag{4.25}$$

where

$p = 0.17 + 0.33\exp(-24/\mathrm{Re})$, $\alpha_1 = 2.405$, $\tau_b = 1.4$

4.2.4 Number of Transfer Units (NTU)

One way to determine the rate-limiting steps in a chromatography process is to calculate the number of transfer units (*NTU*) of each mass transfer and surface-binding steps. The *NTU* is related to the *HETP* by the expression (LeVan et al., 1997),

$$NTU = \frac{2L}{HETP}\left(\frac{k_i^{\#}}{1+k_i^{\#}}\right)^2 \tag{4.26}$$

where $k_i^{\#}$ is the retention factor given by $k_i^{\#} = (1-\varepsilon_b)(\varepsilon_p + K_i)/\varepsilon_b$; K_i is the equilibrium constant. In the absence of adsorption, it is equal to zero. LeVan et al. (1997) also provide an expression for the *NTU* for each step in the adsorption process,

Film mass transfer: $N_f = \frac{3(1-\varepsilon_b)k_f L}{R_p u \varepsilon_b}$ (4.27)

Pore diffusion: $N_p = \frac{15 D_p L}{R_p^2 u}\frac{\varepsilon_p(1-\varepsilon_b)}{\varepsilon_b}$ (4.28)

Axial dispersion: $N_d = \frac{uL}{D_b}$ (4.29)

Surface adsorption on site I: $N_{k,1} = \frac{k_{a,1}(1-\varepsilon_t)Q_{m,1}^{*}L}{u\varepsilon_b}$ (4.30)

Surface adsorption on site II: $N_{k,2} = \frac{k_{a,2}(1-\varepsilon_t)Q_{m,2}^{*}L}{u\varepsilon_b}$ (4.31)

The steps with the smallest number of transfer units are rate-limiting steps and therefore control the adsorption process.

4.3 Experimental

4.3.1 Synthesis of Peptide Resins

Peptides YYWLHH were synthesized directly onto Toyopearl AF Amino 650M (TA650M) resins (Tosoh Biosep, Montgomeryville, PA) using standard fluorenylmethyloxycarbonyl (Fmoc) chemistry as described by (Buettner et al., 1996). The methacrylate-based resins have an average particle size of 65 μm with a 1000 Å average pore diameter. The aminated amino resins were modified with an alanine residue prior to peptide synthesis. To control the peptide density to final substitution levels from 6 to 220 μmol peptide/g resin, a mixture of Fmoc-L-Alanine and tBoc-L-Alanine was coupled to the aminated resins as described by Buettner et al. (Buettner et al., 1997). The tBoc group was released with TFA and the free amino functionality was acetylated with acetic anhydride. No further peptide synthesis occurred at these acetylated sites. Subsequently, the Fmoc protecting groups were released with piperidine and the free L-Alanine was used to attach Fmoc-protected amino acids until the last cycle was finished.

4.3.2 Adsorption Isotherm Measurements

Adsorption isotherms were measured in a set of batch experiments at 20°C. 0.5 ml centrifugal filters with 0.45 μm Durapore membranes (Millipore, Milford, MA) were used as adsorption vessels. Resins (10 mg resins in each vessel) were equilibrated for at least one hour in 400 μl of binding buffer, 0.5M NaCl in phosphate buffer saline (PBS), pH 7.4,

purchased from Sigma Chemical (St. Louis, MO). After draining by centrifugation, 400 μl of SEB solution with concentrations ranging from 0.09 to 1.80 mg/ml in binding buffer were added to the reaction vessel and incubated by using an orbital shaker for 2 hours. The unbound SEB was collected by centrifugation and the amount of unbound SEB was determined by Micro-BCA Assay (Pierce, Rockford, IL). The amount of bound SEB was calculated by mass balance.

4.3.3 Pulse Experiments

The base resin, deprotected Fmoc-ala (acetyl) TA650M resin without peptides, cannot retain SEB (data not shown), and hence it was used to estimate the mass transfer properties of SEB. The TA650M resins were packed into a Metal-Free PEEK-Lined column (4.6mm ID × 15cm) from Alltech (Deerfield, IL) based on manufacturer's instructions (Tosoh Biosep, Montgomeryville, PA). The pulse experiments were carried out using a Waters 616 LC system (Millipore, Milford, MA) with a UV detector (Knauer, Germany) and a 50μl sample loop (Thomson, Springfield, VA). Highly purified SEB was purchased from Toxin Technology (Sarasota, FL). The concentration of SEB was set at 1.5 mg/ml in the binding buffer (PBS + 0.5 M NaCl). The flow rates were 0.1, 0.2, 0.3, 0.4, 0.5ml/min, which corresponded to superficial velocities in the column of approximately 0.01, 0.02, 0.03, 0.04, 0.05 cm/s. To account for extra-column contributions to the first moments and *HETP*, pulse injections of SEB were made under the same conditions with the column off-line. The first moment or *HETP* results with the column off-line were then subtracted from those obtained

with the column on-line. It was impossible to find a void volume marker that could be excluded from the relatively large 1000Å pore size of TA650M resin to allow measurement of the external void fraction. A column packed with HW-40C Toyopearl resin (Tosoh Biosep, Montgomeryville, PA) which has a pore size of 50Å and an average diameter of 75 μm was employed to determine the first moments using blue dextran (Sigma, St. Louis, MO). The resulting interstitial porosity was used to approximate the interstitial porosity of the column with the TA650M resin. All pulse experiments were conducted at 20°C.

The first moment was calculated numerically using exported raw data from HPLC software,

$$\mu_1 = \frac{\sum_i C(L,t_i)t_i\Delta t}{\sum_i C(L,t_i)\Delta t} \tag{4.32}$$

The *HETP* could be estimated from the moment theory from Eqn. (4.22). However, if the chromatography peak is a Gaussian peak, the *HETP* can be estimated from,

$$\begin{aligned} HETP &= \frac{\mu_2^* L}{\mu_1^2} \\ &= \frac{L}{5.54}\left(\frac{t_{w,0.5}}{t_r}\right)^2 \end{aligned} \tag{4.33}$$

where the first absolute moment (μ_1) is identical to the retention time (t_r) of the Gaussian peak, and the second central moment (μ_2^*) is proportional to square of the peak width at half-height of the Gaussian peak by a factor 1/5.54 (Horvath and Melander, 1983).

4.3.4 Construction of Breakthrough Curves

Synthesized resins were packed into a Metal-Free PEEK-Lined column (2.1mm ID × 30mm) from Alltech (Deerfield, IL) in order to minimize the amount of SEB used. The experiments to construct the breakthrough curves were carried out at 20°C using the same HPLC system described above. The column was pre-equilibrated with the binding buffer (0.5M NaCl + PBS). 0.25 mg/ml of SEB in the binding buffer was loaded into a 10 ml loop (Thomson, Springfield, VA) and delivered to the column at a flow rate of 0.1 ml/min. Samples were collected at the exit of the column and the concentration of SEB was determined by Micro-BCA assay (Pierce, Rockford, IL). The bound SEB was eluted by 2% acetic acid and then the column was regenerated with ~50 column volumes of binding buffer. The maximal capacity of the column decreased slightly after ~10 runs, but remained at least 95 percent of the original value that was obtained from the batch isotherm experiments.

4.4 Results and Discussion

4.4.1 Moment and HETP Analysis

The analysis of the first moments gives an accurate estimation of the total porosity of the column even if the elution profile is not a Gaussian peak, while the application of the HETP equation requires a Gaussian peak (Arnold et al., 1985; Boyer and Hsu, 1992b; Natarajan and Cramer, 2000). As seen in Figure 4.1, a typical chromatogram of SEB under unretained conditions exhibits only a small amount of tailing in comparison with the

Gaussian fit. As a result, there is no question that the HETP method can be used for the determination of mass transfer parameters. The total porosity of the column was determined to be 0.787 from the slope of the first moment plot shown in Figure 4.2(a). Because the pore size of Toyopearl resins (1000 Å) is big enough to hold molecules up to 5M Da in size, the widely used void volume marker, blue dextran (Mw 2M Da), cannot be used to determine the interstitial porosity of such a column. Alternatively, a size-exclusion Toyopearl resin, HW-40C, which has the same backbone polymer and a similar particle size but much smaller pore size (50 Å) than the TA650M resin, was packed into a same column. The void fraction (interstitial porosity) of the column was determined to be 0.29 from the first moment analysis using blue dextran in pulse injections (Figure 4.2(a)). The particle porosity was then calculated to be 0.70 by Eqn. (4.20). The interstitial porosity (0.29) is slightly lower than with other polymer beads with similar particle size, such as agorose and sepharose beads, which lead to interstitial porosity in the range of 0.3~0.4 in well-packed columns (Boyer and Hsu, 1992a; Boyer and Hsu, 1992b; Natarajan and Cramer, 2000). Although the void fraction of a column packed with TA650M resin cannot be measured directly, as pointed out by Kaczmarski et al. (2001), any error made in its estimate has a small influence on the frontal or zone spreading analysis. Having the porosities and film mass transfer coefficient calculated from Eqn. (4.21), the axial dispersion coefficient and intraparticle diffusion coefficient were ready to be determined from the intercept and slope of the HETP line in Figure 4.2(b). The estimated intraparticle diffusion coefficient of SEB is $4.83\times10^{-11}m^2/s$. Compared to the molecular diffusivity (D_m) of SEB ($7.70\times10^{-11}m^2/s$) (Wagman et al., 1965), the diffusion of SEB inside the pores of TA650M resins is not restricted as much as other

proteins with similar size to SEB in agarose matrix (Boyer and Hsu, 1992a). This is mainly because the large pore size of TA650M resins reduces the pore diffusion resistance. The intraparticle diffusion coefficient is related to molecular diffusivity by the particle tortuosity factor (τ_p):

$$D_p = \frac{D_m}{\tau_p} \tag{4.34}$$

Because the intraparticle diffusion coefficient has been measured using pulse experiments, the tortuosity is calculated to be 1.6 in the TA650M resin using Eqn (4.34). There are several empirical equations for the particle tortuosity in the literature (Guiochon et al., 1994; Suzuki and Smith, 1972; Wakao and Smith, 1962). The expression developed by Wakao and Smith (1962) can be used to estimate the particle tortuosity and then the intraparticle diffusion coefficient in the TA650M resin,

$$\tau_p = \frac{1}{\varepsilon_p} \tag{4.35}$$

With ε_p=0.70, this gives a tortuosity of 1.4, very close to the measured value. The value of the axial dispersion coefficient estimated from the HETP method (1.43×10^{-7} m^2/s) is also very close to that obtained from Gunn's correlation (1.42×10^{-7} m^2/s) (Eqn. (4.25)).

The GR model using the estimated parameters was used to fit SEB pulses elution peak and breakthrough curves at the end of the column under unretained conditions. Because there is no protein bound to the stationary phase, the spreading of the pulses or breakthrough curves are only due to mass transfer effects. As seen in Figure 4.3, the simulations fit the experimental data well indicating that proper mass transfer parameters have been obtained.

Due to extra-column effects, the experimental data show a little more spreading than the simulations.

4.4.2 Equilibrium and Dynamic Studies of SEB Adsorption

The equilibrium and dynamic behavior of SEB binding to the peptide (YYWLHH) resin were thoroughly studied at a peptide density of 100μmol/g. Accurate isotherm constants are critical to the accuracy of model calculations. Both the Langmuir equation and the bi-Langmuir equation fit the isotherm data well although the bi-Langmuir fit is better than the Langmuir fit. Figure 4.4 shows the bi-Langmuir fit to the experimental data. The dissociation constants (K_d) and maximum capacities (Q_m^*) in the bi-Langmuir equation are listed in Table 4.1. There are two apparent binding sites for SEB on the resins, a high affinity binding site and a low affinity binding site. The total maximum SEB binding capacity of the resins is approximately 42.92 mg/g ($Q_{m,1}^* + Q_{m,2}^*$). A monolayer of protein adsorbs at a density of approximately 2 mg/m^2. The internal surface area of the pores of the Toyopearl particles is approximately 30 m^2/g (Kaufman et al., 2002), so the maximum SEB binding capacity is indicative of coverage of one monolayer or less. We can formulate two rate equations using bi-Langmuir kinetics, one is for the adsorption-desorption process on the high-energy binding site (type I site, Eqn (4.6)), the other is for the adsorption-desorption process on the low-energy binding site (type II site, Eqn (4.7)). These are used to model the breakthrough curves under adsorptive conditions.

The GR model was used to study the dynamic adsorption of SEB on YYWLHH in a fixed bed. In order to reduce the amount of toxin used, a small column with dimensions of 2.1mm (ID) × 30mm was used. The interstitial porosity and particle porosity of this small column were checked to make sure they are the same as in the column for the estimation of mass transfer parameters. Table 4.1 lists the geometrical, fluid flow, and mass transfer and isotherm parameters employed in the GR model at a flow rate of 0.1 ml/min. As shown in Figure 4.5 (a), the GR model fits the experimental results well. The values of the adsorption rate constants ($k_{a,1}$, $k_{a,2}$) were estimated using a nonlinear least-squares regression to the experimental breakthrough curve. The adsorption rate constant on the type II sites ($k_{a,2}$) is at least 10 times smaller than the adsorption rate constant on the type I sites ($k_{a,1}$). The desorption rate constants ($k_{d,1}$, $k_{d,2}$) were calculated using the equation,

$$k_d = K_d k_a \tag{4.36}$$

The analysis of number of transfer units (NTU) described in the theory section give the relative contributions of mass transfer steps and intrinsic adsorption rates. As shown in Table 4.1, the NTU of axial dispersion is significantly larger than the others. Thus axial dispersion is the fastest step and hence has little influence on the adsorption rate. If axial dispersion is neglected, that is, setting the Peclet number (Pe) to be infinite in the GR model, the simulation is almost unchanged (Figure 4.5 (a)). Other NTUs have similar values so that several steps limit the adsorption rate of SEB on YYWLHH in a fixed bed, primarily intraparticle mass transfer and adsorption-desorption rates. As seen in Figure 4.5 (a), if we assume local equilibrium holds, that is, setting the Damkolher number (Da^a) to be infinite in

the GR model, the simulation cannot match the experimental data. Thus our results confirm previous findings that the adsorption-desorption rates involve a slow process in affinity chromatography for proteins (Liapis, 1989; Liapis, 1990). The breakthrough curves also can be predicted properly by the GR model at different flow rates (Figure 4.5 (b)) and inlet concentrations of SEB (Figure 4.5 (c)). The film mass transfer coefficient and axial dispersion coefficient are related to the flow velocity, and they were adjusted based on Eqn. (4.21) and (4.25) respectively for different flow velocities. The intraparticle diffusion coefficient and rate constants remain the same in those simulations.

Several simple models including the lumped pore diffusion (POR) model, transport-dispersive (TD) model and reaction-dispersive (RD) model have been compared to the GR model. The formulation of these models is in the Appendix. The POR model considers all mass transfer effects like the GR model but greatly reduces the mathematical complexity. If the intraparticle diffusion coefficient is not too small, the POR model could give a prediction that is as good as the GR model (Kaczmarski et al., 2001). As seen in Figure 4.6 (a), the results of the POR model considering proper adsorption-desorption kinetics are almost identical to those of the GR model and provide a good fit to the experimental breakthrough curve. If we assume local equilibrium exists, which is a general assumption in ion-exchange and reverse phase chromatography, the simulated breakthrough curve becomes steeper leading to mismatch with the experimental data. The TD model with solid film driving force fails to model the breakthrough curve because it cannot take into account properly the adsorption-desorption kinetics, which is one of the rate-limiting steps (Figure 4.6 (b)). The failure of the RD model shown in Figure 4.6 (c) is because it neglects film mass transfer and

pore diffusion. The RD model might be improved using the lumped rate constants (Eqn. (4-A32)) that include film mass transfer and intraparticle diffusion coefficient in addition to the intrinsic rate constants (Boyer and Hsu, 1992b). As seen in Figure 4.6 (c), the lumped adsorption rate constants are too small so that the simulation deviates from the experimental data. This indicates that the influences of the film mass transfer and pore diffusion are comparable to those of the adsorption-desorption rates. The RD model is best to model chromatographic process in which intrinsic adsorption-desorption kinetics are the only rate-limiting step, the RD model with the lumped rate parameters breaks down here. The success of the GR and POR models and the failure of the TD and RD models further confirm the conclusion from the NTU analysis, that is, both film and intraparticle mass transfer and surface adsorption-desorption rates are rate-limiting.

4.4.3 Effect of Peptide Density on SEB Adsorption

The measured adsorption isotherms at different peptide densities are shown in Figure 4.7. Each isotherm was fitted to both the bi-Langmuir (Figure 4.7 (a)) and the Langmuir equation (Figure 4.7(b)) by nonlinear least-squares regressions. The results of dissociation constants (K_d) and maximum capacities (Q_m^*) are listed in Table 4.2. As seen in Figure 4.7, the bi-Langmuir equation fits the equilibrium data ($R^2 \geq 0.99$) better than the Langmuir equation ($R^2 \approx 0.96$) especially at high concentrations of SEB.

The effects of peptide density on dissociation constant and maximum capacity can be seen in Figure 4.8. As seen in Figure 4.8 (a), the dissociation constants either from the bi-

Langmuir equation or the Langmuir equation increase first, then decrease to reach a nearly constant value with increasing peptide density. This indicates the binding affinity of SEB on peptide ligands is high at very low peptide density, and then decreases with increasing density, followed by another decrease at high peptide density. Except for a dramatic drop when the peptide density increases from 6 μmol/g to 9 μmol/g, the maximum capacity increases with increases in the peptide density as might be expected (Figure 4.8 (b)). As shown in Figure 4.8 (b), the total maximum capacity of each resin is less than 50 mg/g, indicating the coverage of SEB on the surface of TA650M resin is a monolayer. An SEB molecule has the shape of an ellipsoid with dimensions of 50 Å ×45 Å ×34 Å (Papageorgiou et al., 1998). It covers an area of approximately 1415 $Å^2$. Using this information, the number of peptides covered by one SEB molecule at different peptide densities was calculated (Table 4.3). At low peptide density, the interactions between SEB molecules and peptides are approximately monovalent and are probably bio-specific. Increases in ligand density from low values apparently introduce steric hindrances so that the affinity of the ligands tends to decrease and hence the dissociation constant increases. After the peptide density reaches a certain level, the adsorption mechanism may switch to multivalent interactions from monovalent interactions. The multivalent interaction is a combination of specific and nonspecific interactions between the protein and several peptides. In this case, the interactions between SEB molecules and peptides are strengthened and hence the dissociation constant decreases with increasing ligand density. The transition of the binding mechanism can also explain the variation in the maximum capacity with peptide density. For single point and bio-specific binding, the increase in peptide density introduces more steric

hindrances for SEB binding, and therefore causes the maximum capacity to decrease. If the binding mechanism switches to multipoint binding, the maximum capacity typically increases with increase in peptide density. The transition zone of peptide density in which SEB undergoes from monovalent binding to multivalent binding is located from 9 to 20 μmol/g as shown in Figure 4.8.

The dynamic behavior of SEB binding to YYWLHH with different peptide densities was studied using frontal chromatography. The breakthrough curves are shown in Figure 4.9. The GR model was used to fit all these curves using both the bi-Langmuir and the Langmuir kinetics. It is shown that the bi-Langmuir kinetics provides a better fit to the breakthrough curve than the Langmuir kinetics. As shown previously, the adsorption rate constants were obtained using a nonlinear least-squares regression to fit the breakthrough curve, and the desorption rate constants were calculated by Eqn. (4.36). All the rate constants at different peptide densities are listed in Table 4.4. In comparison with Table 4.2, it can be seen that smaller dissociation constants, which indicate higher affinity, are associated with larger adsorption rate constants. The bi-Langmuir kinetics results show a larger variation of adsorption rate constants than desorption rate constants with increases in peptide density on the type I binding sites, while contrary results were obtained on the type II binding sites. Namely, the adsorption rate constants (k_a) seem more sensitive to the peptide density than the desorption rate constants on the type I binding sites, while the contrary is true on the type II binding sites. These results indicate different binding mechanisms on these two kinds of binding sites. At high ligand density, the desorption constant tends to be

small indicating the contribution from strong nonspecific interactions may denature the protein so as to make the elution more difficult.

The relative contributions of mass transfer and intrinsic adsorption rates were also investigated at different peptide densities. The number of transfer units for each mass transfer step and intrinsic adsorption rates were calculated by Eqn. (4.27~4.31). As shown in Table 4.5, whether a bi-Langmuir or Langmuir isotherm is used, the intrinsic adsorption step always has the smallest number of transfer units. Therefore, SEB adsorption on YYWLHH with various peptide densities from 6~220 μmol/g is adsorption-rate limited. But film mass transfer and pore diffusion need to be properly considered because their numbers of transfer units are not large enough to be neglected.

4.5 Conclusions

The mass transfer rates and intrinsic adsorption-desorption kinetics of SEB adsorption on YYWLHH attached on TA650M resins at a ligand density of 100 μmol/g have been evaluated. The HETP equation for pulses under unretained conditions were used for the estimation of mass transfer parameters. It has been found that the SEB diffusion in TA650M resins is moderately restricted due to the large pore size of TA650M resins. A better fit to the equilibrium experimental data using the bi-Langmuir equation than the Langmuir equation indicates that the adsorption of SEB to the YYWLHH resin is heterogeneous. The GR model using the estimated mass transfer parameters was subsequently used to fit the dynamic breakthrough curves to obtain rate constants using a nonlinear least-squares

regression. An analysis of number of transfer units revealed that film mass transfer and pore diffusion and intrinsic adsorption are rate-limiting steps. In comparison with the GR model, the application of simple models, such as POR model, TD model and RD model, further confirmed this point.

The same methodology was used for peptide ligands at different densities. An analysis of the dissociation constant and maximum capacity suggested that a bio-specific interaction at low peptide density might switch to a combination of specific and nonspecific interactions between SEB molecules and peptide ligands with increases in ligand density. The breakthrough curves at different peptide densities were well predicted by the GR model. It was found that the intrinsic adsorption has the smallest number of transfer units for all peptide densities, indicating intrinsic adsorption is the slowest process, with film and intraparticle diffusion also contributing to rate limitations.

4.6 Acknowledgement

The authors would like to thank Dr. Patrick V. Gurgel for the helpful discussions on the effects of peptide density on protein adsorption.

4.7 Nomenclature

a	Parameters in the dimensionless Langmuir isotherm, Q_m^*/K_d
b	Parameters in the dimensionless Langmuir isotherm, C_0/K_d

Bi	Biot number, $k_f R_p/(\varepsilon_p D_p)$
C_0	Feed concentration
C_b	Concentration in the bulk phase
c_b	Dimensionless concentration in the bulk phase, C_b/C_0
C_p	Concentration in the stagnant fluid phase inside the particle pores
c_p	Dimensionless concentration in the stagnant fluid phase inside the particle pores, C_p/C_0
$\overline{C_p}$	Average concentration in the stagnant fluid phase inside the particle pores
$\overline{c_p}$	Dimensionless average concentration in the stagnant fluid phase inside the particle pores, $\overline{C_p}/C_0$
D_b	Axial dispersion coefficient
D_m	Molecular diffusion coefficient
D_p	Intraparticle diffusion coefficient, D_m/τ_p
Da^a	Damkolher number for adsorption, Lk_aC_0/u
Da^d	Damkolher number for desorption, Lk_d/u
F	Phase ratio, $(1-\varepsilon_t)/\varepsilon_t$
$HETP$	Height equivalent to a theoretical plate
K	Slope of isotherm chord
K_i	Equilibrium constant
K_d	Dissociation constant
k_a	Adsorption rate constant

k_{al}	Lumped adsorption rate constant
k_d	Desorption rate constant
k_i	Internal mass transfer coefficient
$k_i^{\#}$	Retention factor
k_f	Film mass transfer coefficient
k_m	Overall mass transfer coefficient in the TD model
k_t	Lumped mass transfer coefficient in the POR model
L	Column length
Mw	Molecular weight of SEB
N_d	Number of transfer units for the axial dispersion
N_f	Number of transfer units for the film mass transfer
N_k	Number of transfer units for the adsorption kinetics
N_p	Number of transfer units for the pore diffusion
p	Parameter in Gunn correlation
Pe	Peclet number in the GR model and the POR model, uL/D_b
$Pe^{\#}$	Peclet number in the TD model and the RD model, u_tL/D_b
Q	Concentration in the solid phase (based on unit volume of particle skeleton)
q	Dimensionless concentration in the solid phase, Q/C_0
Q_m^*	Adsorption saturation capacity (based on unit volume of particle skeleton)
q_m^*	Dimensionless adsorption saturation capacity, Q_m^*/C_0

$\overline{Q}$	Average concentration in the solid phase
$\overline{q}$	Dimensionless average concentration in the solid phase, $\overline{Q}/C_0$
R	Radial coordinate
r	Dimensionless radial coordinate, R/R_p
R_p	Particle radius
R_c	Column radius
r_s	Separation factor
Re	Reynolds number, $2R_p\rho u\varepsilon_b/\mu$
Sc	Schmidt number, $\mu/(\rho D_m)$
Sh	Sherwood number, $k_f(2R_p)/D_m$
St	Stanton number in the GR model, $3k_f L/(R_p u)$
$St^{\#}$	Stanton number in the POR model, $3k_t L/(R_p u)$
$St^{\#\#}$	Stanton number in the TD model, $k_m L/u_t$
t	Time
t_r	Retention time
$t_{w,0.5}$	Width at half-height of a peak
u	Interstitial velocity, u_0/ε_b
u_0	Superficial velocity
u_t	Chromatographic velocity, u_0/ε_t
Z	Axial coordinate
z	Dimensionless axial coordinate, Z/L

Greek Letters

α_1	First root of the zero-order Bessel function
ε_b	Interstitial porosity
ε_p	Particle porosity
ε_t	Total porosity
η	Dimensionless constant, $St/(3Bi)$
μ	Mobile phase viscosity
μ_1	First absolute moment of peak
μ_2	Second central moment of peak
ρ	Mobile phase density
τ	Dimensionless time, tu/L
τ_b	Column tortuosity
τ_p	Particle tortuosity
ξ	Dimensionless constant, $(1-\varepsilon_b)St/\varepsilon_b$
$\xi^{\#}$	Dimensionless constant, $(1-\varepsilon_b)St^{\#}/\varepsilon_b$

Subscripts

1, 2	Type I binding sites, type II binding sites

Superscripts

*	Equilibrium value

4.8 References

Amatschek K, Necina R, Hahn R, Schallaun E, Schwinn H, Josic D, Jungbauer A. 2000. Affinity chromatography of human blood coagulation factor VIII on monoliths with peptides from a combinatorial library. J High Resol Chromatogr 23:47-58.

Arnold FH, Blanch HW, Wilke CR. 1985. Analysis of affinity separations II: The characterization of affinity columns by pulse techniques. Chem Eng J 30:B25-B36.

Balaban N, Rasooly A. 2000. Review: Staphylococcal enterotoxins. Int J Food Microbiol 61:1-10.

Bastek PD. 2000. Purification of alpha-1-proteinase inhibitor using ligands from combinatorial peptide libraries [Doctoral dissertation]. Raleigh, NC: North Carolina State University.

Bastek PD, Land JM, Baumbach GA, Hammond DH, Carbonell RG. 2000. Discovery of Alpha-1-proteinase inhibitor binding peptides from the screening of a solid phase combinatorial peptide library. Separation Sci Technol 35:1681-1706.

Boyer PM, Hsu JT. 1992a. Effects of ligand concentration on protein adsorption in dye-ligand adsorbents. Chem Eng Sci 47:241-251.

Boyer PM, Hsu JT. 1992b. Experimental studies of restricted protein diffusion in an agrose matrix. AIChE J 38:259-272.

Buettner JA, Dadd CA, Baumbach GA, Hammond DJ; 1997. Fibrinogen binding peptides. U.S. patent 5,723,579.

Buettner JA, Dadd CA, Baumbach GA, Masecar BL, Hammond DJ. 1996. Chemically derived peptide libraries: A new resin and methodology for lead identification. Int J Peptide Protein Res 47:70-83.

Finlayson BA. 1980. Nonlinear analysis in chemical engineering. New York: McGraw-Hill.

Glueckauf E. 1955. Theory of chromatography. X. Formulas for diffusion into spheres and their application to chromatography. Trans Faraday Soc 51:1540-1551.

Gu T. 1995. Mathematical modeling and scale-up of liquid chromatography. New York: Springer.

Guiochon G, Shirazi SG, Katti AM. 1994. Fundamentals of preparative and nonlinear chromatography. New York: Academic Press.

Gunn DJ. 1987. Axial and radial dispersion in fixed beds. Chem Eng Sci 42:363-373.

Gurgel PV, Carbonell RG, Swaisgood HE. 2001. Fractionation of whey proteins with a hexapeptide ligand affinity resin. Bioseparation 9:385-392.

Horvath C, Melander WR. 1983. Theory of chromatography. In: Heftmann E, editor. Chromatography, Part A. Amsterdam: Elsevier. p A28-A135.

Huang PY, Baumbach GA, Dadd CA, Buettner JA, Masecar BL, Hentsch M, Hammond DJ, Carbonell RG. 1996. Affinity purification of von Willebrand Factor using ligands derived from peptide libraries. Bioorg Med Chem 4:699-708.

Huang PY, Carbonell RG. 1995. Affinity purification of proteins using ligands derived from peptide libraries. Biotechnol Bioeng 47:288-297.

Kaczmarski K, Antos D, Sajonz H, Sajonz P, Guiochon G. 2001. Comparative modeling of breakthrough curves of bovine serum albumin in anion-exchange chromatography. J Chromatogr A 925:1-17.

Kaufman DB, Hentsch ME, Baumbach GA, Buettner JA, Dadd CA, Huang PY, Hammond DJ, Carbonell RG. 2002. Affinity purification of fibrinogen using a ligand from a peptide library. Biotechnol Bioeng 77:278-289.

LeVan MD, Carta G, Yon CM. 1997. Adsorption and ion exchange. In: Perry RH, Green DW, editors. Chemical Engineer's Handbook. New York: MacGraw-Hill.

Li H, Llera A, Malchiodi EL, Mariuzza RA. 1999. The structural basis of T cell activation by superantigens. Annu Rev Immunol 17:435-466.

Liapis AI. 1989. Theoretical aspects of affinity chromatography. J Biotechnol 11:143-160.

Liapis AI. 1990. Modeling affinity chromatography. Sep Purif Methods 19:133-210.

Liu X, Kaczmarski K, Cavazzini A, Szabelski P, Zhou D, Guiochon G. 2002. Modeling of preparative reversed-phase HPLC of insulin. Biotechnol Prog 18:796-806.

Miyabe K, Guiochon G. 1999. Kinetic study of the concentration dependence of the mass transfer rate coefficient in anion-exchange chromatography of bovine serum albumin. Biotechnol Prog 15:740-752.

Morbidelli M, Servida A, Storti G, Carra S. 1982. Simulation of multicomponent adsorption beds. Model analysis and numerical solution. Ind Eng Chem Fundam 21:123-131.

Morbidelli M, Storti G, Carra S. 1984. Study of a separation process through adsorption of molecular sieves. Chem Eng Sci 39:383-393.

Natarajan V, Cramer SM. 2000. A methodology for the characterization of ion-exchange resins. Separation Sci Technol 35:1719-1742.

Papageorgiou AC, Tranter HS, Acharya KR. 1998. Crystal structure of microbial superantigen staphylococcal enterotoxin B at 1.5Å resolution: Implications for superantigen recognition by MHC class II molecules and T -cell receptors. J Mol Biol 277:61-79.

Pflegerl K, Podgornik A, Berger E, Jungbauer A. 2002. Screening for peptide affinity ligands on CIM monoliths. Biotechnol Bioeng 79:733-740.

Suzuki M, Smith JM. 1972. Axial dispersion in beds of small particles. Chem Eng J 3:256-264.

Villadsen J, Michelsen ML. 1978. Solutions of differential equation models by polynomial approximation. Englewood Cliff: Prentice Hall.

Wagman J, Edwards RC, Schantz EJ. 1965. Molecular size, homogeneity, and hydrodynamic properties of purified staphylococcal enterotoxin B. Biochemistry 4:1017-1023.

Wakao N, Oshima T, Yagi S. 1958. Mass transfer from packed beds of particles to a fluid. Kagaku Kogaku 22:780-785.

Wakao N, Smith JM. 1962. Diffusion in catalyst pellets. Chem Eng Sci 17:825-834.

Wang G, De J, Schoeniger JS, Roe DC, Carbonell RG. 2003. A hexamer peptide ligand that binds selectively to staphylococcal enterotoxin B (SEB): Isolation from a solid phase combinatorial peptide library. Chapter 3.

Yu Q, Wang N-HL. 1989. Computer simulations of the dynamics of multicomponent ion exchange and adsorption in fixed beds - gradient-directed moving finite element method. Computers Chem Eng 13:915-926.

Zhou D, Liu X, Kaczmarski K, Felinger A, Guiochon G. 2003. Prediction of band profiles of mixtures of Bradykinin and Kallidin from data acquired by competitive frontal analysis. Biotechnol Prog 19(3):945-954.

4.9 Appendix I: Numerical Techniques

Only numerical solutions are available for the GR model for nonlinear chromatography. The most efficient choice to discretize the bulk phase partial differential equation (PDE) is either the Galerkin finite element method (Gu, 1995) or orthogonal collocation on finite elements (Yu and Wang, 1989). Both of them deal well with stiff systems. For the pore phase governing equation, orthogonal collocation is an accurate, efficient and simple method for discretization (Gu, 1995; Yu and Wang, 1989). In this work we used the finite element method to discretize the bulk phase PDE and the orthogonal collocation method to discretize the pore phase PDE. Since the finite element method (Gu, 1995) and orthogonal collocation method (Finlayson, 1980; Villadsen and Michelsen, 1978) are discussed in length in the literature, only a brief description is given here.

4.9.1 Finite Element Method in the Bulk Phase

The first step is to derive the weak form of this problem. The weak form is defined as the weighting integral of the differential equation over the region of integration. We multiply a testing function *v(z)* to both sides of the bulk phase PDE and integrate from 0 to 1 to get

$$\int_0^1 v\left[\frac{\partial c_b}{\partial \tau}-\frac{1}{Pe_b}\frac{\partial^2 c_b}{\partial z^2}+\frac{\partial c_b}{\partial z}+\xi\left(c_b-c_p\big|_{r=1}\right)\right]dz=0 \qquad \text{(4-A1)}$$

Using integration by parts, this results in,

$$\int_0^1 v\frac{\partial c_b}{\partial \tau}dz+\int_0^1\frac{1}{Pe_b}\frac{\partial c_b}{\partial z}\frac{\partial v}{\partial z}dz-\frac{1}{Pe_b}v\frac{\partial c_b}{\partial z}\Big|_0^1+\int_0^1\left(v\frac{\partial c_b}{\partial z}+\xi v c_b\right)dz=\int_0^1\xi v c_p\big|_{r=1}dz \qquad \text{(4-A2)}$$

Substituting the boundary conditions at $z = 0$ and $z = 1$ and rearranging the equation results in the weak form,

$$\int_0^1 v\frac{\partial c_b}{\partial \tau}dz + (vc_b)\Big|_{z=0} + \int_0^1\left(\frac{1}{Pe_b}\frac{\partial c_b}{\partial z}\frac{\partial v}{\partial z} + v\frac{\partial c_b}{\partial z} + \xi v c_b\right)dz = \int_0^1 \xi v c_p\Big|_{r=1}dz + v\Big|_{z=0} \tag{4-A3}$$

Next a triangulation (interval) over the integration space [0, 1] is generated. Usually a uniform Cartesian grid is used to get the intervals. An interval is also called a finite element. The finite element method uses continuous piecewise lower order (linear, quadratic or cubic) interpolation polynomials as base functions over the triangulation. The finite element solution can be written as

$$c_b = \sum_{m=1}^{n_f} c_{bi,m}(\tau)\phi_m(z) \tag{4-A4}$$

where $\phi_m(z)$ are the base functions. The dimension of the finite element space (n_f) is related to the number of the elements (n_e) and the type of the base function used. We choose the testing function v equal to the base functions, that is

$$v = \phi_n,\ n = 1, 2, \ldots, n_f \tag{4-A5}$$

Substitution of c_b and v into the weak form gives the following equation,

$$\begin{aligned}\sum_{m=1}^{n_f}\left(\frac{\partial c_{bi,m}}{\partial \tau}\int_0^1 \phi_m\phi_n dz\right) + \sum_{m=1}^{n_f}\left\{c_{bi,m}\left[\int_0^1\left(\frac{1}{Pe_b}\frac{\partial \phi_m}{\partial z}\frac{\partial \phi_n}{\partial z} + \phi_n\frac{\partial \phi_m}{\partial z} + \xi\phi_m\phi_n\right)dz + (\phi_m\phi_n)\Big|_{z=0}\right]\right\} \\ = \int_0^1 \xi\phi_n c_p\Big|_{r=1}dz + \phi_n\Big|_{z=0}, n = 1, 2, \ldots, n_f\end{aligned} \tag{4-A6}$$

This results in a set of ordinary differential equations (ODE) that can be expressed in the matrix form,

$$[MI][\frac{\partial c_{bi}}{\partial \tau}]^T + [MII][c_{bi}]^T = [MIII] \tag{4-A7}$$

where

$$[MI] = \sum_{m=1}^{n_f} \left(\int_0^1 \phi_m \phi_n dz \right), n = 1, 2, \ldots, n_f \tag{4-A8}$$

$$[MII] = \sum_{m=1}^{n_f} \left[\int_0^1 \left(\frac{1}{Pe_b} \frac{\partial \phi_m}{\partial z} \frac{\partial \phi_n}{\partial z} + \phi_n \frac{\partial \phi_m}{\partial z} + \xi \phi_m \phi_n \right) dz + (\phi_m \phi_n)\big|_{z=0} \right], n = 1, 2, \ldots, n_f \tag{4-A9}$$

[MII] is called the stiffness matrix.

$$[MIII] = \int_0^1 \xi \phi_n c_p \big|_{r=1} dz + \phi_n \big|_{z=0} , n = 1, 2, \ldots, n_f \tag{4-A10}$$

[MIII] is called the load vector.

$[c_{bi}]$ is exactly the solution of c_b at nodal points in the axial direction. Due to the fact that the base functions are piecewise over the triangulation, most of the base functions are zero on a specific element. There are two, three and four non-zero base functions in each element for linear, quadratic and cubic polynomials respectively. Thus it is more efficient for computation to break up the integration element by element, and then form the matrices above by assembling element by element. In our simulation, quadratic polynomials were used as the base functions. Considering a mixed boundary condition at $z = 0$ and a Newman boundary condition at $z = 1$, the dimension of the finite element space (n_f) is equal to $2n_m+1$, which is also the number of total nodal points (n_d). Therefore, ($2n_m+1$) ODEs need to be solved in the bulk phase. The integrals are evaluated using fourth order Gaussian quadrature.

4.9.2 Orthogonal Collocation in the Pore Phase

In the orthogonal collocation method the unknown solutions are expanded into trial functions, which are sets of orthogonal polynomials. The collocation points are taken as the roots of the polynomials and the differential equations are satisfied at each collocation point. The polynomials used in the pore phase automatically satisfy the boundary conditions at r = 0 as shown in equation (4.17). The PDE in the pore phase is discretized into the following ordinary ODE by the orthogonal collocation method

$$\left[\left(1-\varepsilon_p\right)\frac{\partial q}{\partial \tau}+\varepsilon_p\frac{\partial c_p}{\partial \tau}\right]_h=\eta\sum_{k=1}^{n_p+1}B_{h,k}(c_p)_k,\ h=1, 2, \ldots, n_p \tag{4-A11}$$

The value of $(c_p)_{n_p+1}$, i.e. $c_p\big|_{r=1}$, can be obtained from the boundary condition at r = 1,

$$\sum_{i=1}^{n_p+1}A_{n_p+1,i}(c_p)_i=Bi\left(c_b-c_p\big|_{r=1}\right) \tag{4-A12}$$

or

$$c_p\big|_{r=1}=\frac{Bic_b-\sum_{i=1}^{n_p+1}A_{n_p+1,i}(c_p)_i}{A_{n_p+1,n_p+1}+Bi} \tag{4-A13}$$

where A and B are the matrices defined by Finlayson (1980).

A MATLAB code was written to solve the GR model. Figure 4.10 summarizes the numerical procedure. The resulting ODEs (4-A7) and (4-A11), coupled with equations (4.5), (4.6) and (4.7), are normally stiff differential equations. The built-in function *ode15s* in MATLAB was used to solve the stiff ODEs. The nonlinear regression function *lqvcurvefit* was used to estimate the adsorption rate constants. Typically ten elements in the axial

direction and two collocation points in the radial direction are enough to get good convergence at our experimental conditions; further increase in the number of elements and collocation points gave little influence on the simulation results. If the adsorption rate constants were pre-set, the typical computing time to generate the breakthrough curve on a Dell Pentium III-based desk computer was around 2 minutes. The computing time to estimate adsorption rate constants using a nonlinear regression was variable based on the initial value chosen to start the simulation.

There is only one PDE in the POR, TD and RD models. The finite element method used to solve this equation is similar to that used in the GR model.

4.10 Appendix II: Other Models

4.10.1 Lumped Pore Diffusion (POR) Model

The POR model is a simplification of the GR model and can be derived from the GR model by integrating Eqn. (4.4) over the particle volume (Morbidelli et al., 1982; Morbidelli et al., 1984). The adsorbate concentration in the mobile phase in the pores is taken as the average concentration over the particle. The influences of the external mass transfer (k_f) and pore diffusion (D_p) are lumped together and characterized by a lumped mass transfer coefficient (k_t). The POR model has been extensively used to describe the zone profiles and breakthrough curves in preparative liquid chromatography (Kaczmarski et al., 2001; Liu et al., 2002; Zhou et al., 2003). The formulation of the POR model is almost the same as in the literature except for the consideration of the kinetics of surface reaction.

$$\frac{\partial c_b}{\partial \tau} - \frac{1}{Pe}\frac{\partial^2 c_b}{\partial z^2} + \frac{\partial c_b}{\partial z} + \xi^{\#}\left(c_b - \overline{c_p}\right) = 0 \tag{4-A14}$$

$$\left(1-\varepsilon_p\right)\frac{\partial \overline{q}}{\partial \tau} + \varepsilon_p \frac{\partial \overline{c_p}}{\partial \tau} - St^{\#}\left(c_b - \overline{c_p}\right) = 0 \tag{4-A15}$$

As in the GR model, bi-Langmuir kinetics are used.

$$\overline{q} = \overline{q_1} + \overline{q_2} \tag{4-A16}$$

$$\frac{\partial \overline{q_1}}{\partial \tau} = Da_1^a c_p\left(q_{m,1}^* - \overline{q_1}\right) - Da_1^d \overline{q_1} \tag{4-A17}$$

$$\frac{\partial \overline{q_2}}{\partial \tau} = Da_2^a c_p\left(q_{m,2}^* - \overline{q_2}\right) - Da_2^d \overline{q_2} \tag{4-A18}$$

If local equilibrium exists, then Eqn. (4-A17) and (a-A18) reduce to the form,

$$\overline{q_1^*} = \frac{a_1 \overline{c_p}}{1 + b_1 \overline{c_p}} \tag{4-A19}$$

$$\overline{q_2^*} = \frac{a_2 \overline{c_p}}{1 + b_2 \overline{c_p}} \tag{4-A20}$$

The initial and boundary conditions are similar to those used in the GR model.

The lumped mass transfer coefficient (k_t) is given by the relationship (Morbidelli et al., 1982)

$$\frac{1}{k_t} = \frac{1}{k_f} + \frac{1}{k_i \varepsilon_p} \tag{4-A21}$$

where k_i is the internal mass transfer coefficient proposed by (Glueckauf, 1955).

$$k_i = \frac{5D_p}{R_p} \tag{4-A22}$$

4.10.2 Transport-Dispersive (TD) Model

The formulation of the TD model appears elsewhere (Guiochon et al., 1994; Kaczmarski et al., 2001; Natarajan and Cramer, 2000). A solid film driving force model is employed to describe the adsorption on each type of binding site when bi-Langmuir kinetics is employed.

$$\frac{\partial c_b}{\partial \tau} + F\frac{\partial q}{\partial \tau} - \frac{1}{Pe^{\#}}\frac{\partial^2 c_b}{\partial z^2} + \frac{\partial c_b}{\partial z} = 0 \tag{4-A23}$$

$$q = q_1 + q_2 \tag{4-A24}$$

$$\frac{\partial q_1}{\partial \tau} = St^{\#\#}(q_1^* - q_1) \tag{4-A25}$$

$$\frac{\partial q_2}{\partial \tau} = St^{\#\#}(q_2^* - q_2) \tag{4-A26}$$

The initial and boundary conditions are similar to those used in the GR model.

The overall mass transfer coefficient (k_m) in the solid film linear driving force model is given by the following equation (Guiochon et al., 1994; Miyabe and Guiochon, 1999),

$$\frac{1}{k_m} = \frac{K}{F}\left(\frac{R_p}{3k_f} + \frac{R_p^2}{15\varepsilon_p D_p}\right) \tag{4-A27}$$

where K (the slope of the isotherm chord) is given by

$$K = F\frac{\Delta Q^*}{\Delta C} \tag{4-A28}$$

4.10.3 Reaction-Dispersive (RD) Model

The RD model assumes that the adsorption-desorption kinetics is the rate-limiting step (Natarajan and Cramer, 2000).

$$\frac{\partial c_b}{\partial \tau} + F\frac{\partial q}{\partial \tau} - \frac{1}{Pe^{\#}}\frac{\partial^2 c_b}{\partial z^2} + \frac{\partial c_b}{\partial z} = 0 \tag{4-A29}$$

$$\frac{\partial q_1}{\partial \tau} = Da_1^a c_p\left(q_{m,1}^* - q_1\right) - Da_1^d q_1 \tag{4-A30}$$

$$\frac{\partial q_2}{\partial \tau} = Da_2^a c_p\left(q_{m,2}^* - q_2\right) - Da_2^d q_2 \tag{4-A31}$$

If the mass transfer effects have a minor influence but cannot be neglected, a lumped adsorption coefficient (k_{al}) could replace the intrinsic adsorption coefficient (k_a) in the Damkolher number (Da^a) to account for mass transfer effects (Boyer and Hsu, 1992a).

$$\frac{1}{k_{al}} = \frac{1}{k_a} + \frac{Q_m^*(1+r_s)R_p^2}{30 r_s}\left(\frac{1}{\varepsilon_p D_p} + \frac{5}{k_f R_p}\right) \tag{4-A32}$$

Where r_s is the separation factor defined by

$$r_s = 1 + \frac{C_0}{K_d} \tag{4-A33}$$

Table 4.1 Parameters involved in the general rate model in Figure 4.5(a).

Parameter	*Definition*	*Value*
L	Column length	0.03 m
R_c	Column radius	1.05×10^{-3} m
R_p	Particle radius	32.5×10^{-6} m
C_f $(=C_0)$	Inlet concentration	9.05×10^{-3} mol/m^3
Mw	SEB molecular weight	28,366
ρ	Mobile phase density	1000 kg/m^3
u_0	Superficial velocity	4.81×10^{-4} m/s
ε_b	Interparticle void fraction	0.29
ε_p	Particle Porosity	0.70
μ	Mobile phase viscosity	0.001 Pa·s
D_b	Axial dispersion coefficient	2.40×10^{-7} m^2/s
D_m	Molecular diffusion coefficient	7.70×10^{-11} m^2/s
D_p	Diffusion coefficient inside the pores	4.83×10^{-11} m^2/s
k_f	Film mass transfer coefficient	9.51×10^{-6} m/s
$Q_{m,1}^*$	Capacity constant of type I sites	0.43 mol/m^3 (8.50 mg/g)
$Q_{m,2}^*$	Capacity constant of type II sites	1.74 mol/m^3 (34.42 mg/g)
$K_{d,1}$	Dissociation constant of type I sites	6.75×10^{-5} mol/m^3 (1.91×10^{-3} mg/ml)

Table 4.1 (continued)

$K_{d,2}$	Dissociation constant of type II sites	3.60×10^{-3} mol/m^3 (0.10 mg/ml)
$k_{a,1}$	Adsorption rate constant on type I sites	5.95 m^3 mol^{-1} s^{-1}
$k_{a,2}$	Adsorption rate constant on type II sites	0.40 m^3 mol^{-1} s^{-1}
$k_{d,1}$	Desorption rate constant on type I sites	4.01×10^{-4} s^{-1}
$k_{d,2}$	Desorption rate constant on type II sites	1.45×10^{-3} s^{-1}
N_d	NTU of axial dispersion	207.49
N_f	NTU of film mass transfer	38.85
N_p	NTU of pore diffusion	21.23
$N_{k,1}$	NTU of adsorption on type I sites	33.96
$N_{k,2}$	NTU of adsorption on type II sites	9.35

Note:
NTU: number of transfer units; flow rate: 0.1 ml/min

Table 4.2 Isotherm parameters at different peptide densities.

Peptide	(μmol/g)	6	9	20	36	52	100	220
density	(mol/m^3)	8.68	13.02	28.93	52.08	75.23	142.86	318.26
				Bi-Langmuir isotherm				
$Q_{m,1}^*$	(mg/g)	11.47	9.31	8.07	13.74	10.49	8.50	13.94
	$(mol/m^3)^*$	0.56	0.48	0.41	0.70	0.54	0.43	0.71
$Q_{m,2}^*$	(mg/g)	32.86	24.35	27.30	23.65	25.78	34.42	33.26
	$(mol/m^3)^*$	1.68	1.24	1.39	1.21	1.32	1.74	1.70
$K_{d,1}$	$(mg/ml)\times10^3$	5.80	19.12	22.95	29.60	15.06	1.91	1.56
	$(mol/m^3)\times10^4$	2.04	6.74	8.09	10.43	5.31	0.68	0.55
$K_{d,2}$	(mg/ml)	0.19	0.36	0.68	0.60	0.38	0.10	0.047
	$(mol/m^3)\times10^3$	6.84	12.80	23.92	21.19	13.26	3.60	1.67
				Langmuir isotherm				
Q_m^*	(mg/g)	35.75	25.85	25.34	26.91	29.85	39.54	44.27
	$(mol/m^3)^*$	1.82	1.32	1.29	1.37	1.52	2.00	2.26
K_d	$(mg/ml)\times10^2$	4.70	8.66	14.73	8.32	10.36	4.55	1.73
	$(mol/m^3)\times10^3$	1.66	3.05	5.19	2.93	3.65	1.60	0.61

Note: the bulk density of resins is 320 ± 4 mg/ml; *: based on unit volume of particle skeleton

Table 4.3 Surface area estimates

Peptide density (μmol/g)	Number of peptides covered by one SEB molecule
6	1.7
9	2.6
20	5.7
36	10.2
52	14.8
100	28.4
220	62.5

Table 4.4 Adsorption rate constants at different peptide densities

Peptide density	(μmol/g)	6	9	20	36	52	100	220
				Bi-Langmuir kinetics				
$k_{a,1}$	(m^3 mol^{-1} s^{-1})	1.24	1.14	0.60	0.45	1.02	5.95	9.11
$k_{d,1}$	(s^{-1})×10^4	2.52	7.67	4.85	4.70	5.43	4.01	5.02
$k_{a,2}$	(m^3 mol^{-1} s^{-1})	0.36	0.14	0.32	0.19	0.13	0.40	0.50
$k_{d,2}$	(s^{-1})×10^4	24.6	18.03	75.65	40.64	17.74	14.54	8.33
				Langmuir kinetics				
k_a	(m^3 mol^{-1} s^{-1})	0.62	0.39	0.51	0.38	0.40	0.58	0.67
k_d	(s^{-1})×10^4	10.29	11.82	26.28	11.24	14.70	9.26	4.11

Table 4.5 Number of mass transfer units at different peptide densities

Peptide density (μmol/g)	6	9	20	36	52	100	220
N_d	207.49	207.49	207.49	207.49	207.49	207.49	207.49
N_f	38.85	38.85	38.85	38.85	38.85	38.85	38.85
N_p	21.23	21.23	21.23	21.23	21.23	21.23	21.23
			Bi-Langmuir kinetics				
$N_{k,1}$	9.59	7.17	3.27	4.19	7.27	33.96	86.00
$N_{k,2}$	8.01	2.31	5.84	3.07	2.34	9.35	11.23
			Langmuir kinetics				
N_k	15.05	6.78	8.68	6.97	8.13	15.34	20.16

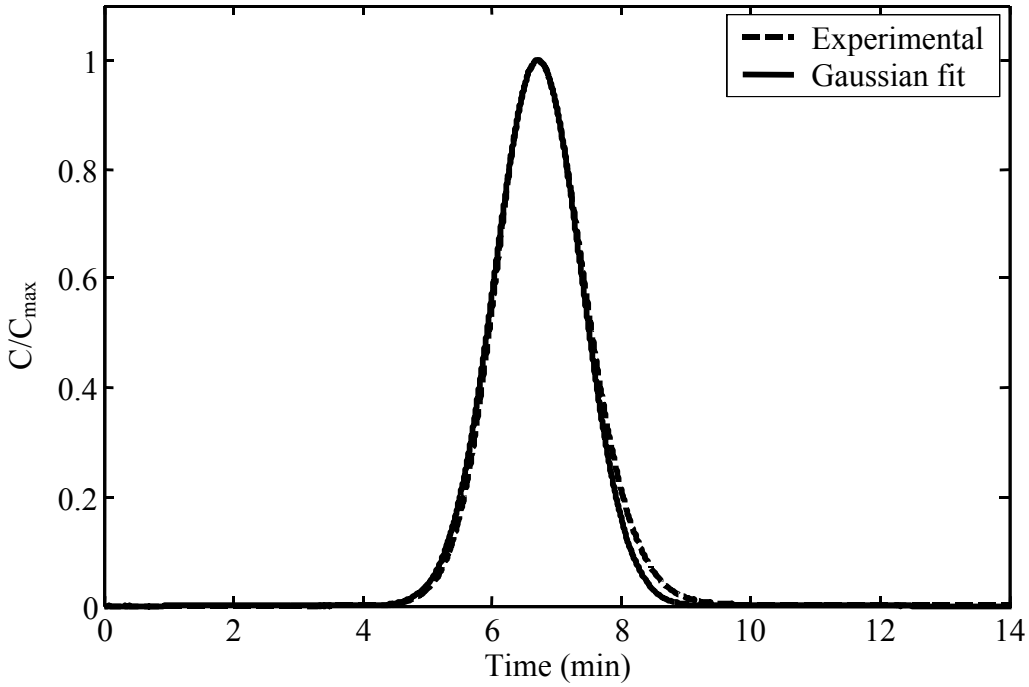

Figure 4.1 Gaussian fit to experimental peak profile. Dashed line: experimental data. Solid line: Gaussian fit. Flow rate: 0.3 ml/min.

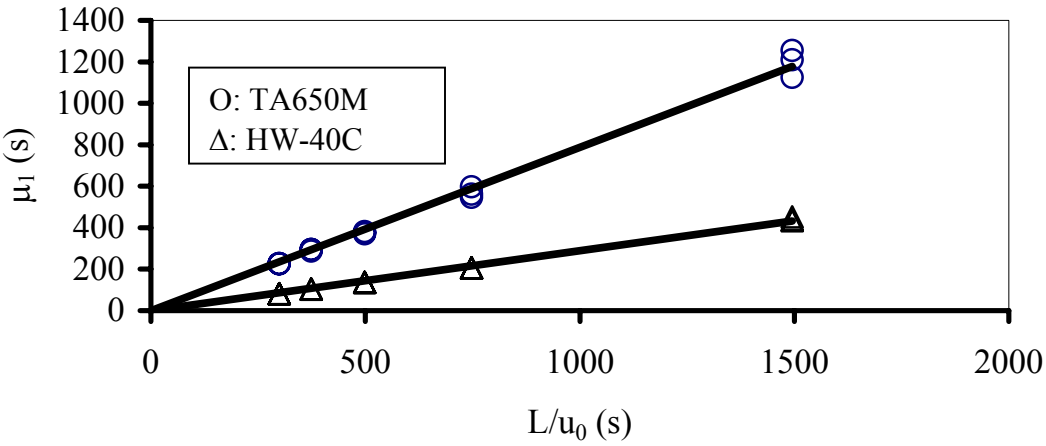

(a)

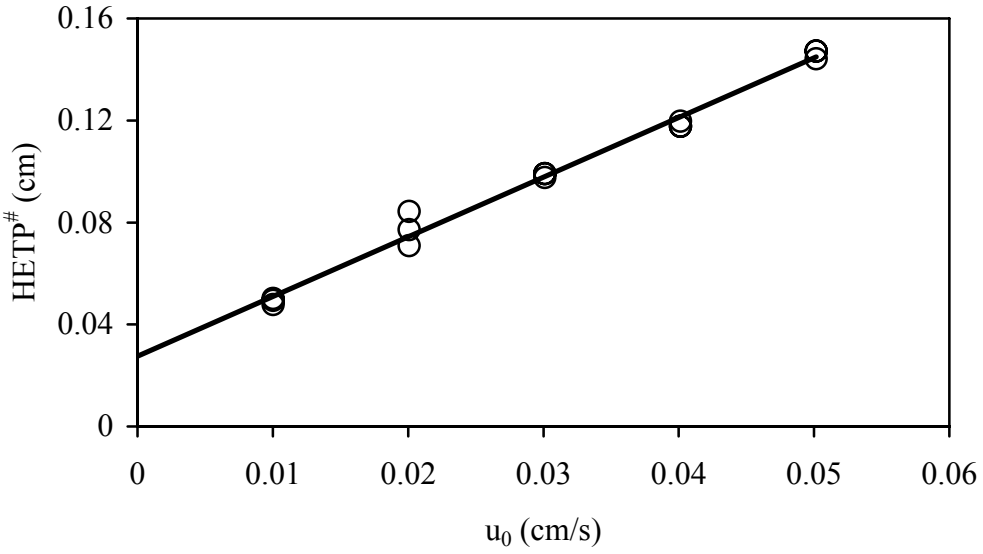

(b)

Figure 4.2 **(a)** First moments of chromatography peaks under unretained conditions. **(b)** HETP plots under unretained conditions.

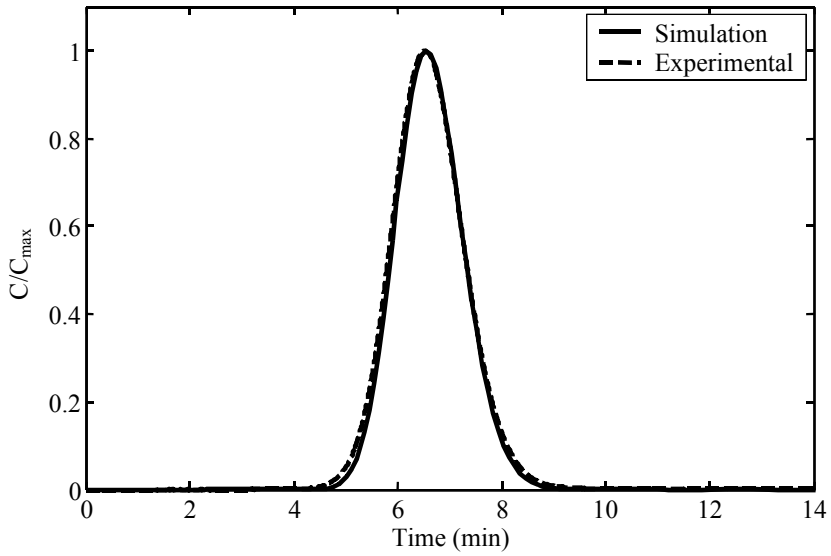

(a)

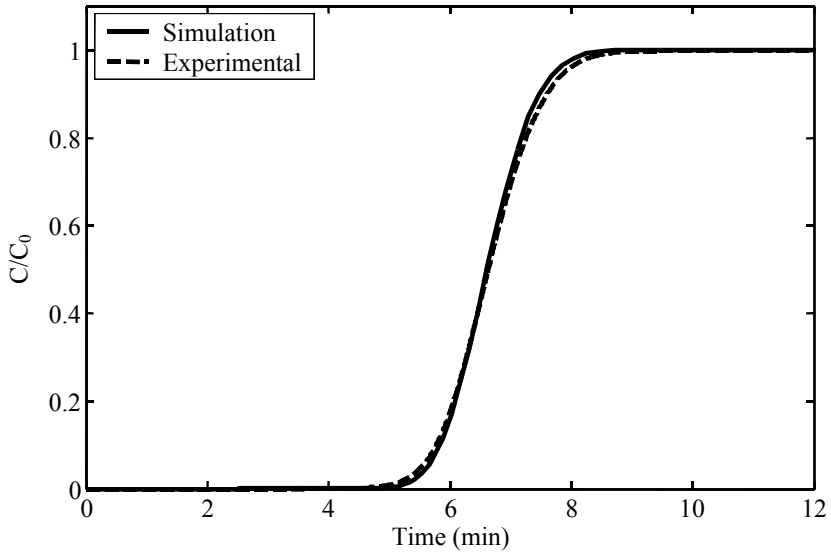

(b)

Figure 4.3 Comparison of simulation (general rate model using mass transfer parameters determined from HETP equation) and experimental results under unretained conditions. **(a)** A pulse injection. **(b)** A breakthrough curve. Flow rate: 0.3 ml/min.

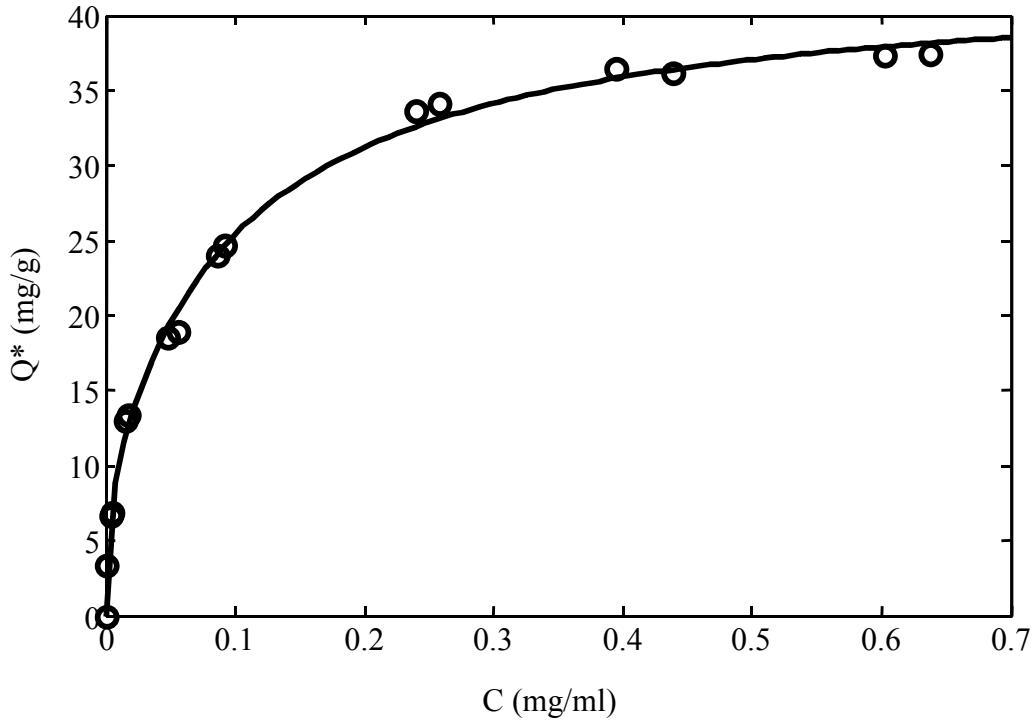

Figure 4.4 The bi-Langmuir isotherm for SEB binding to YYWLHH.

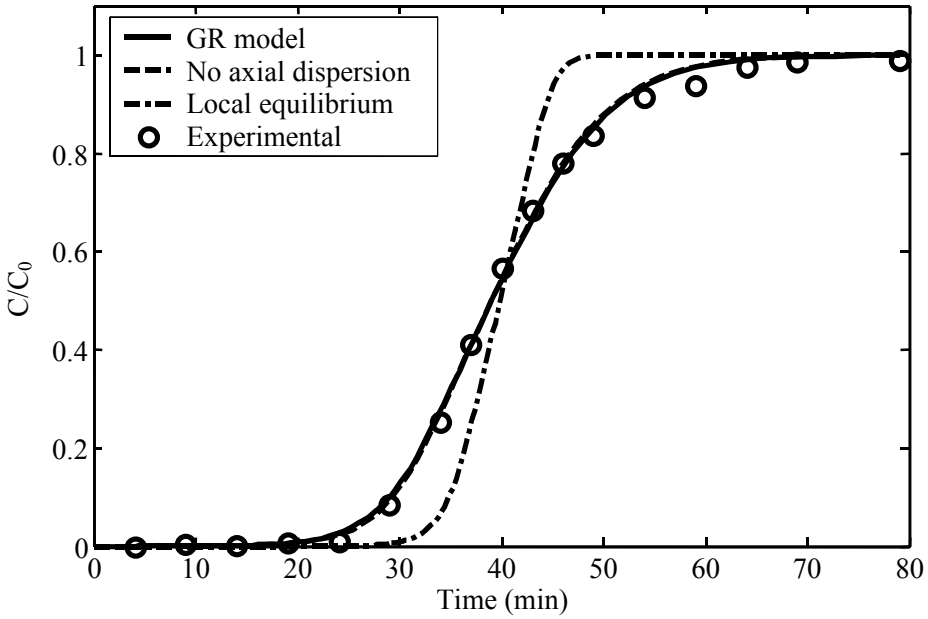
GR model
No axial dispersion
Local equilibrium
Experimental
C/C0
Time (min)
0
0.2
0.4
0.6
0.8
1
0
10
20
30
40
50
60
70
80

(a)

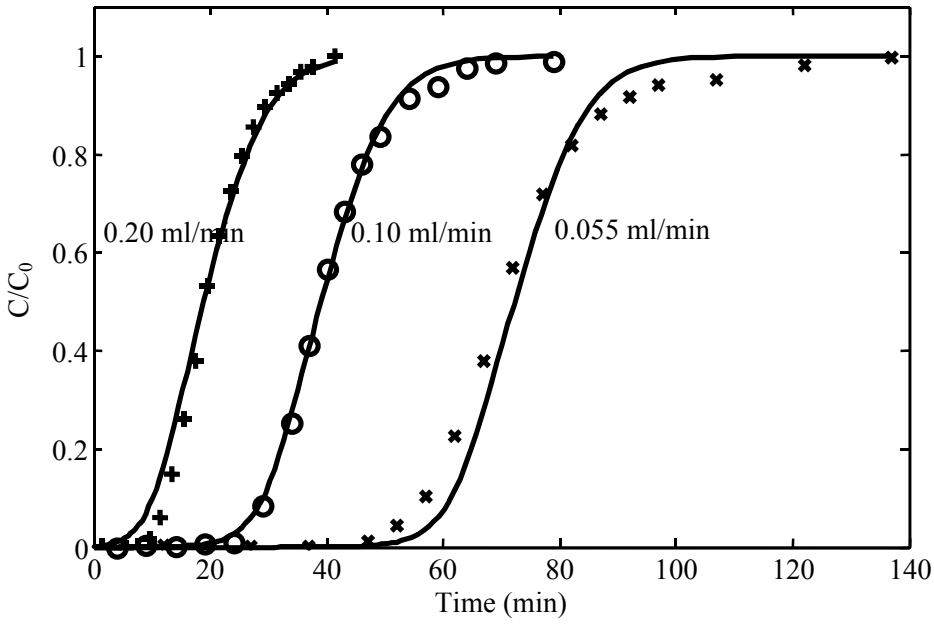
0.20 ml/min
0.10 ml/min
0.055 ml/min
C/C0
Time (min)
0
0.2
0.4
0.6
0.8
1
0
20
40
60
80
100
120
140

(b)

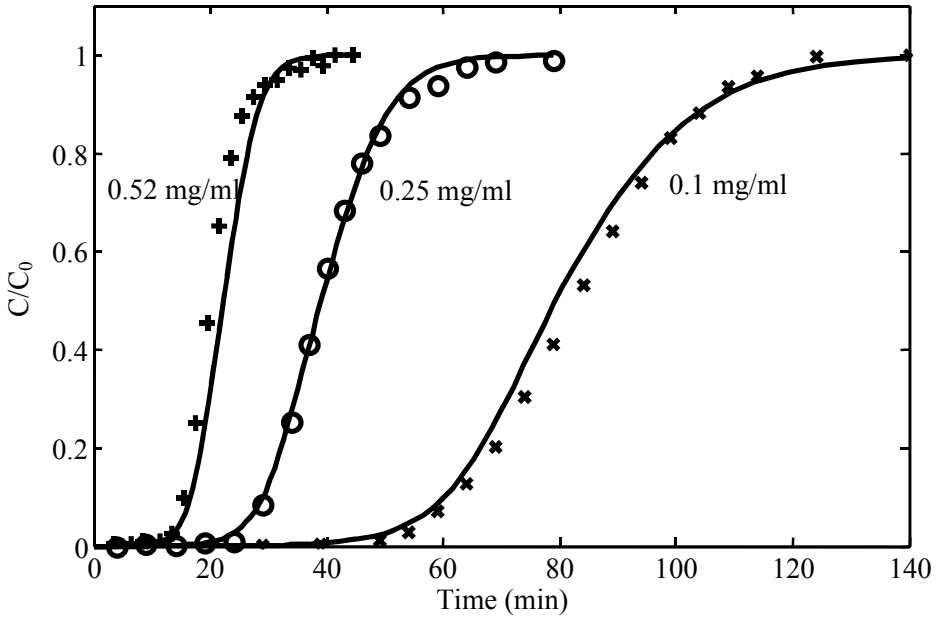

(c)

Figure 4.5 Experimental (symbols) vs. simulated (lines) breakthrough curves using the GR model. **(a)** At base case. (—) GR model, (---) GR model only considering the rate-limiting steps, (-·-) GR model with the local equilibrium. Feed concentration: 0.25 mg/ml; flow rate: 0.1 ml/min. **(b)** At different flow rates. (+) 0.2 ml/min, (o) 0.1 ml/min, (×) 0.055 ml/min. Feed concentration: 0.25 mg/ml. **(c)** At different feed concentrations. (+) 0.52 mg/ml, (o) 0.25 mg/ml, (×) 0.10 mg/ml. Flow rate: 0.1 ml/min.

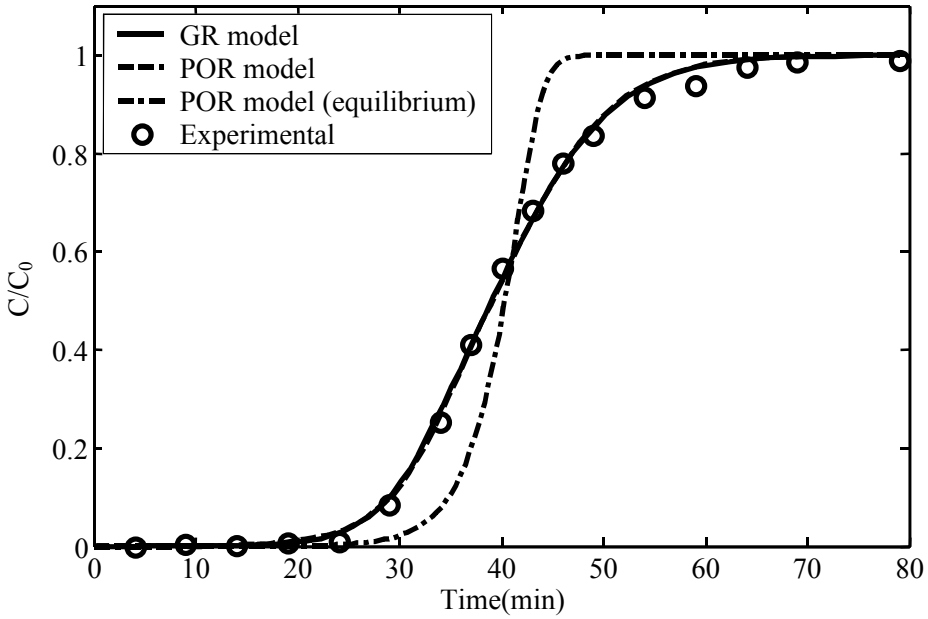
GR model
POR model
POR model (equilibrium)
Experimental
C/C0
Time(min)
0
0.2
0.4
0.6
0.8
1
0
10
20
30
40
50
60
70
80

(a)

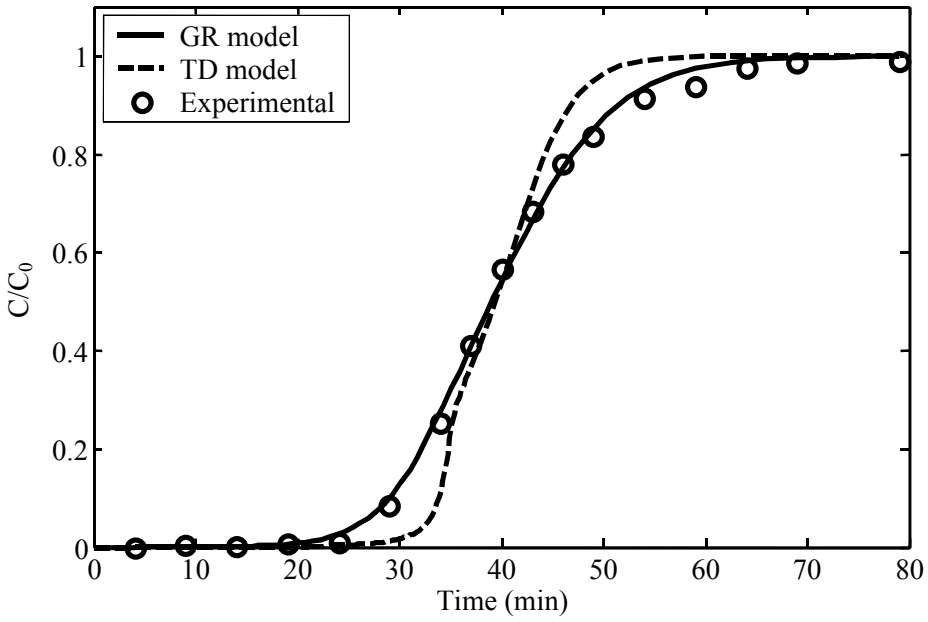
GR model
TD model
Experimental
C/C0
Time (min)
0
0.2
0.4
0.6
0.8
1
0
10
20
30
40
50
60
70
80

(b)

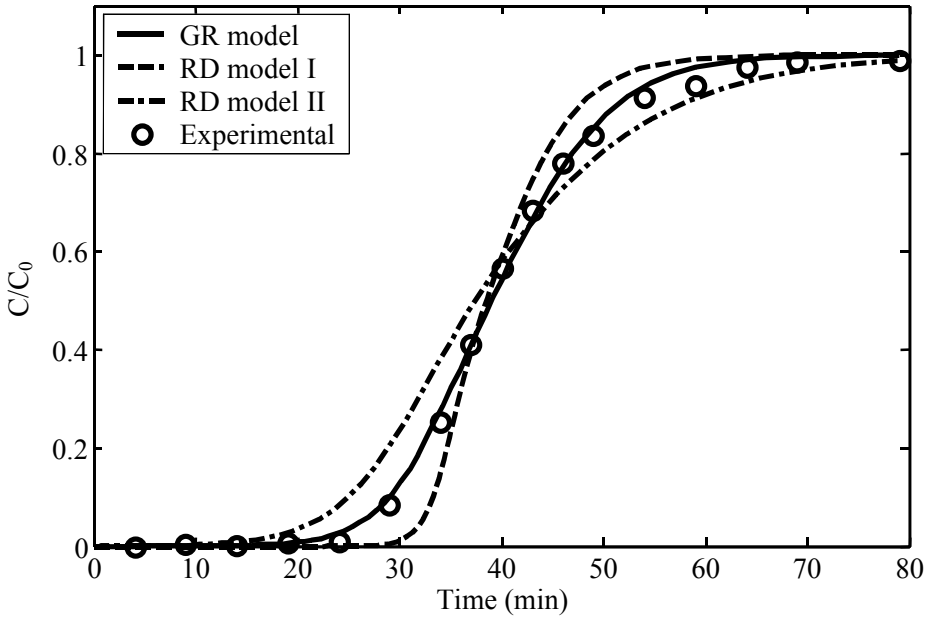

(c)

Figure 4.6 **(a)** Comparison between the POR model and the GR model. (o) Experimental data, (—) GR model, (---) POR model, (-··-) POR model with local equilibrium. **(b)** Comparison between the TD model and the GR model. (o) Experimental data, (—) GR model, (---) TD model. **(c)** Comparison between the RD model and the GR model. (o) Experimental data, (—) GR model, (---) RD model with the intrinsic rate parameters, (-··-) RD model with the lumped rate parameters. Flow rate: 0.1 ml/min; feed concentration: 0.25 mg/ml.

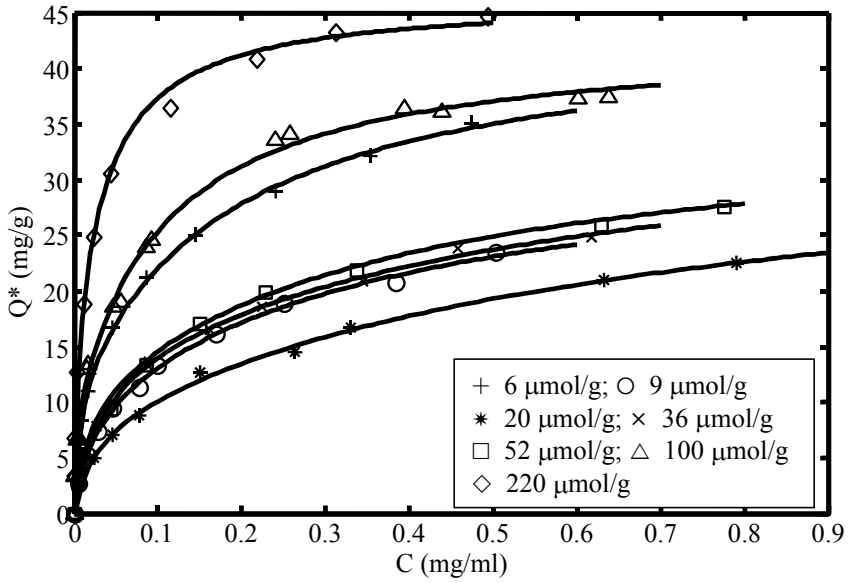

(a)

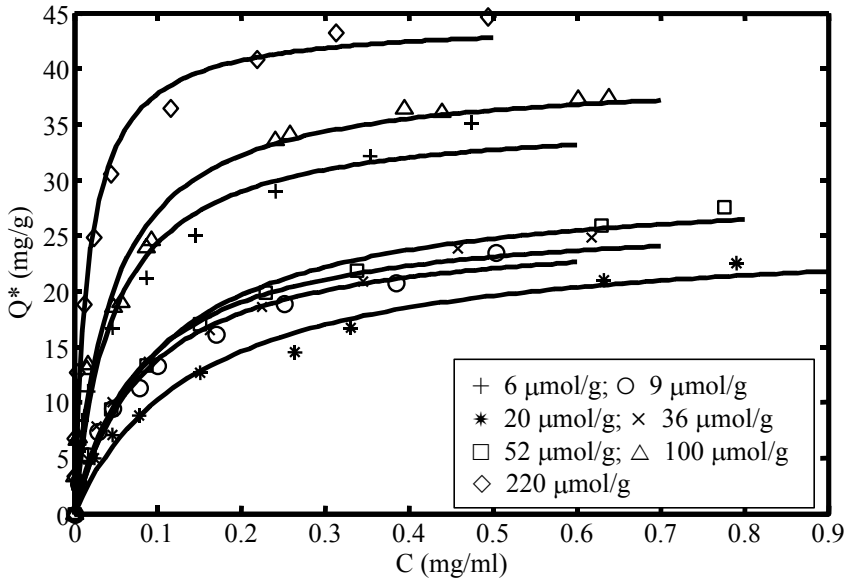

(b)

Figure 4.7 Isotherms for SEB binding to YYWLHH at different peptide densities. **(a)** A bi-Langmuir fit. **(b)** A Langmuir fit.

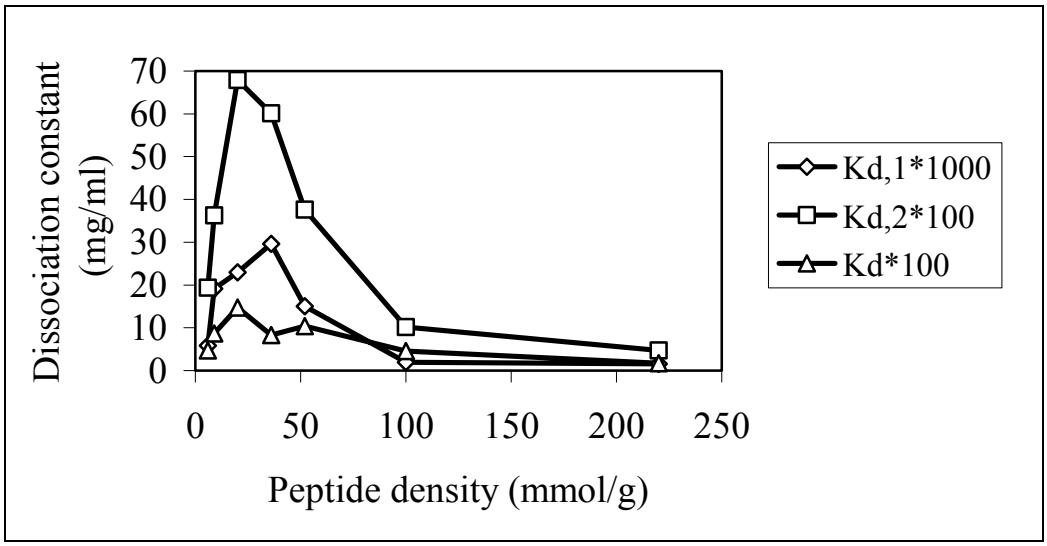

(a)

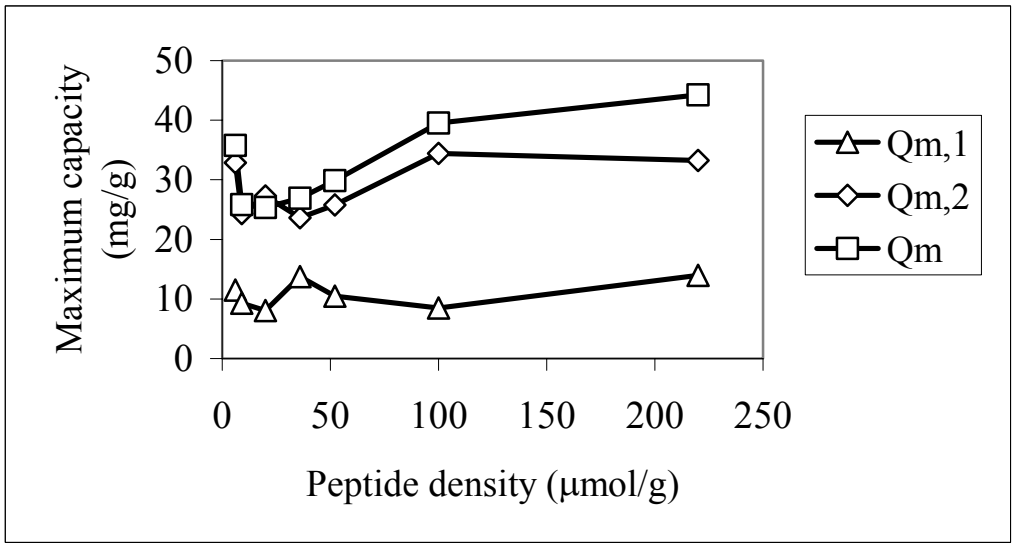

(b)

Figure 4.8 **(a)** Variation of dissociation constant for SEB adsorption on YYWLHH with peptide density. **(b)** Variation of maximum capacity for SEB adsorption on YYWLHH with peptide density.

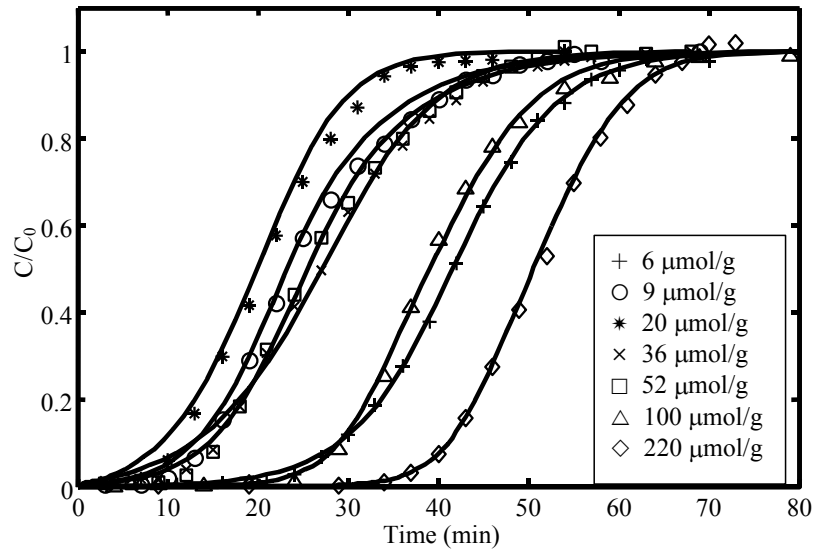

(a)

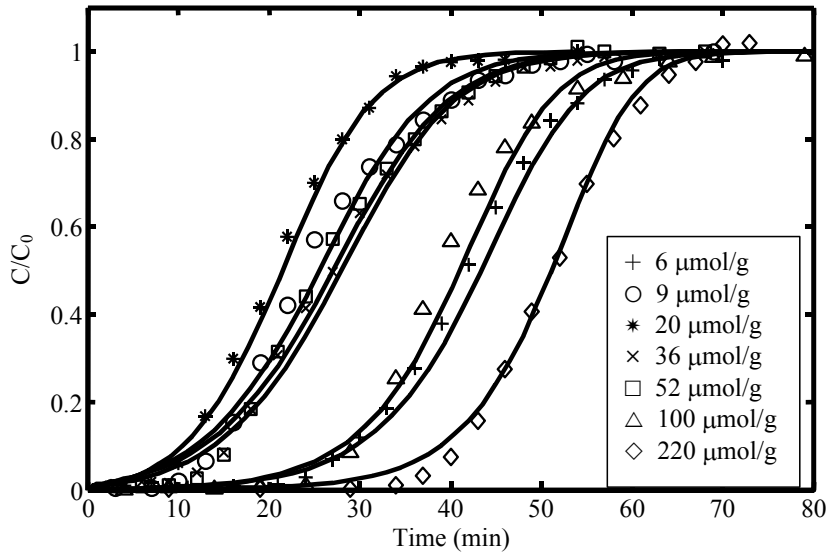

(b)

Figure 4.9 Experimental (symbols) vs. simulated (lines) breakthrough curves using the GR model at different peptide densities. **(a)** Bi-Langmuir kinetics. **(b)** Langmuir kinetics. Flow rate: 0.1 ml/min; feed concentration: 0.22 mg/ml for resins with a density of 6 μmol/g, 0.25 ± 0.1 mg/ml for others.

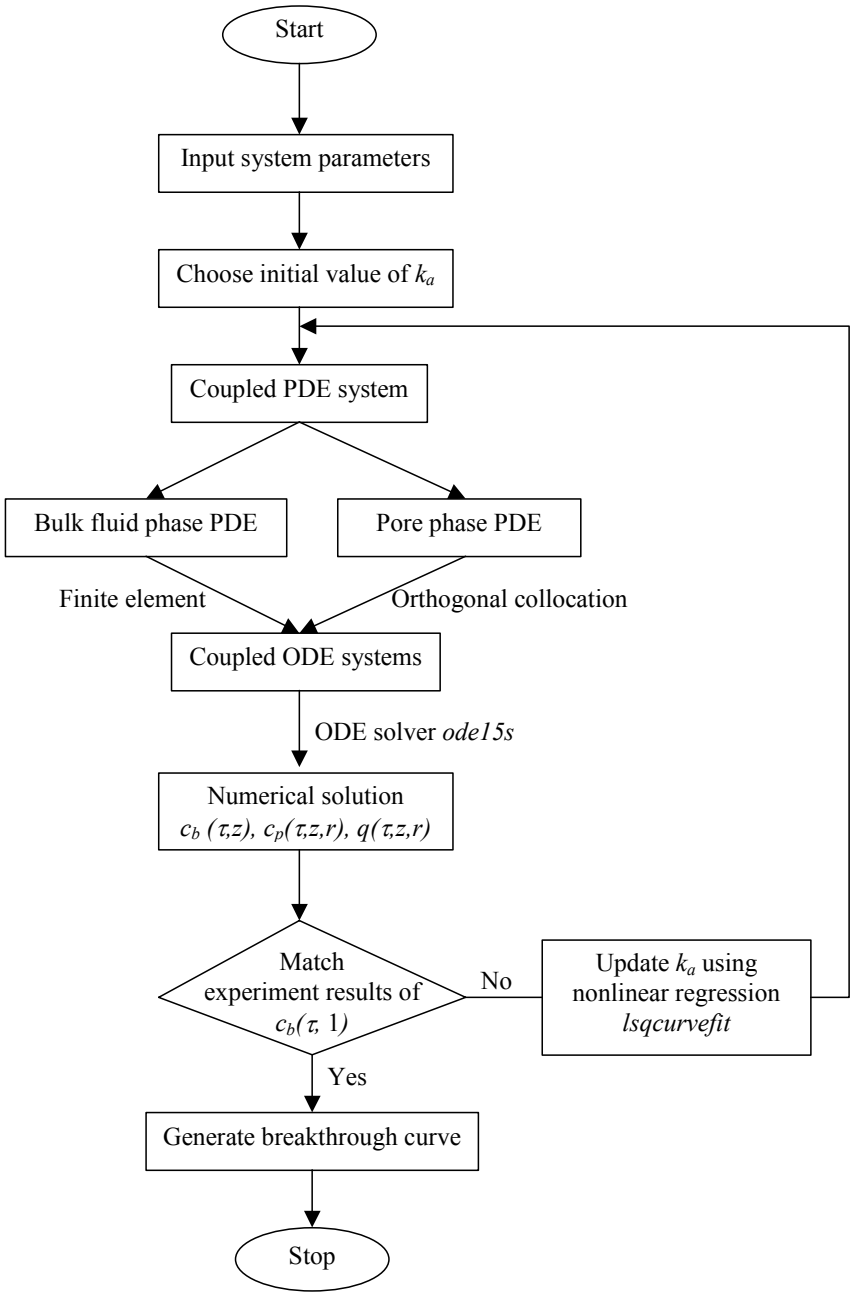

Figure 4.10 Flow chart of the computer simulation program.

CHAPTER 5

DESIGN OF ADSORPTIVE COLUMNS FOR SPECIFIC PATHOGEN REMOVAL: APPLICATION TO STAPHYLOCOCCAL ENTEROTOXIN B (SEB)

Guangquan Wang, Ruben G. Carbonell

Department of Chemical Engineering, North Carolina State University

1017 Main Campus Drive, Centennial Campus

Partner's Building I, Suite 3200, Box 7006

Raleigh, NC 27695-7006

This is a manuscript in preparation for submission to

Biotechnology and Bioengineering

Abstract

The potential presence of pathogenic agents such as toxins, viruses, bacteria and prions in blood and plasma sources, in mammalian culture media, fermentation broths, milk, and aqueous streams of various types has gained increasing importance in ensuring product safety and in combating the effects of acts of bioterrorism. Adsorption chromatography can play an important role in helping to remove such pathogens from solution without affecting other desirable components in a product stream. Because these are potential infectious agents, the design of an adsorptive column to effect such removal has to have as a goal the removal of several logs of infectious units. This requirement is significantly more stringent than the high yield requirements associated with adsorptive separations aimed at product recovery in a process stream. This paper considers the design of an adsorptive column aimed at reducing the concentration of an infectious agent from a known volume of a process stream by several logs in a fixed amount of time. The general rate (GR) model of chromatography is used in the analysis, including all major transport and kinetic steps in the adsorption process. Two design options are analyzed, one fixing the column length and varying the fluid velocity, the other fixing the fluid velocity and varying the column length. The results indicate that the reduction in pathogen concentration is highly dependent on the residence time in the column, which is in turn dependent on the flow rate and column geometry. The theory, with no adjustable parameters, is shown to predict with great accuracy the effect of residence time on the log removal of staphylococcal enterotoxin B

(SEB) from an aqueous stream using an affinity resin with a small peptide (YYWLHH) that has been found to bind specifically to this toxin.

Keywords: column design; pathogen removal; peptide-affinity ligands; staphylococcal enterotoxin B

5.1 Introduction

Various biological products derived from either human or animal origins contain an inherent risk of pathogen contamination. For example, the dominant pathogens in blood and blood products are bacteria and viruses, which are potential threats for disease transmission. In addition, a potential threat to the safety of plasma products is the possibility that transmissible spongiform encephalopathies (TSEs), such as bovine spongiform encephalopathy (BSE) in cattle and Creutzfeldt-Jakob disease (CJD) in humans, which are associated with the pathogenic and infectious prion protein (Lee et al., 2002; Miller et al., 2001). Dairy foods such as milk are potentially contaminated by a bacterium, *Staphylococcus aureus*, which releases staphylococcal enterotoxins that are leading causes in food poisoning (Evenson et al., 1988). Thus the detection and removal of such pathogens would be valuable to the safety of food and blood products. Various methods have been used for pathogen removal and clearance, i.e. heat inactivation, ultraviolet light irradiation, chemical inactivation, filtration, chromatographic and precipitation process steps (Lee et al., 2002; Miller et al., 2001). Note that bacteria can sometimes be removed through filtration due to their relatively large size. In order to maximize pathogen control while maintaining good product quality, it is desirable to develop novel pathogen removal methods with high selectivity and capacity for the target pathogen and low affinity for other components in the process stream. Adsorption chromatography has been widely used in protein recovery, and may also be used to remove pathogens efficiently from aqueous biological media due to its higher selectivity in comparison with other pathogen removal methods. It has been shown

that short peptide ligands, which can be obtained by screening a combinatorial peptide library, have high affinity and chemical stability in protein purification (Bastek et al., 2000; Gurgel et al., 2001b; Wang et al., 2003). A similar screening strategy could also be applied to a specific pathogen, and the resultant peptide ligand would be a suitable candidate to be used in adsorption chromatography for pathogen removal. A detailed procedure for identification of peptide ligands for a specific target has been well addressed elsewhere (Bastek et al., 2000; Gurgel et al., 2001a; Wang et al., 2003) and will not be discussed further here.

It is generally required to remove several logs of infectious units of a pathogen to ensure product safety. An adsorption column should be properly designed to meet this requirement, which is significantly more stringent than the high yield requirements associated with adsorptive separations aimed at product recovery in a process stream. In this paper we demonstrate an approach to column design for pathogen removal with staphylococcal enterotoxin B (SEB) as the example. SEB is a primary toxin in food poisoning, which can cause emesis as a gastrointestinal toxin, and in addition, functions as a superantigen to interact with the major histocompatibility complex class II molecules (MHCII) and T cells bearing particular Vβ elements, triggering a massive release of T cell-derived cytokines followed by allergic and autoimmune symptoms (Balaban and Rasooly, 2000; Li et al., 1999). Due to its extreme toxicity and inherent stability, SEB is considered a significant bioterrorism threat as either an aerosol or food and water contaminant (Franz et al., 1997), and is listed by the CDC as a select agent (Enserink and Malakoff, 2001). A short peptide ligand that selectively binds to SEB, YYWLHH, has been identified from a solid

phase combinatorial peptide library (Wang et al., 2003). Besides its application in SEB detection and purification, this peptide ligand has a potential use to remove SEB from contaminated food and water due to its high affinity and selectivity for SEB.

A column design strategy is presented in this paper to obtain prescribed log removals of SEB from solution. The column design is approached by fixing the volume to be processed and the time required for processing. This can be done by either fixing the column length and varying the fluid velocity or fixing the velocity and varying the column length. This can give rise to different logs of removal because of the effects of flow rate on fluid phase mass transfer. The concentration at the exit of the column can be calculated as a function of time using the general rate (GR) model of chromatography, including all major transport and kinetic steps in the adsorption process. All the parameters used in the calculation have been determined for the SEB – YYWLHH system in our lab (Wang and Carbonell, 2003). The described strategies of column design are generally applicable to all kinds of pathogens that can be captured and removed by the use of porous affinity chromatography resins, and is not limited to SEB.

5.2 Calculation Strategy

If the volume of fluid that needs to be processed (V_m) and the time available to complete the removal (t_m) are fixed, then the flow rate (Q_f) in the column is fixed by the ratio of the volume of fluid to be processed to the time available for processing. The required column dimensions can be calculated using two different methods: (a) Fix the column length

(L) and calculate the log removal at the maximum process time as a function of fluid velocity (u_0) (the superficial velocity in the chromatography bed); (b) Fix the fluid velocity and calculate the log removal at the maximum process time as a function of column length. The value of the log removal at the maximum process time is given by

$$F_r = -\log_{10}\left(\frac{C_{out}(t_m)}{C_0}\right) \tag{5.1}$$

where $C_{out}(t_m)$ is the SEB concentration at the outlet of the column at the maximum process time (t_m), and C_0 is the feed concentration of SEB. The column volume (V_c) and the flow rate (Q_f) can be described as

$$V_c = A_c L \tag{5.2}$$

$$Q_f = \frac{V_m}{t_m} = A_c u_0 \tag{5.3}$$

where A_c is the cross-section area of the column. For the first column design strategy, increasing the fluid velocity decreases the cross-section area of the column according to equation (5.3), and therefore leads to a smaller column volume according to equation (5.2). For the second column design strategy, the cross-section area is a constant because the fluid velocity is fixed according to equation (5.3), and therefore increasing the column length linearly increases the column volume according to equation (5.2). At a desired log removal at the maximum process time (3 or 5 logs for example) there are several combinations of length and area that will meet the desired objective. The residence times associated with these individual columns can be computed form the ratio of the column length to the fluid velocity. In this chapter, the rate constant for binding was varied to understand the effect of

this parameter on column volume. A special calculation was done assuming that the binding rate is infinite (equilibrium calculation). This gives the minimum required volume of column. The effects of other factors such as mass transfer parameters and SEB concentration on the log removal at the maximum process time were also investigated.

5.3 Design Constraints

The inlet concentration chosen in the calculations for SEB was 0.15 μg/ml, which corresponds to the amount sufficient to cause symptoms of intoxication in humans (Evenson et al., 1988). This is much lower than the magnitude of the dissociation constant for adsorption shown in Table 5.1. The volume of fluid to be processed was assumed to be 500 ml. The time required for processing was chosen to be 40 minutes. This corresponds to a volumetric flow rate of 12.5 ml/min. All mass transfer parameters that are needed in the GR model and physical properties of the peptide affinity resins are listed in Table 5.1.

5.4 Theory

5.4.1 Isotherm Model

It has been shown that the adsorption isotherm data of SEB to YYWLHH fit well to the bi-Langmuir isotherm (Wang and Carbonell, 2003),

$$Q^* = Q_1^* + Q_2^* \tag{5.4}$$

$$Q_1^* = \frac{Q_{m,1}^* C}{K_{d,1} + C} \tag{5.5}$$

$$Q_2^* = \frac{Q_{m,2}^* C}{K_{d,2} + C} \tag{5.6}$$

Thus there are two types of binding sites for SEB, a high affinity binding site and a low affinity binding site. The capacities and dissociation constants are listed in Table 5.1.

5.4.2 General Rate (GR) Model

The outlet concentration of SEB was calculated using the GR model, which considers all major mass transfer and kinetic effects including the effects of mass transfer from the bulk fluid to the particle surface, diffusion into the particles, the kinetics of adsorption to the surface of the resin, and axial dispersion (Gu, 1995; Guiochon et al., 1994; Wang and Carbonell, 2003).

The mass balance of SEB in the mobile-phase stream is governed by

$$\frac{\partial C_b}{\partial t} - D_b \frac{\partial^2 C_b}{\partial Z^2} + u \frac{\partial C_b}{\partial Z} = \left(\frac{1 - \varepsilon_b}{\varepsilon_b} \right) \left(\frac{3}{R_p} \right) k_f \left(C_b - C_p (R = R_p) \right) \tag{5.7}$$

The mass balance of SEB in the pores of the stationary phase is given by

$$\left(1 - \varepsilon_p\right) \frac{\partial C_p}{\partial t} + \varepsilon_p \frac{\partial C_p}{\partial t} = \varepsilon_p D_p \left(\frac{1}{R^2} \frac{\partial}{\partial R} \left(R^2 \frac{\partial C_{p,i}}{\partial R} \right) \right) \tag{5.8}$$

The intrinsic adsorption-desorption rate is of the form consistent with bi-Langmuir kinetics,

$$Q = Q_1 + Q_2 \tag{5.9}$$

$$\frac{\partial Q_1}{\partial t} = k_{a,1} C_p \left(Q^*_{m,1} - Q_1 \right) - k_{d,1} Q_1 \tag{5.10}$$

$$\frac{\partial Q_2}{\partial t} = k_{a,2} C_p \left(Q^*_{m,2} - Q_2 \right) - k_{d,2} Q_2 \tag{5.11}$$

If local equilibrium holds, equations (5.5) and (5.6) can be used to describe the surface adsorption instead of equations (5.10) and (5.11).

The initial conditions are

$$t = 0,\ C_b = 0;\ C_p = 0;\ Q = 0;\ Q_1 = 0;\ Q_2 = 0 \tag{5.12}$$

The boundary conditions at the inlet and outlet of the column are the conventional Dankwerts conditions (Danckwerts, 1953),

$$Z = 0,\ \frac{\partial C_b}{\partial Z} = \frac{u}{D_b}(C_b - C_0);\ Z = L,\ \frac{\partial C_b}{\partial Z} = 0 \tag{5.13}$$

The boundary conditions for the particle phase in equation (5.8) are

$$R = 0,\ \frac{\partial C_p}{\partial R} = 0;\ R = R_p,\ \frac{\partial C_p}{\partial R} = \frac{k_f}{\varepsilon_p D_p}\left(C_b - C_p \Big|_{R=R_p} \right) \tag{5.14}$$

We assume that the interstitial porosity, particle porosity, and the pore diffusion coefficient are constant, with values that have been previously determined (Wang and Carbonell, 2003). The film mass transfer coefficient and the axial dispersion coefficient are related to the fluid velocity, and thus have to be adjusted according to the variation of the fluid velocity in the calculations using the GR model. The film mass transfer coefficient is estimated using the correlation by Wakao et al. (1958),

$$sh = 2 + 1.45\,\mathrm{Re}^{1/2}\,Sc^{1/3} \tag{5.15}$$

where Sh, Re, and Sc are the Sherwood, Renolds, and Schmidt numbers, respectively. The correlation from Gunn (1987) is used to estimate the axial dispersion coefficient,

$$\frac{D_b}{2R_p u} = \left\{ \frac{\mathrm{Re}\,Sc}{4\alpha_1^2(1-\varepsilon_b)}(1-p)^2 + \frac{\mathrm{Re}^2\,Sc^2}{16\alpha_1^4(1-\varepsilon_b)^2}\,p(1-p)^3 \times \left[\exp\left(\frac{-4\alpha_1^2(1-\varepsilon_b)}{p(1-p)\,\mathrm{Re}\,Sc} \right) - 1 \right] \right\} + \frac{\varepsilon_b}{\tau_b\,\mathrm{Re}\,Sc} \tag{5.16}$$

where

$p = 0.17 + 0.33\exp(-24/\mathrm{Re})$, $\alpha_1 = 2.405$, $\tau_b = 1.4$

Table 5.1 lists all the parameters needed in the calculation using the GR model.

The GR model equations were solved numerically using the finite element method to discretize the bulk phase partial differential equation and the orthogonal collocation method to discretize the pore phase partial differential equation, and then the built-in function *ode15s* in Matlab was used to solve the resultant ordinary differential equations.

5.5 Experimental

5.5.1 Synthesis of Peptide Resins

Peptides YYWLHH were synthesized directly onto Toyopearl AF Amino 650M (TA650M) resins (Tosoh Biosep, Montgomeryville, PA) using standard fluorenylmethyloxycarbonyl (Fmoc) chemistry as described by (Buettner et al., 1996). The

methacrylate-based resins have an average particle size of 65 μm with a 1000 Å average pore diameter. The aminated amino resins were modified with an alanine residue prior to peptide synthesis. To control the peptide density to a final substitution level of 100 μmol peptide/g resin, a 1:1 mixture of Fmoc-L-Alanine and tBoc-L-Alanine was coupled to the aminated resins. The tBoc group was released with TFA and the free amino functionality was acetylated with acetic anhydride. No further peptide synthesis occurred at these acetylated sites. Subsequently, the Fmoc protecting groups were released with piperidine and the free L-Alanine was used to attach Fmoc-protected amino acids until the last cycle was finished.

5.5.2 Log Removal Measurement

Synthesized resins were packed into a relatively small Metal-Free PEEK-Lined column (2.1mm ID × 30mm) from Alltech (Deerfield, IL) in order to minimize the amount of SEB used. The experiments to measure the log removal were carried out using a Waters 616 LC system (Millipore, Milford, MA) at 20°C. The column was pre-equilibrated with the binding buffer, 0.5M NaCl in phosphate buffer saline (PBS), pH 7.4, purchased from Sigma Chemical (St. Louis, MO). The binding buffer spiked with SEB was delivered to the column at a flow rate of 0.075, 0.10, 0.15, and 0.25 ml/min corresponding to superficial velocities of 2.17, 2.89, 4.33 and 7.22 cm/min, respectively. Samples were collected at the exit of the column when the processing time reached 40min. The concentrations of SEB in the collections were determined using ELISA. Under the same conditions for the superficial velocities and the column length, the values of the log removal were calculated using the GR

model when the processing time reached 40min and compared to the experimental log removal results.

5.5.3 ELISA for SEB

A 96-well ELISA plate (Nunc-Immuno Module, Nalge Nunc, Naperville, IL) was coated with 100 μl of 10 μg/ml affinity purified IgG antitoxin solution (Toxin Technology, Sarasota, FL) in each well. The coating buffer was 0.01 M Na_2CO_3, pH 9.6. The coated ELISA plate was incubated overnight at room temperature on a flatbed shaker (MTS4; Ika-Schuttler, Staufen, Germany) at 100 rpm. The next day, the ELISA plate was washed three times with 250μl PBS-Tween (Sigma, St. Louis, MO) added to each well. The third wash was allowed to stand in the wells for at least 15 minutes. 250μl of Superblocker (Pierce, Rockford, IL) was added to each well and incubated for 1 hour in order to reduce background signals. Next, 100 μl of sample solution were added to the wells, and incubated at room temperature for two hours on the flatbed shaker (MTS4; Ika-Schuttler, Staufen, Germany) at 100 rpm. Each sample was done in triplicate. The plate was then washed three times with 250μl PBS-Tween in each well. 100 μl of diluted IgG antitoxin conjugated with horseradish peroxidase (Toxin Technology, Sarasota, FL) was added to each well and incubated for one hour at room temperature on the flatbed shaker (MTS4; Ika-Schuttler, Staufen, Germany) at 100 rpm. After the incubation, the plate was washed ten times with 250μl PBS-Tween in each well. A peroxidase substrate, ABTS (1-Step™ ABTS, Pierce, Rockford, IL), was added

with 100 μl in each well. The solution was incubated at room temperature for 20 minutes and read photometrically at 410 nm.

5.6 Results and Discussion

5.6.1 Simulation Results

Figure 5.1(a) shows the results from the first calculation strategy, namely, fixing the column length to a particular value and changing the fluid velocity to calculate the log removal at the maximum process time as a function of fluid velocity. As shown in Figure 5.1 (a), the log removal as a function of fluid velocity for four different column lengths, 1, 3, 5, and 10 cm, were calculated. Larger fluid velocityies result in a smaller residence time in the column preventing binding of SEB. All the curves except the curve of the 1 cm length in Figure 5.1(a) are nearly parallel. Obviously, longer columns lead to higher log removals due to their longer residence times. For a prescribed log removal (3 or 5 logs), the corresponding fluid velocity can be located in Figure 5.1(a) for a column of fixed length. The residence time can be obtained by dividing the column length by the fluid velocity. Because the flow rate is fixed (12.5 ml/min) as mentioned in the design constraints, the cross-sectional area and column volume can be calculated. Table 5.2 (a) lists the fluid velocities, column dimensions, and residence times of these four columns with different fixed lengths for prescribed log removals (3 and 5 logs). It can be seen that narrow columns are more efficient because of the faster fluid velocity that leads to larger mass transfer rate to the particle

surface. But the increase in mass transfer will be eventually hampered by the rate-limiting steps, film and pore diffusion and surface adsorption-desorption. Both the effective pore diffusion coefficient and the rate constants of the adsorption-desorption do not change with fluid velocity. But the rate of either of these two processes relative to the fluid velocity, namely the number of transfer units (Wang and Carbonell, 2003), tends to be smaller at higher fluid velocities. Therefore, beyond a certain value of the fluid velocity, the pore diffusion and surface adsorption-desorption will dominate the apparent adsorption rate and thus further increases in the fluid velocity make no difference in log removal.

Figure 5.1 (b) shows the results from the second calculation strategy, in which the fluid velocity is fixed and the log removal at the maximum process time is calculated as a function of column length. The log removal as a function of column length for four different fluid velocities, 1, 3, 5, and 10 cm/min, were calculated. Figure 5.1 (b) demonstrates the same trends shown in Figure 5.1 (a) but from a different point to view. The log removal is a nearly linear function of the column length at a fixed fluid velocity. When the fluid velocity is fixed, the mass transfer parameters are constant. For a given fluid velocity, the longer the column, the bigger the column capacity (if the cross-sectional area is specified), which leads to a higher log removal. Meanwhile, a longer column leads to a longer residence time that allows more time for SEB to adsorb to the column. At different fluid velocities, the mass transfer rates that affect the log removals are different. This is the reason why the curves in Figure 5.1(b) have different slopes. Table 5.2 (b) lists the column dimensions and residence times at these four fixed fluid velocities for prescribed log removals (3 and 5 logs). These

results also indicate that narrow columns are more efficient because of the faster fluid velocity that leads to faster intraparticle mass transfer rates.

As a summary of Table 5.2, for 3 logs of removal with the measured rate constants for SEB, the required residence times were in the range of $0.66 < t_r < 0.92$ minutes. The required column dimensions are as follows:

Smallest column: $L = 10$ cm, $A_c = 0.83$ cm^2, $V_c = 8.3$ cm^3

Largest column: $L = 0.92$ cm, $A_c = 12.5$ cm^2, $V_c = 11.51$ cm^3

Similarly, the residence times for 5 logs of removal were in the range of $1.10 < t_r < 1.61$ minutes. The required column dimensions are as follows:

Smallest column: $L = 10.97$ cm, $A_c = 1.25$ cm^2, $V_c = 13.71$ cm^3

Largest column: $L = 1$ cm, $A_c = 20.13$ cm^2, $V_c = 20.13$ cm^3

It is interesting to note that two additional log removals can be achieved with relatively small increases in column volume if longer columns are used.

5.6.2 Effects of Inlet Concentration

In these calculations, the inlet concentration of SEB was set to 0.15 μg/ml, which is much lower than the dissociation constants, 1.9 μg/ml and 102 μg/ml for those two respective binding sites listed in Table 5.1. In this range the isotherms in equation (5.5) and (5.6) tend to be linear. In addition, the desorption rate is fairly small in comparison with the adsorption rate at such a low adsorbed solute concentration. Thus the rate equations (5.10) and (5.11) also tend to be linear. Therefore, the log removal results are essentially

independent of inlet concentration. Figure 5.2 shows the log removal results at a fixed column length (3 cm) and fluid velocity (3 cm/min), respectively. The calculation results are almost identical when the inlet concentration is set to 0.15, 0.015, and 0.0015 μg/ml. When the inlet concentration increases to 15 μg/ml, which is significantly larger than the dissociation constant of the first type of binding site and not significantly smaller than the dissociation constant of the second type of binding site, the isotherm and rate equation become nonlinear. The log removal results are then a function of the inlet concentration. Figure 5.2 shows the effects of the transition from linear chromatography to nonlinear chromatography on log removal results.

Table 5.3 gives the fluid velocities, column dimensions, and residence times at different inlet concentrations for prescribed log removals (3 and 5 logs) based on Figure 5.2 and the design constraints. The column volume for a prescribed log removal remains nearly constant when the inlet concentration is below 0.15 μg/ml. When the inlet concentration increases beyond 0.15 μg/ml, a somewhat larger column is needed to achieve the same log removal.

5.6.3 Effects of Axial Dispersion

Axial dispersion involves molecular diffusion and eddy diffusion. It reduces the efficiency of the chromatography, namely, increases the Height Equivalent to a Theoretical Plate (HETP) of the column. Thus a larger axial dispersion requires a larger column to achieve the same log removal due to the reduction of the column efficiency. Previous results

have shown that the axial dispersion is not a rate-limiting step and its resistance to the mass transfer rate can be neglected in a nonlinear peptide affinity chromatography (Wang and Carbonell, 2003). A comparison of log removal with and without axial dispersion is shown in Figure 5.3 at a fixed column length (3 cm) and fluid velocity (3 cm/min). The log removal curves with axial dispersion included are below the log removal curves without the axial dispersion, indicating that the axial dispersion erodes the column efficiency, but the effect is fairly small.

All the parameters and dimensions required to design columns for prescribed log removals (3 and 5 logs) have been calculated using the same procedure as in the previous sections and listed in Table 5.4. The column volume increases slightly (< 6%) as a result of axial dispersion under these operating conditions.

5.6.4 Effects of Pore Diffusion

Pore diffusion is a rate-limiting step that restricts the mass transfer rate in peptide affinity chromatography (Wang and Carbonell, 2003). The tortuosity of the packing material extends the diffusion path of molecules in the pores so that pore diffusion is slower than the molecular diffusion. The effective diffusivity is determined by dividing the free molecular diffusivity by the tortuosity to account for the effects of pore structure on the diffusion rate. The tortuosity can vary in a fairly large range for different packing materials (Guiochon et al., 1994; LeVan et al., 1997). It is more reliable to treat the tortuosity as an empirical constant that is determined experimentally for any particular chromatography beads. The use

of a value of 4 is recommended when no other information is available (LeVan et al., 1997). The particle effective diffusivity for SEB (D_p) in Toyopearl beads has been determined experimentally to be 4.83×10^{-11} m/s (Wang and Carbonell, 2003). In comparison with the free molecular diffusivity of SEB ($D_m = 7.70\times 10^{-11}$ m/s), the diffusion inside the pores is mildly retarded due to the relatively large pore size (1000 Å) of Toyopearl resins. The effect of the pore diffusion on the log removal is shown in Figure 5.4 when the column length is fixed to 3 cm and the fluid velocity is 3 cm/min. First, in order to know the potential to maximize the efficiency of the column for log removals by increasing the pore diffusion rate, the pore diffusion coefficient is set to its extreme value, the free molecular diffusivity. A general case in which the tortuosity is set to 4 empirically is also compared to the real case in Figure 5.4. It is obvious that intraparticle diffusion has a deleterious effect on column performance. The empirical value of the pore diffusion coefficient (D_m / 4) is too small in this case so that the corresponding log removal results are much smaller than the real case, indicating that the effective diffusivity should be accurately determined experimentally for any specified resin.

Table 5.5 shows the required column dimension and residence time with different effective diffusivities. The larger the pore diffusion rate is, the smaller the column dimension and residence time. It is also seen here that in this case the empirical value of the tortuosity (τ_p=4) results in a column volume that is 33-35% larger than necessary.

5.6.5 Preference for Binding Sites

As mentioned at above, the isotherms approximate linear equations due to the low concentration of SEB. Thus equation (5.5) and (5.6) can be rewritten in the following forms,

$$Q_1^* = K_1 C \tag{5.17}$$

where $K_1 = \dfrac{Q_{m,1}^*}{K_{d,1}}$

$$Q_2^* = K_2 C \tag{5.18}$$

where $K_2 = \dfrac{Q_{m,2}^*}{K_{d,2}}$

The ratio K_1 to K_2 is 13. Thus 93% of adsorbed SEB adsorbes on the first type of binding site at equilibrium. The kinetics of the adsorption–desorption process for SEB has also been considered because it is a rate-limiting step for dynamic SEB binding. As shown in Table 5.1, the adsorption rate constant for the first type of binding site is greater than that for the second type of binding site, while the corresponding desorption rate constant for the first type of binding site is smaller than that for the second type of binding site. Therefore, SEB favors the first type of binding site thermodynamically and kinetically, and hence the contribution from the second type of binding site to the consequent log removal is trivial. In Figure 5.5, the log removal curves in considering both types of binding site in action are compared to calculations with only the first type of binding site when the column length is fixed to 3 cm and the fluid velocity to 3 cm/min. The elimination of SEB binding on the second type of binding site leads to a small error in prediction.

As done in previous sections, the fluid velocities, column dimensions, and residence times for prescribed log removals (3 and 5 logs) are shown in Table 5.6. The results considering that only one type of binding site are in use results in an error of less than 10%.

5.6.6 Effects of Rate Constant

As shown in (Wang and Carbonell, 2003), the intrinsic adsorption-desorption process is the rate-limiting step for chromatography. Equation (5.10) and (5.11) are the rate equations for these two binding sites, respectively. The effects of varying of the rate constants relative to the real rate constants on log removal results are shown in Figure 5.6 when the column length is fixed to 3 cm and the fluid velocity to 3 cm/min, respectively. A limiting case is that the rate constants on both binding sites go to infinity, namely an instant local equilibrium is reached so that the isotherm equations (5.5) and (5.6) are used to calculate the log removal results in the GR model instead of using equations (5.10) and (5.11). It can be seen that the log removal curve at equilibrium is well above the log removal curve of the real case, indicating that the adsorption-desorption rate is crucial in determining column efficiency. If the rate constants of both sites increase by a factor of 10, the log removal curve is fairly close to the equilibrium curve, and the adsorption-desorption process is no longer the rate-limiting step. On the other hand, the column efficiency is dramatically reduced if the rate constants in both sites decrease by a factor of 10.

Table 5.7 lists the required fluid velocities, column dimensions, and residence times for prescribed log removals (3 and 5 logs) based on Figure 5.5 and the design constraints.

Fast adsorption-desorption rates require smaller columns and residence times to achieve the same goal for SEB removal. Noticeably, if the rate constants decrease 10 times in size, the column volume climbs to a value more than 3 times larger than that obtained using the real rate constants. It has been found that higher peptide density leads to larger rate constants and capacities (Wang and Carbonell, 2003). Provided no nonspecific binding was introduced, the use of peptide resins with a high density would reduce the column size for a prescribed log removal.

5.6.7 Simulation Results at Equilibrium

Peptide affinity chromatography is generally rate limited by the intrinsic adsorption-desorption process (Kaufman et al., 2002; Wang and Carbonell, 2003). This has been confirmed by the influences of rate constants on log removal results in Figure 5.5. In a column design, it is desirable to know the maximum potential of the column to favor column optimization.

The data used to generate Figure 5.7 is the same as that of Figure 5.1 except that a local equilibrium was assumed in the simulation. The fluid velocities, column dimensions, and residence times for prescribed log removals (3 and 5 logs) based on Figure 5.7 and the design constraints are presented in Table 5.8. For 3 logs of removal with local equilibrium for SEB, the residence times are in the range of $0.35 < t_r < 0.66$ minutes. The required column dimensions are as follows:

Smallest column: $L = 10$ cm, $A_c = 0.434$ cm^2, $V_c = 4.34$ cm^3

Largest column: L = 0.66 cm, A_c = 12.5 cm^2, V_c = 8.30 cm^3

Similarly, the residence times for 5 logs of removal are in the range of $0.54 < t_r < 1.05$ minutes. The required column dimensions are as follows:

Smallest column: L = 10 cm, A_c = 0.68 cm^2, V_c = 6.8 cm^3

Largest column: L = 1 cm, A_c = 13.07 cm^2, V_c = 13.07 cm^3

It is interesting to note that a longer column can give rise to a smaller resin volume to achieve two additional logs of removal under adsorption equilibrium conditions. In comparison with those calculated with the measured rate constants, the column dimensions assuming adsorption equilibrium are greatly reduced, suggesting increasing rate constants for binding is the best way to minimize column dimension. In addition, as observed earlier, narrow columns lead to smaller column dimensions due to faster fluid velocities that result in larger intraparticle mass transfer rates.

5.6.8 Pressure Drop

Although narrow columns facilitate mass transfer leading to small column dimensions, the pressure drop could increase to a level that is too high to be practicable. The pressure drop in the column can be estimated using the Ergun equation (Bird et al., 1960),

$$\frac{\Delta P}{L} = 150\mu \frac{(1-\varepsilon_b)^2}{d_p^2 \varepsilon_b^3} u_0 + 1.75 \frac{1-\varepsilon_b}{\varepsilon_b^3} \frac{\rho}{d_p} u_0^2 \qquad (5.19)$$

The first term on the right side of equation (5.19) is important at low fluid velocities where the pressure drop in the column is primarily determined by the shear forces. The second term

is more important at higher fluid velocities where the inertial forces of the fluid colliding with the particles contributes significantly to the pressure drop. In most chromatography separations, only the leading term is important. Note that the pressure drop per unit length of column is dependent on the column void fraction, the particle diameter, the fluid density and viscosity and the superficial velocity. Substituting the values of these parameters in Table 5.1 into Equation (5.19), we obtained the pressure drop per unit length of the column in SI units,

$$\frac{\Delta P}{L} = 7.34 \times 10^{8} u_0 + 7.84 \times 10^{8} u_0^2 \qquad (5.20)$$

The fluid velocities in the column were in the range of 0.5 to 15 cm/min (8.33×10^{-5} to 2.50×10^{-3} m/s) in the calculations. The higher velocities are needed in the longer columns with smaller cross-sectional areas and the smaller velocities are to be found in the shorter column with larger cross sectional areas. For all these velocities, the second term is not important and will be neglected from now on. Equation (5.20) can be rewritten in pressure drop and velocity units of (mmHg/cm) and (cm/min), respectively,

$$\frac{\Delta P}{L} = 9.17 u_0 \qquad (5.21)$$

Figure 5.8 shows the pressure drop and the cross-sectional area vs. column length for prescribed log removals (3 and 5 logs). The fluid velocities and column lengths for the calculation of the pressure drop are taken from Table 5.2. Each point on the lines shown in Figure 5.8 represents a design option for the prescribed log removal (3 or 5 logs). Although the fluid velocities are not shown in this figure, they can be determined from the cross-

sectional areas shown in Figure 5.8 and the fixed flow rate (12.5 ml/min). The pressure drops are in the range of $8.47<\Delta P<1381.77$ mmHg for 3 logs of removal, and $5.69<\Delta P<1005.61$ mmHg for 5 logs of removal. In considering the cost of pump delivery and the mechanical properties of chromatography beads, there is a maximum fluid velocity that maximizes the mass transfer rate and does not yield intolerably high pressures.

The pressure drop in a column packed with Toyopearl resins is recommended to be less than 3 kg/cm^2 (2.2×10^3 mmHg) to obtain excellent pressure/flow characteristics. This pressure drop is high enough for all the column dimensions obtained from the simulation for 3 and 5 logs of removal under current conditions. Thus the column could be narrowed further until the pressure drop reaches the maximum value.

5.6.9 Experimental Confirmation

Figure 5.9 shows the simulation vs. experimental log removal results in a fixed dimension column (2.1 mm × 3 cm) by varying the fluid velocity. The simulations matched experimental results very well, indicating that the calculation method is reliable to be used for SEB removal. Recalling the log removal curves are insensitive to the inlet concentrations as shown in Figure 5.2, inlet concentrations (1.5 or 15 μg/ml) higher than 0.15 μg/ml in the simulation were used in the experiment to facilitate the detection using ELISA. As described in the experimental section, 100 μl of samples were taken at the outlet of the column after the maximum process time (40min) for ELISA analysis. The inlet concentration for experimental confirmation was set to 1.5 μg/ml at velocities of 2.89, 4.33, and 7.22 cm/min,

respectively, and 15 μg/ml at 2.17 cm/min. The match of the simulations with the experimental data beyond 5 logs cannot be checked due to the detection limit of the ELISA (~0.1 ng/ml).

5.7 Conclusions

Peptide affinity chromatography columns packed with a short peptide ligand, YYWLHH, have demonstrated several log removal of SEB from a feed with a given fixed volume (500 ml) within a given processing time (40 minutes). Two design strategies were investigated, one is to fix the column length and calculate the log removal as a function of fluid velocity at the maximum process time, the other is to fix the fluid velocity and calculate the log removal as a function of column length at the maximum process time. Both strategies led to several design options with various column lengths and cross-sectional areas for prescribed log removals (3 and 5 logs) of SEB. The general rate (GR) model with previously determined mass transfer parameters was used to do these calculations. It has been found that narrow columns are more efficient because of the faster fluid velocity (larger mass transfer rate). Various factors that could affect the column design have been investigated. If the inlet concentration of SEB is significantly smaller than the dissociation constants in the isotherm, the column dimensions for prescribed log removals are the same for different inlet concentrations because the isotherm and rate equations are linear. Although there are two types of binding sites on the adsorbent, most of SEB molecules tend to bind the higher affinity sites because both sites are not saturated at such low inlet concentrations of protein.

The neglect of the second type of binding site with weaker affinities led to only slightly different log removal results. Axial dispersion showed a very small increase in column dimensions for prescribed log removals, confirming a previously drawn conclusion that the axial dispersion is a fast process and not a rate-limited step (Wang and Carbonell, 2003). Pore diffusion is a rate-limiting step and showed a much larger effect than axial dispersion on column dimensions. It is recommended to have an accurate effective diffusivity because the results from empirical correlation can yield a large error. The intrinsic adsorption-desorption is rate limiting as well (Wang and Carbonell, 2003). An increase in the rate constants to approximate an instant equilibrium can dramatically increase the column efficiency and reduce the column dimensions for prescribed log removals. Although a narrow column gives high efficiency, the high pressure drop built in it may limit its use in practice. The Toyopearl resin used in these studies can withstand the resulting pressure drops under conditions of the simulation. Finally, the results of an experimental study matched the simulation results very well demonstrating the reliability of the column design strategy.

5.8 Nomenclature

A_c	Cross-sectional area of the column
C_0	Feed concentration
C_b	Concentration in the bulk phase
C_p	Concentration in the stagnant fluid phase inside the particle pores
C_{out}	Outlet concentration, $C_b(Z=L)$
D_b	Axial dispersion coefficient
D_p	Effective diffusion coefficient inside the particle pores
D_m	Molecular diffusion coefficient
d_p	Particle diameter
F_r	Log removal factor, $-\log_{10}\left(\frac{C_{out}(t_m)}{C_f}\right)$
K	Distribution constant, $\frac{Q_m^*}{K_d}$
K_d	Dissociation constant
k_a	Adsorption rate constant
k_d	Desorption rate constant
k_f	Film mass transfer coefficient
L	Column length
Mw	Molecular weight of SEB
p	Probability of the axial displacement

ΔP	Pressure drop
Q	Concentration in the solid phase (based on unit volume of particle skeleton)
Q_m^*	Adsorption saturation capacity (based on unit volume of particle skeleton)
R	Radial coordinate
R_p	Particle radius
Re	Reynolds number, $2R_p\rho u\varepsilon_b/\mu$
Sc	Schmidt number, $\mu/(\rho D_m)$
Sh	Sherwood number, $k_f(2R_p)/D_m$
t	Time
t_r	Retention time
t_m	Maximum processing time
u	Interstitial velocity, u_0/ε_b
u_0	Superficial fluid velocity
V_c	Column volume
V_m	Volume of fluid that needs to be processed
Z	Axial coordinate

Greek Letters

α_1	First root of the zero-order Bessel function
ε_b	Interstitial porosity
ε_p	Particle porosity

μ	Mobile phase viscosity
ρ	Mobile phase density
τ_b	Column tortuosity
τ_p	Particle tortuosity

Subscripts

1, 2	Type I binding sites, type II binding sites

Superscripts

*	Equilibrium value

5.9 References

Balaban N, Rasooly A. 2000. Review: Staphylococcal enterotoxins. Int J Food Microbiol 61:1-10.

Bastek PD, Land JM, Baumbach GA, Hammond DH, Carbonell RG. 2000. Discovery of Alpha-1-proteinase inhibitor binding peptides from the screening of a solid phase combinatorial peptide library. Separation Sci Technol 35:1681-1706.

Bird RB, Stewart WE, Lightfoot EN. 1960. Transport Phenomena. N. Y.: J. Wiley & Sons.

Buettner JA, Dadd CA, Baumbach GA, Masecar BL, Hammond DJ. 1996. Chemically derived peptide libraries: A new resin and methodology for lead identification. Int J Peptide Protein Res 47:70-83.

Danckwerts PV. 1953. Continuous flow system: Distribution of residence times. Chem Eng Sci 2:1-18.

Enserink M, Malakoff D. 2001. Bioterrorism: Congress weighs select agent update. Science 294:1438-1438.

Evenson ML, Hinds MW, Bernstein RS, Bergdoll MS. 1988. Estimation of human dose of staphylococcal enterotoxin A from a large outbreak of staphylococcal food poisoning involving chocolate milk. Int J Food Microbiol 7:311-316.

Franz DR, Jahrling PB, Friedlander AM, McClain DJ, Hoover DL, Bryne WR, Pavlin JA, Christopher CW, Eitzen EM. 1997. Clinical recognition and management of patients exposed to biological warfare agents. J Am Med Assoc 278:399-411.

Gu T. 1995. Mathematical modeling and scale-up of liquid chromatography. New York: Springer.

Guiochon G, Shirazi SG, Katti AM. 1994. Fundamentals of preparative and nonlinear chromatography. New York: Academic Press.

Gunn DJ. 1987. Axial and radial dispersion in fixed beds. Chem Eng Sci 42:363-373.

Gurgel PV, Carbonell RG, Swaisgood HE. 2001a. Fractionation of whey proteins with a hexapeptide ligand affinity resin. Bioseparation 9:385-392.

Gurgel PV, Carbonell RG, Swaisgood HE. 2001b. Identification of peptide ligands generated by combinatorial chemistry that bind alpha-Lactalbumin. Separation Sci Technol 36:2411-2431.

Kaufman DB, Hentsch ME, Baumbach GA, Buettner JA, Dadd CA, Huang PY, Hammond DJ, Carbonell RG. 2002. Affinity purification of fibrinogen using a ligand from a peptide library. Biotechnol Bioeng 77:278-289.

Lee DC, Miller JLC, Petteway SR. 2002. Pathogen safety of manufacturing processes for biological products: special emphasis on KOGENATE Bayer. Haemophilia 8:6-9.

LeVan MD, Carta G, Yon CM. 1997. Adsorption and ion exchange. In: Perry RH, Green DW, editors. Chemical Engineer's Handbook. New York: MacGraw-Hill.

Li H, Llera A, Malchiodi EL, Mariuzza RA. 1999. The structural basis of T cell activation by superantigens. Annu Rev Immunol 17:435-466.

Miller JLC, Petteway SR, Lee DC. 2001. Ensuring the pathogen safety of intravenous immunoglobulin and other human plasma-derived therapeutic proteins. J Allergy Clin Immunol 108:S91-94.

Wagman J, Edwards RC, Schantz EJ. 1965. Molecular size, homogeneity, and hydrodynamic properties of purified staphylococcal enterotoxin B. Biochemistry 4:1017-1023.

Wakao N, Oshima T, Yagi S. 1958. Mass transfer from packed beds of particles to a fluid. Kagaku Kogaku 22:780-785.

Wang G, Carbonell RG. 2003. Characterization of a peptide ligand that binds selectively to staphylococcal enterotoxin B (SEB). Chapter 4.

Wang G, De J, Schoeniger JS, Roe DC, Carbonell RG. 2003. A hexamer peptide ligand that binds selectively to staphylococcal enterotoxin B (SEB): Isolation from a solid phase combinatorial peptide library. Chapter 3.

Table 5.1 Parameters needed in the GR model (Wang and Carbonell, 2003).

Parameter	*Definition*	***Value***
R_p	Particle radius	32.5×10^{-6} m
C_f	Inlet concentration	0.15 g/m^3
Mw	SEB molecular weight	28,366
ρ	Mobile phase density	1000 kg/m^3
ε_b	Interparticle void fraction	0.29
ε_p	Particle Porosity	0.70
μ	Mobile phase viscosity	0.001 Pa·s
D_b	Axial dispersion coefficient	Equation (5.14)
D_m	Molecular diffusion coefficient	7.7×10^{-11} m^2/s (Wagman et al., 1965)
D_p	Diffusion coefficient inside the pores	4.827×10^{-11} m^2/s
k_f	Film mass transfer coefficient	Equation (5.13)
$Q_m^*{}_{,1}$	Capacity constant of type I sites	0.430 mol/m^3 * (8.496 mg/g)
$Q_m^*{}_{,2}$	Capacity constant of type II sites	1.742 mol/m^3 * (34.421 mg/g)
$K_{d,1}$	Dissociation constant of type I sites	6.745×10^{-5} mol/m^3 (1.913×10^{-3} mg/ml)
$K_{d,2}$	Dissociation constant of type II sites	3.595×10^{-3} mol/m^3 (0.102 mg/ml)
$k_{a,1}$	Adsorption rate constant on type I sites	5.949 m^3 mol^{-1} s^{-1}
$k_{a,2}$	Adsorption rate constant on type II sites	0.404 m^3 mol^{-1} s^{-1}
$k_{d,1}$	Desorption rate constant on type I sites	4.013×10^{-4} s^{-1}
$k_{d,2}$	Desorption rate constant on type II sites	1.454×10^{-3} s^{-1}

Note: the bulk density of resins is 320 ± 4 mg/ml; (*): based on unit volume of particle skeleton

Table 5.2 Cross-sectional area, column volume, and residence time for 3 and 5 log removal of SEB. **(a)** Fixed column length. **(b)** Fixed fluid velocity.

(a)

Column length (L) (cm)	Fluid velocity (u_0) (cm/min)	Cross area (A) (cm^2)	Column volume (V) (cm^3)	Residence time (t_r) (min)
		3 log removal		
1	1.1022	11.3410	11.3410	0.9073
3	3.9648	3.1527	9.4581	0.7567
5	7.0405	1.7754	8.8770	0.7102
10	15.0684	0.8296	8.2960	0.6636
		5 log removal		
1	0.6210	20.1288	20.1288	1.6103
3	2.2959	5.4445	16.3335	1.3067
5	4.1497	3.0123	15.0615	1.2049
10	9.0319	1.3840	13.8400	1.1072

(b)

Fluid velocity (u_0) (cm/min)	Column length (L) (cm)	Cross area (A) (cm^2)	Column volume (V) (cm^3)	Residence time (t_r) (min)
		3 log removal		
1	0.9211	12.5000	11.5138	0.9211
3	2.3533	4.1667	9.8055	0.7844
5	3.6847	2.5000	9.2118	0.7369
10	6.8705	1.2500	8.5881	0.6871
		5 log removal		
1	1.4902	12.5000	18.6275	1.4902
3	3.7805	4.1667	15.7522	1.2602
5	5.9031	2.5000	14.7578	1.1806
10	10.9663	1.2500	13.7079	1.0966

Table 5.3 Cross-sectional area, column volume, and residence time for 3 and 5 log removal of SEB at various loading concentrations. **(a)** Fixed column length (3 cm). **(b)** Fixed fluid velocity (3 cm/min).

(a)

Inlet concentration	Fluid velocity (u_0) (cm/min)	Cross area (A) (cm^2)	Column volume (V) (cm^3)	Residence time (t_r) (min)
		3 log removal		
C_0/100	3.9685	3.1498	9.4494	0.7560
C_0/10	3.9681	3.1501	9.4503	0.7560
C_0	3.9648	3.1527	9.4581	0.7567
10*C_0	3.9303	3.1804	9.5412	0.7633
100*C_0	3.5675	3.5039	10.5117	0.8409
		5 log removal		
C_0/100	2.2970	5.4419	16.3257	1.3061
C_0/10	2.2969	5.4421	16.3263	1.3061
C_0	2.2959	5.4445	16.3335	1.3067
10*C_0	2.2854	5.4695	16.4085	1.3127
100*C_0	2.1852	5.7203	17.1609	1.3729

(b)

Inlet concentration	Column length (L) (cm)	Cross area (A) (cm^2)	Column volume (V) (cm^3)	Residence time (t_r) (min)
		3 log removal		
C_0/100	2.3512	4.1667	9.7967	0.7837
C_0/10	2.3514	4.1667	9.7976	0.7838
C_0	2.3533	4.1667	9.8055	0.7844
10*C_0	2.3722	4.1667	9.8842	0.7907
100*C_0	2.5766	4.1667	10.7359	0.8589
		5 log removal		
C_0/100	3.7789	4.1667	15.7455	1.2596
C_0/10	3.7791	4.1667	15.7464	1.2597
C_0	3.7805	4.1667	15.7522	1.2602
10*C_0	3.7946	4.1667	15.8110	1.2649
100*C_0	3.9558	4.1667	16.4826	1.3186

Note: C_0=0.15 g/m^3.

Table 5.4 Effect of axial dispersion on cross-sectional area, column volume, and residence time for 3 and 5 log removal of SEB. **(a)** Fixed column length (3 cm). **(b)** Fixed fluid velocity (3 cm/min).

(a)

Axial dispersion (D_b)	Fluid velocity (u_0) (cm/min)	Cross area (A) (cm^2)	Column volume (V) (cm^3)	Residence time (t_r) (min)
		3 log removal		
+	3.9648	3.1527	9.4581	0.7567
-	4.1427	3.0174	9.3222	0.7242
		5 log removal		
+	2.2959	5.4445	16.3335	1.3067
-	2.4442	5.1141	15.3423	1.2274

(b)

Axial dispersion (D_b)	Column length (L) (cm)	Cross area (A) (cm^2)	Column volume (V) (cm^3)	Residence time (t_r) (min)
		3 log removal		
+	2.3533	4.1667	9.8055	0.7844
-	2.2520	4.1667	9.3834	0.7507
		5 log removal		
+	3.7805	4.1667	15.7522	1.2602
-	3.6107	4.1667	15.0447	1.2036

Note: (+): with axial dispersion; (-): without axial dispersion

Table 5.5 Effect of pore diffusion on cross-sectional area, column volume, and residence time for 3 and 5 log removal of SEB. **(a)** Fixed column length (3 cm). **(b)** Fixed fluid velocity (3 cm/min).

(a)

Diffusion coefficient	Fluid velocity (u_0) (cm/min)	Cross area (A) (cm^2)	Column volume (V) (cm^3)	Residence time (t_r) (min)
		3 log removal		
D_p	3.9648	3.1527	9.4581	0.7567
D_m	4.5485	2.7482	8.2446	0.6596
D_m/τ_p	2.9336	4.2610	12.7830	1.0226
		5 log removal		
D_p	2.2959	5.4445	16.3335	1.3067
D_m	2.5947	4.8175	14.4525	1.1562
D_m/τ_p	1.7200	7.2674	21.8022	1.7442

(b)

Diffusion coefficient	Column length (L) (cm)	Cross area (A) (cm^2)	Column volume (V) (cm^3)	Residence time (t_r) (min)
		3 log removal		
D_p	2.3533	4.1667	9.8055	0.7844
D_m	2.1155	4.1667	8.8146	0.7052
D_m/τ_p	3.0644	4.1667	12.7684	1.0215
		5 log removal		
D_p	3.7805	4.1667	15.7522	1.2602
D_m	3.3943	4.1667	14.1430	1.1314
D_m/τ_p	4.9221	4.1667	20.5089	1.6407

Note: $\tau_p = 4$.

Table 5.6 Effect of binding sites on cross-sectional area, column volume, and residence time for 3 and 5 log removal of SEB. **(a)** Fixed column length (3 cm). **(b)** Fixed fluid velocity (3 cm/min).

(a)

Binding sites	Fluid velocity (u_0) (cm/min)	Cross area (A) (cm^2)	Column volume (V) (cm^3)	Residence time (t_r) (min)
		3 log removal		
I+II	3.9648	3.1527	9.4581	0.7567
I	3.7036	3.3751	10.1253	0.8100
		5 log removal		
I+II	2.2959	5.4445	16.3335	1.3067
I	2.1403	5.8403	17.5209	1.4017

(b)

Binding sites	Column length (L) (cm)	Cross area (A) (cm^2)	Column volume (V) (cm^3)	Residence time (t_r) (min)
		3 log removal		
I+II	2.3533	4.1667	9.8055	0.7844
I	2.5006	4.1667	10.4193	0.8335
		5 log removal		
I+II	3.7805	4.1667	15.7522	1.2602
I	4.0319	4.1667	16.7997	1.3440

Note:

- (I+II): consideration of both types of binding sites.
- (I): consideration of the first type of binding site.

Table 5.7 Effect of rate constants on cross-sectional area, column volume, and residence time for 3 and 5 log removal of SEB. **(a)** Fixed column length (3 cm). **(b)** Fixed fluid velocity (3 cm/min).

(a)

Adsorption rate constant	Fluid velocity (u_0) (cm/min)	Cross area (A) (cm^2)	Column volume (V) (cm^3)	Residence time (t_r) (min)
		3 log removal		
k_a/10	1.1958	10.4533	31.3599	2.5088
k_a	3.9648	3.1527	9.4581	0.7567
10*k_a	6.2287	2.0068	6.0204	0.4816
∞	6.8631	1.8213	5.4639	0.4371
		5 log removal		
k_a/10	0.7002	17.8520	53.5560	4.2845
k_a	2.2959	5.4445	16.3335	1.3067
10*k_a	3.6622	3.4132	10.2396	0.8192
∞	4.0761	3.0667	9.2001	0.7360

(b)

Adsorption rate constant	Column length (L) (cm)	Cross area (A) (cm^2)	Column volume (V) (cm^3)	Residence time (t_r) (min)
		3 log removal		
k_a/10	7.2022	4.1667	30.0094	2.4007
k_a	2.3533	4.1667	9.8055	0.7844
10*k_a	1.6585	4.1667	6.9105	0.5528
∞	1.5514	4.1667	6.4642	0.5171
		5 log removal		
k_a/10	11.9013	4.1667	49.5891	3.9671
k_a	3.7805	4.1667	15.7522	1.2602
10*k_a	2.5695	4.1667	10.7063	0.8565
∞	2.3732	4.1667	9.8884	0.7911

Table 5.8 Cross-sectional area, column volume, and residence time for 3 and 5 log removal of SEB at equilibrium. **(a)** Fixed column length. **(b)** Fixed fluid velocity.

(a)

Column length (L) (cm)	Fluid velocity (u_0) (cm/min)	Cross area (A) (cm^2)	Column volume (V) (cm^3)	Residence time (t_r) (min)
		3 log removal		
1	1.7009	7.3491	7.3491	0.5879
3	6.8631	1.8213	5.4639	0.4371
5	12.7508	0.9803	4.9015	0.3921
10	28.8116	0.4339	4.3390	0.3471
		5 log removal		
1	0.9564	13.0698	13.0698	1.0456
3	4.0839	3.0608	9.1824	0.7346
5	7.8218	1.5981	7.9905	0.6392
10	18.3842	0.6799	6.7990	0.5439

(b)

Fluid velocity (u_0) (cm/min)	Column length (L) (cm)	Cross area (A) (cm^2)	Column volume (V) (cm^3)	Residence time (t_r) (min)
		3 log removal		
1	0.6641	12.5000	8.3013	0.6641
3	1.5544	4.1667	6.4767	0.5181
5	2.3292	2.5000	5.8230	0.4658
10	4.0887	1.2500	5.1109	0.4089
		5 log removal		
1	1.0359	12.5000	12.9488	1.0359
3	2.3732	4.1667	9.8884	0.7911
5	3.5183	2.5000	8.7958	0.7037
10	6.0861	1.2500	7.6076	0.6086

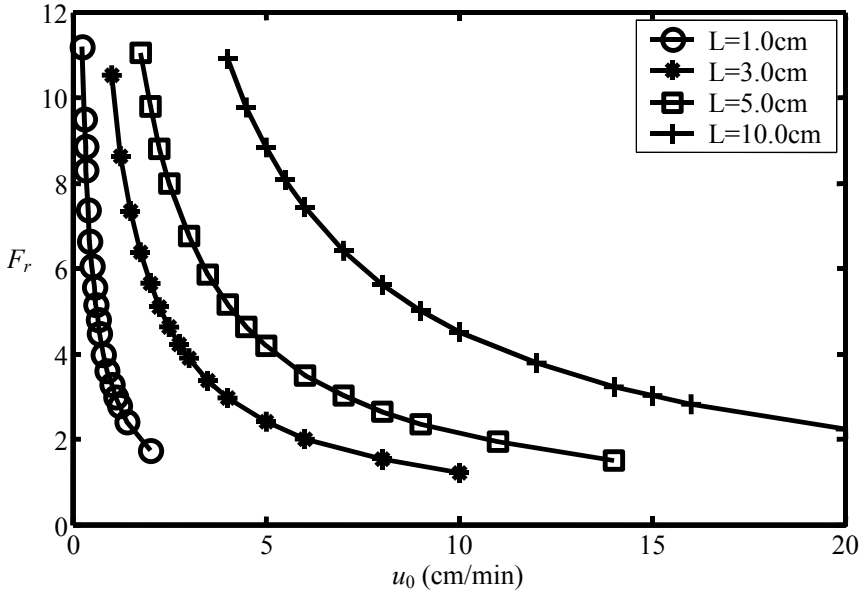

(a)

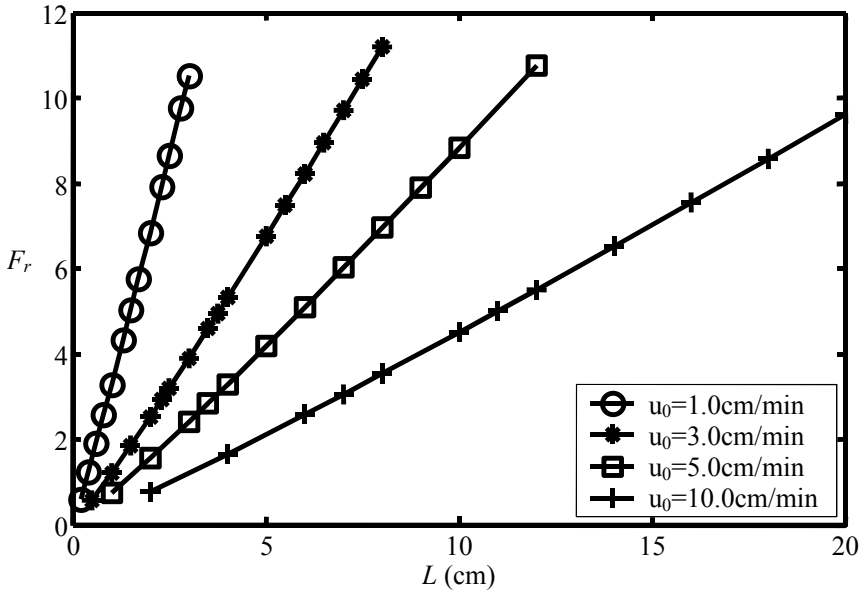

(b)

Figure 5.1 Effect of column length and fluid velocity on log removal of SEB. **(a)** Fixed column length. **(b)** Fixed fluid velocity.

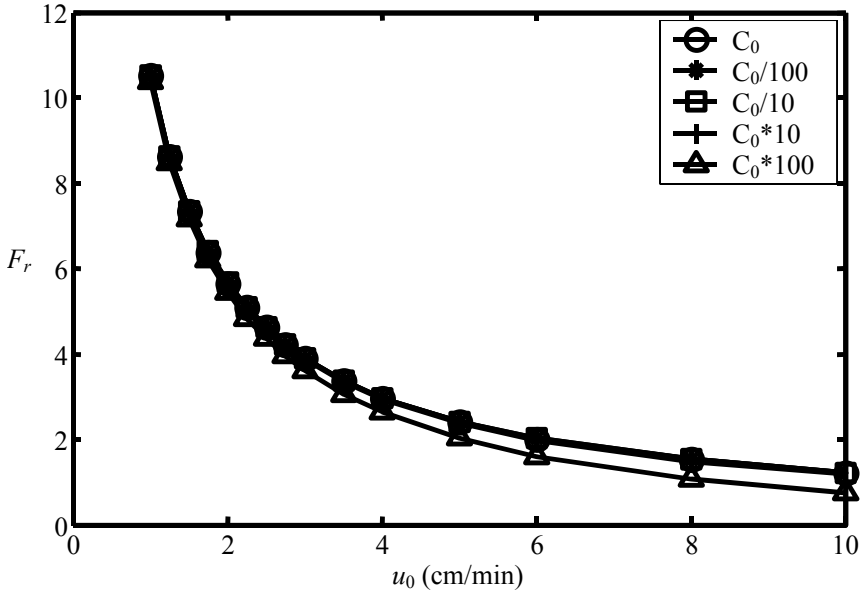

(a)

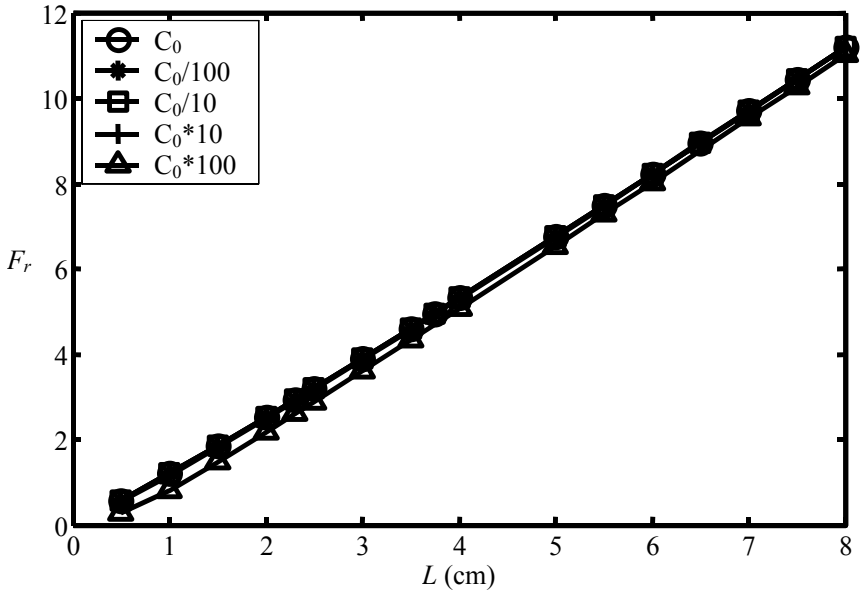

(b)

Figure 5.2 Effect of loading concentration on log removal of SEB. **(a)** Fixed length (3 cm). **(b)** Fixed fluid velocity (3 cm/min).

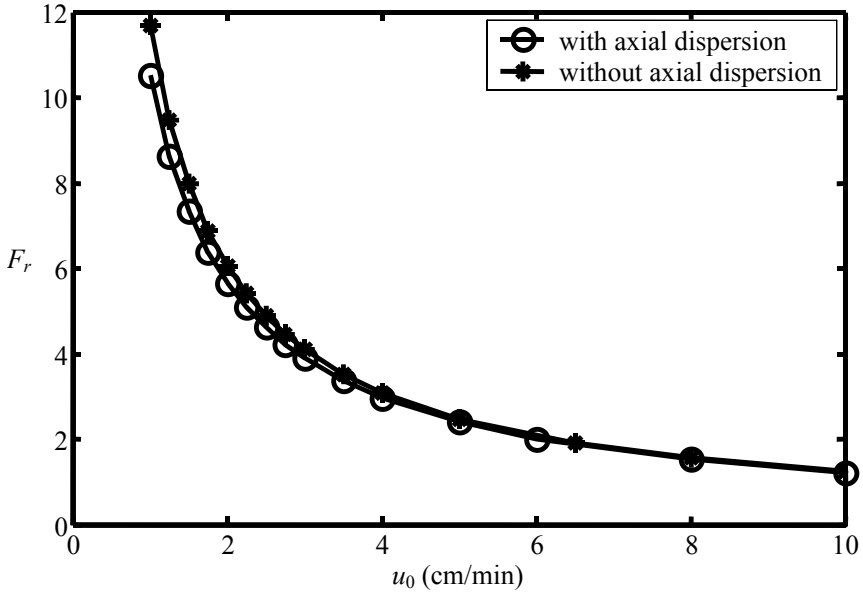

(a)

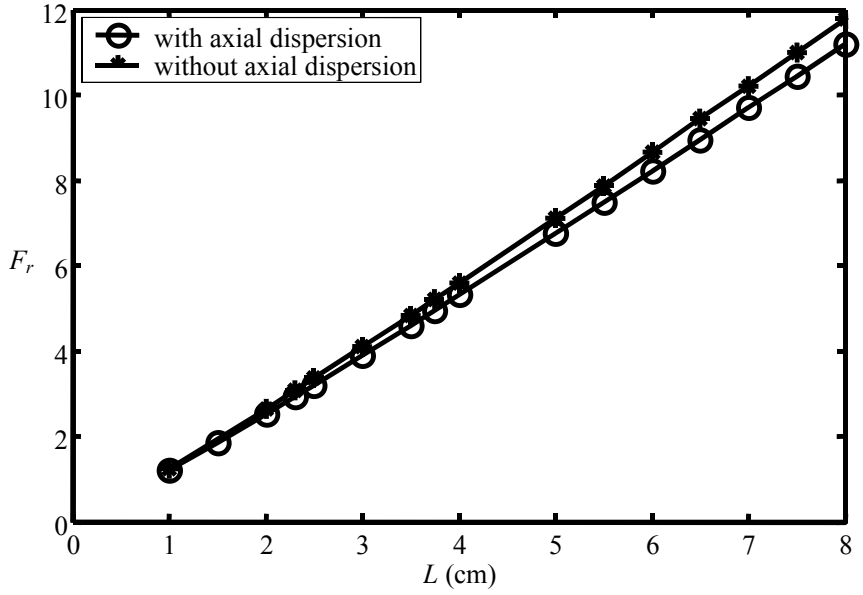

(b)

Figure 5.3 Effect of axial dispersion on log removal of SEB. **(a)** Fixed column length (3cm). **(b)** Fixed fluid velocity (3cm/min).

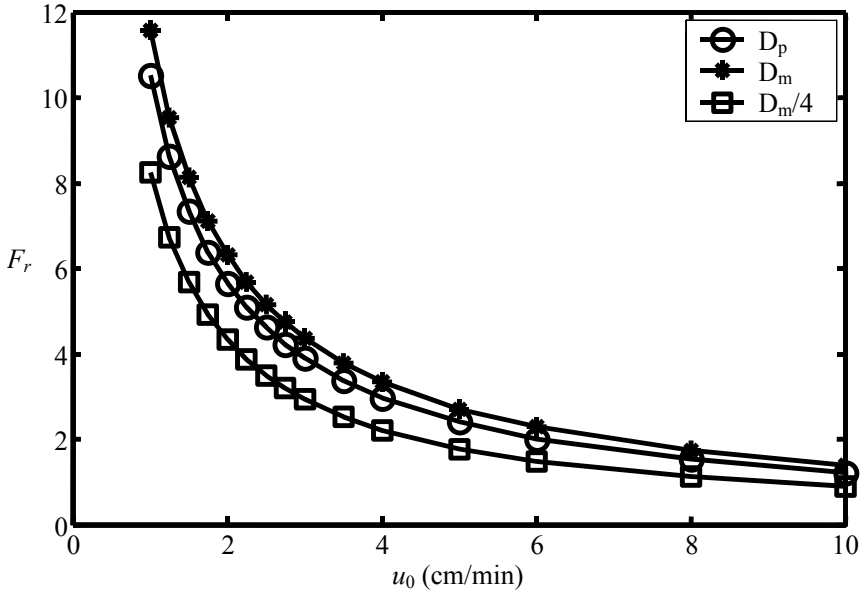

(a)

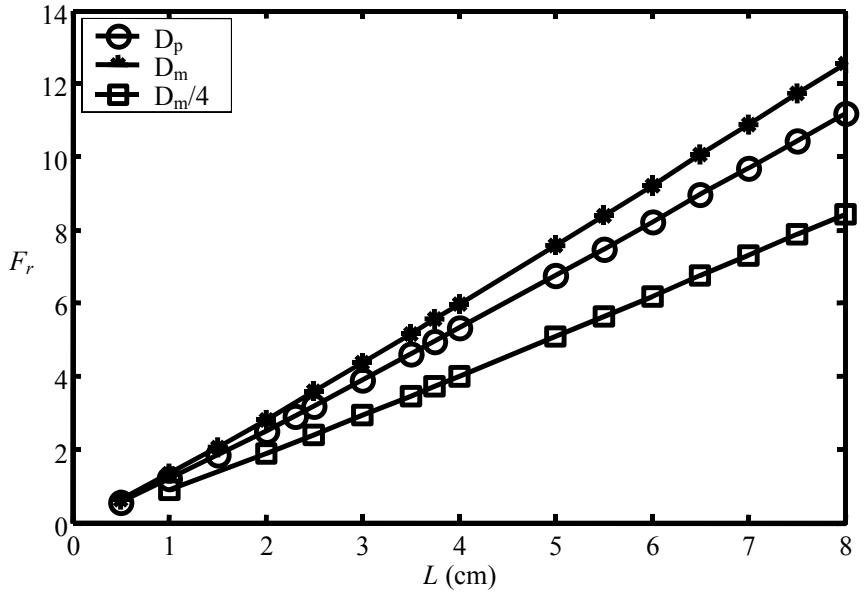

(b)

Figure 5.4 Effect of pore diffusion on log removal of SEB. **(a)** Fixed column length (3 cm). **(b)** Fixed fluid velocity (3 cm/min).

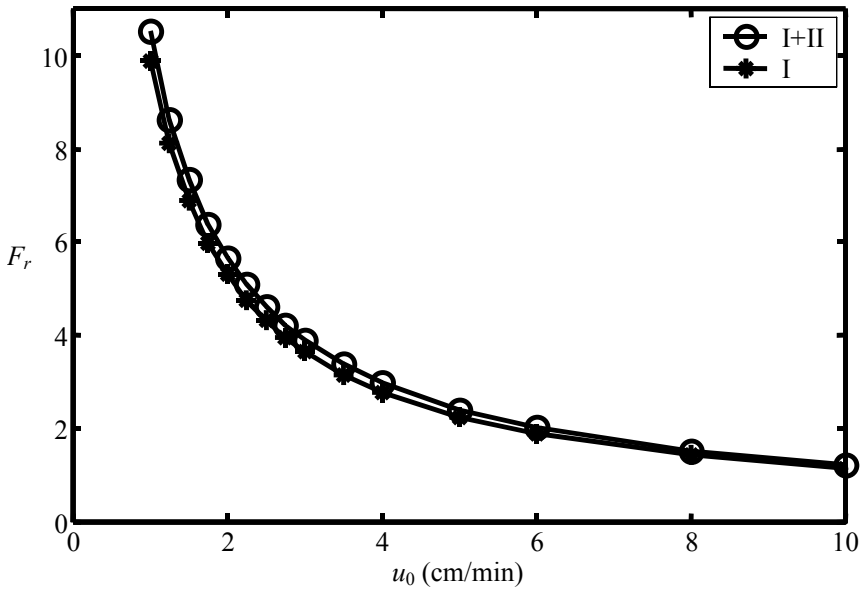

(a)

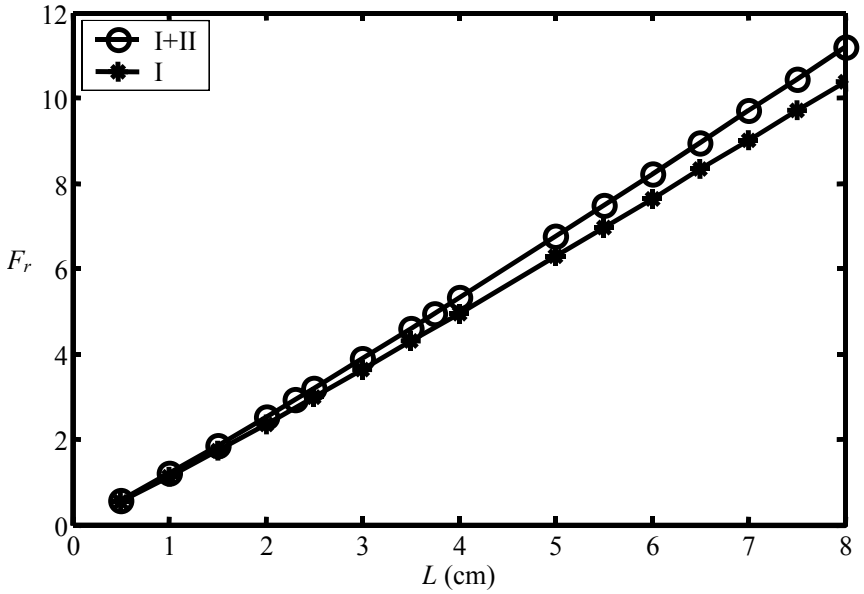

(b)

Figure 5.5 Effect of bonding sites on log removal of SEB. **(a)** Fixed column length (3cm). **(b)** Fixed fluid velocity (3cm/min).

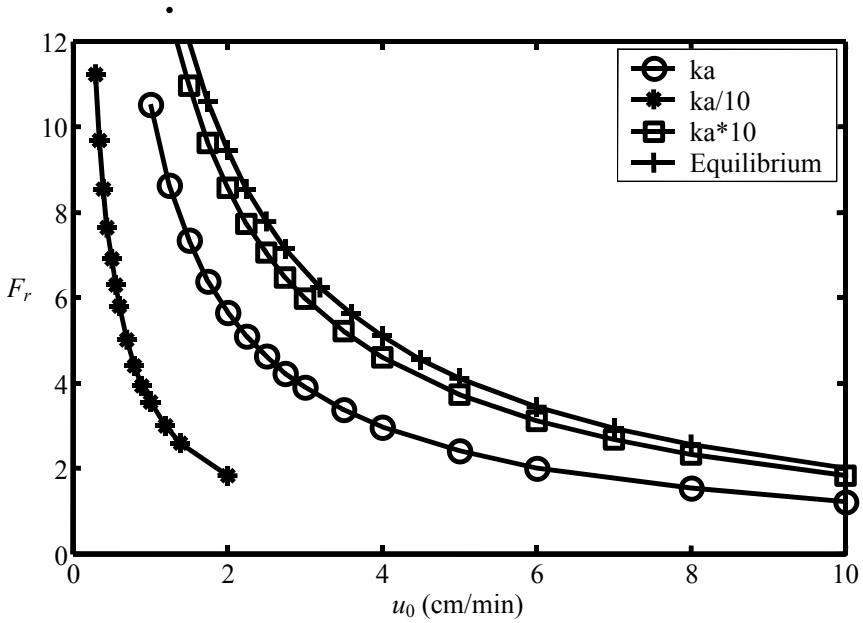

(a)

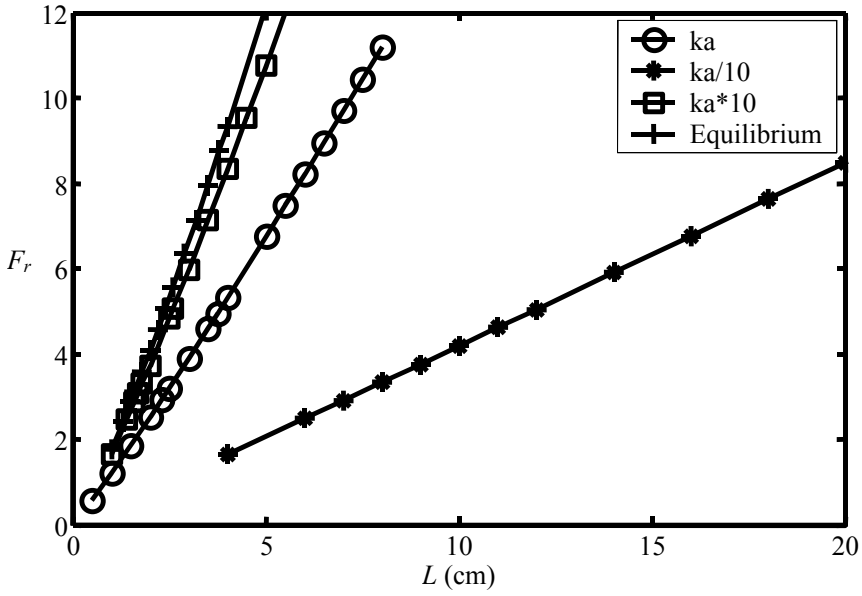

(b)

Figure 5.6 Effect of rate constants on log removal of SEB. **(a)** Fixed column length (3 cm). **(b)** Fixed fluid velocity (3 cm/min).

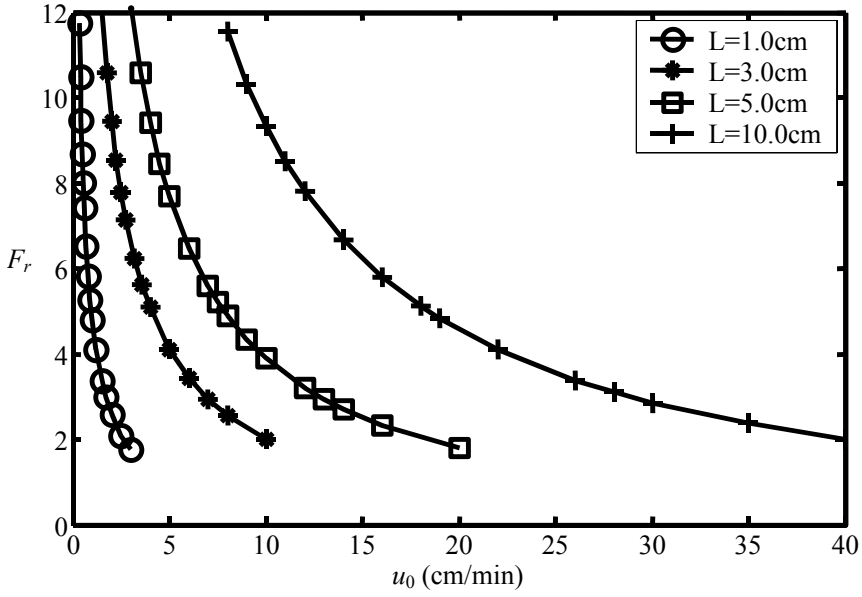

(a)

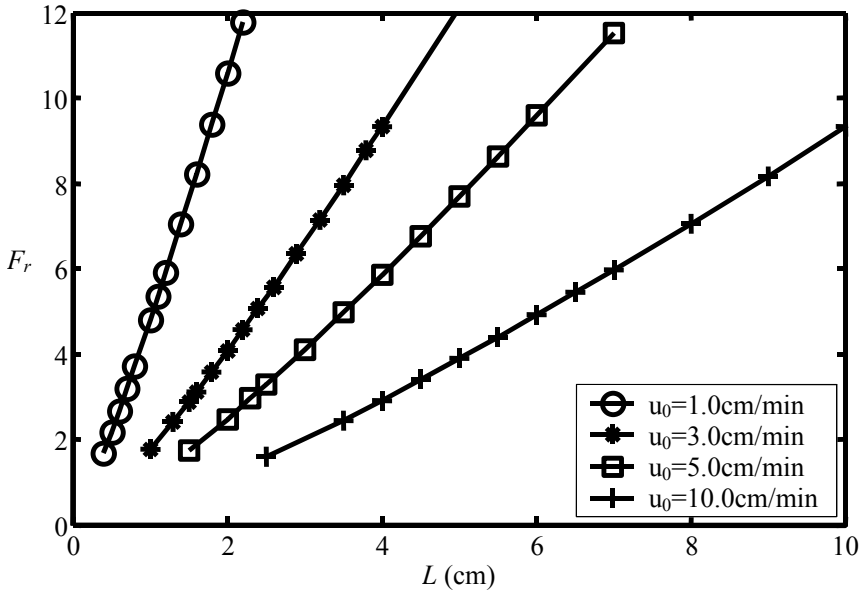

(b)

Figure 5.7 Effect of column length and fluid velocity on log removal of SEB at equilibrium. **(a)** Fixed column length. **(b)** Fixed fluid velocity.

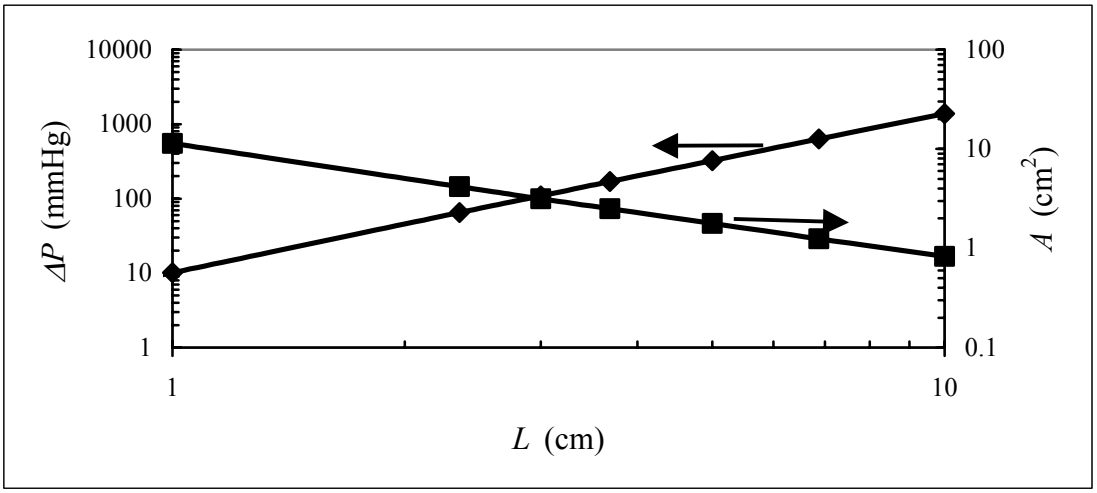

(a)

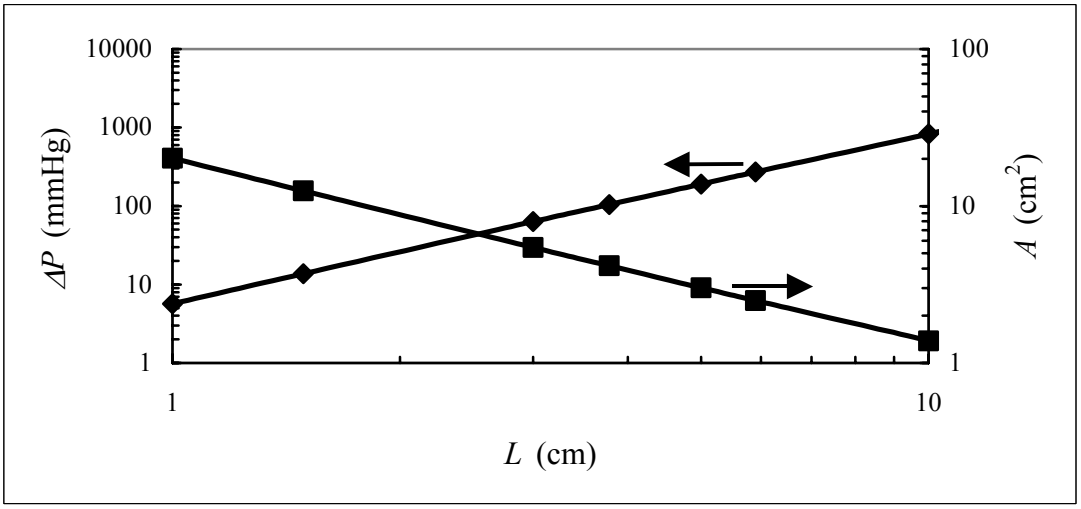

(b)

Figure 5.8 Pressure drop and cross-sectional area for prescribed log removals. **(a)** 3 logs. **(b)** 5 logs.

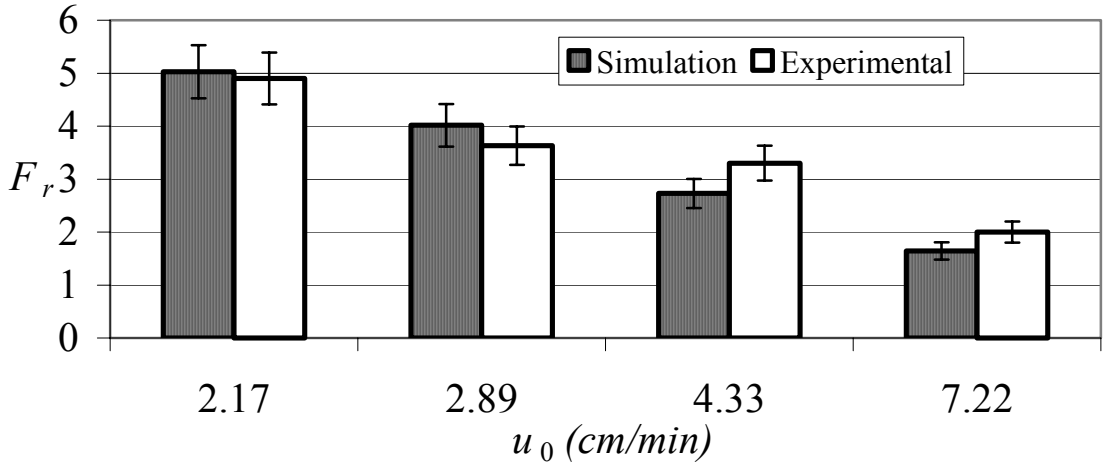

Figure 5.9 Experimental vs. simulated log removal values of SEB in a 2.1mm × 3.0 cm column.

CHAPTER 6

PEPTIDE-AFFINITY SOLID-PHASE EXTRACTION FOR TRACE ANALYSIS OF STAPHYLOCOCCAL ENTEROTOXIN B (SEB)

Guangquan Wang, Ruben G. Carbonell

Department of Chemical Engineering, North Carolina State University

1017 Main Campus Drive, Centennial Campus

Partner's Building I, Suite 3200, Box 7006

Raleigh, NC 27695-7006

This is a manuscript in preparation for submission to

Analytical Chemistry

Abstract

Staphylococcal enterotoxin B (SEB) is a primary toxin that causes food poisoning. It is considered a potential bioterrorism threat as either an aerosol or food and water contaminant and is listed by the Center for Diseases Control (CDC) as a select agent. The detection of trace SEB in biological and environmental samples is a challenging analytical task. Sample extraction and trace enrichment can significantly improve the sensitivity of detection methods for SEB, such as ELISA and HPLC. Due to its high affinity, stability and capacity, peptide ligand resins can be suitable stationary phases that could be used in a solid-phase extraction column for sample preparation. In this paper, it is demonstrated that trace enrichment and clean-up for SEB can be achieved in a single step by using a hexamer peptide YYWLHH, which selectively binds to SEB. 0.5 ng of SEB in 0.1, 1.0, 10, and 100 ml of buffer respectively can be completely captured by the YYWLHH column and eluted in 0.1ml of 2% acetic acid, and then analyzed by ELISA. The sensitivity of ELISA can be improved by a thousand fold (from to 5 ng/ml to 5 pg/ml) by enrichment from peptide-affinity solid-phase extraction. Such an efficient method for sample preparation might have great potential to help detect SEB in food and ground water.

Keywords: ELISA, peptide ligands; solid-phase extraction; staphylococcal enterotoxin B

6.1 Introduction

Staphylococcal enterotoxins (SEs) are leading causes of food poisoning and are potent gastrointestinal toxins (Archer and Young, 1988). They are also superantigens that bind to major histocompatibility complex class II molecules (MHCII) and T cells bearing particular Vβ elements, triggering a massive release of T cell-derived cytokines followed by allergic and autoimmune symptoms (Balaban and Rasooly, 2000) and the eventual disappearance or inactivation of responding T cells (Li et al., 1999). Due to the extreme toxicity of SEs, and their inherent stability, they are considered a significant bioterrorism threat as either an aerosol or food and water contaminant (Franz et al., 1997), and are listed by the CDC as select agents (Enserink and Malakoff, 2001). Therefore it is important to improve the analytical methods available for detecting SEs. Although ELISA is the primary method to detect SEs, its use has been limited by the fact that many antibodies are not specific, and cross-react with other closely related analytes; moreover, ELISA is better suited to detection in biological samples such as blood and urine, rather than complex environmental matrices (Stevenson, 2000). The popular analytical methods, such as high-performance liquid chromatography (HPLC), capillary electrophoresis (CE) and mass spectrometry (MS), could be more widely used if the samples are properly enriched. Sample preparation is the rate-limiting step in the overall detection procedure when dealing with complex matrices, such as dairy food samples. Solid-phase extraction (SPE) has been widely used to prepare samples for many applications in the past 20 years and continues to be a dynamic field in analytical chemistry (Delaunay et al., 2000; Liska, 2000; Stevenson, 2000).

SPE typically has four steps: a priming step to ensure conditions are optimal for retention of the analyte, a retention step where the matrix is applied to the cartridge/column, a rinsing step to wash out the interferences, and an elution step where the purified analyte is collected for analysis (James, 2000). The highly selective SPE method, immuno-affinity SPE, has been coupled to HPLC to detect trace analytes in biological fluids instead of ELISA (Delaunay et al., 2000; Stevenson, 2000). Recently, both immunoaffinity chromatography and cation exchange have been used in the SPE methods to prepare staphylococcal enterotoxin samples for ELISA or western blotting leading to higher sensitivity and efficiency of detection (Balaban and Rasooly, 2001; Lapeyre et al., 2001). Short peptides from combinatorial peptide libraries have shown high affinity and stability for the purification of various proteins (Gurgel et al., 2001; Huang and Carbonell, 1995; Kaufman et al., 2002), and as a result potentially could be used as an SPE method to improve the detection of the corresponding protein. Peptide ligands can be more specific than an ion exchanger and more stable than antibodies making them good candidates in the SPE method.

The aims of this work is to demonstrate a simple protocol for the enrichment and elution (in a small volume) of SEB from a peptide column of YYWLHH to improve the detection limit of ELISA.

6.2 Materials and Methods

6.2.1 Synthesis of Peptide Resins

Peptides YYWLHH were synthesized directly onto Toyopearl AF Amino 650M (TA650M) resins (Tosoh Biosep, Montgomeryville, PA) using standard fluorenylmethyloxycarbonyl (Fmoc) chemistry as described by (Buettner et al., 1996). The methacrylate-based resins have an average particle size of 65 μm with a 1000 Å average pore diameter. The aminated amino resins were modified with an alanine residue prior to peptide synthesis. To control the peptide density to a final substitution level of 100 μmol peptide/g resin, a 1:1 mixture of Fmoc-L-Alanine and tBoc-L-Alanine was coupled to the aminated resins. The tBoc group was released with TFA and the free amino functionality was acetylated with acetic anhydride. No further peptide synthesis occurred at these acetylated sites. Subsequently, the Fmoc protecting groups were released with piperidine and the free L-Alanine was used to attach Fmoc-protected amino acids until the last cycle was finished.

6.2.2 Effect of Flow Rate on SEB Binding

32 mg of peptide beads were packed into a microbore column (2.1 mm ID×30 mm) from Alltech (Deerfield, IL) and tested on a Waters 616 LC system (Millipore, Milford, MA) with a UV detector (Knauer, Germany) at 280 nm. The column was pre-equilibrated with ~50 column volumes binding buffer (PBS + 0.5 M NaCl) at 0.15 ml/min (260 cm/hr). SEB samples (no any other background protein) were injected through a 100 μl loop (Thomson,

Springfield, VA) at various flow rates (0.02, 0.05, 0.10, 0.15, 0.20 and 0.25 ml/min) for 10 minutes. The flow rate was set to 0.15 ml/min for the remainder of the run. The column was washed sequentially with the binding buffer for 10 minutes, 1 M NaCl in PBS for 20 minutes, and then 2% acetic acid in water for another 20 minutes.

6.2.3 Solid-phase Extraction of SEB

Synthesized resins were packed into a relatively small Metal-Free PEEK-Lined column (2.1mm ID × 30mm) from Alltech (Deerfield, IL). The experiments on solid-phase extraction of SEB were carried out using a Waters 616 LC system (Millipore, Milford, MA) at 20°C. The column was pre-equilibrated with the binding buffer, 0.5 M NaCl in phosphate buffer saline (PBS), pH 7.4, purchased from Sigma Chemical (St. Louis, MO). 0.5 ng of SEB in 0.1, 1.0, 10, and 100 ml of binding buffer were loaded into the peptide column at a flow rate of 0.1ml/min. After each injection, the column was rinsed with PBS buffer for 10 minutes. The bound SEB was released in a 2% acetic acid elution step. Samples of eluate (100 μl each) were collected at the exit of the column and neutralized with 2 M Tris, pH 10.5, to bring the pH to 7. The concentrations of SEB in the collected eluate samples were determined using an ELISA as described below. Collected elution samples from the same column with a loading of binding buffer instead of SEB samples were used as the control in the ELISA detection.

6.2.4 ELISA for SEB

A 96-well ELISA plate (Nunc-Immuno Module, Nalge Nunc, Naperville, IL) was coated with 100 μl of 10 μg/ml affinity purified IgG antitoxin solution (Toxin Technology, Sarasota, FL) in each well. The coating buffer is 0.01 M Na_2CO_3, pH 9.6. The coated ELISA plate was incubated overnight at room temperature on a flatbed shaker (MTS4; Ika-Schuttler, Staufen, Germany) at 100 rpm. The next day, the ELISA plate was washed three times with 250μl PBS-Tween (Sigma, St. Louis, MO) added to each well. The third wash was allowed to stand in the wells for at least 15 minutes. 250μl of Superblocker (Pierce, Rockford, IL) was added to each well and incubated for 1 hour in order to reduce background signals. Next, 100 μl of sample solution were added to the wells, and incubated at room temperature for two hours on the flatbed shaker (MTS4; Ika-Schuttler, Staufen, Germany) at 100 rpm. Each sample was done in triplicate. The plate was then washed three times with 250μl PBS-Tween in each well. 100 μl of diluted IgG antitoxin conjugated to horseradish peroxidase (Toxin Technology, Sarasota, FL) was added to each well and incubated for one hour at room temperature on the flatbed shaker (MTS4; Ika-Schuttler, Staufen, Germany) at 100 rpm. After the incubation, the plate was washed ten times with 250μl PBS-Tween in each well. A peroxidase substrate, ABTS (Pierce, Rockford, IL), was added with 100 μl in each well. The solution was incubated at room temperature for 20 minutes and read photometrically at 410 nm.

6.3 Results and Discussion

6.3.1 ELISA for SEB

Figure 6.1 shows a standard curve for the detection of SEB. Under the experimental conditions of the ELISA, the reliable detection range is 1~8 ng/ml of SEB. Any concentration beyond 8 ng/ml will cause a nonlinear standard curve (data not shown). On the other hand, the absorbance is too small to be reliable when the concentration is below 1 ng/ml. Therefore, in order to detect SEB in a sample at a concentration less than 1 ng/ml, an enrichment step, such as solid-phase extraction, is needed. In the section below, we demonstrate the use of the peptide column for this purpose.

6.3.2 Solid-phase Extraction of SEB

The flow rate is an important parameter that affects recoveries of analytes, especially with low-performance sorbents because of their slow mass transfer and binding kinetics (Delaunay et al., 2000). Therefore, high flow rates may prevent the analytes from binding to the immobilized ligands. The loading flow rate for SEB binding to the YYWLHH column was studied in pulse injections (Figure 6.2). The SEB peak area of the elution was almost constant at low flow rates and then decreased when the flow rate was larger than 0.5 ml/min (Table 6.1), indicating that the binding performance is not sensitive to the loading flow rate until the flow rate is larger than 0.5 ml/min (14.44 cm/min). It has been determined earlier that the pore diffusion and binding kinetics are the rate-limiting steps for the binding of SEB

on columns of YYWLHH (Wang and Carbonell, 2003). In order to use the peptide column efficiently, the loading flow rate was kept at 0.1 ml/min to ensure complete binding.

To illustrate the enrichment of SEB in a YYWLHH column, the detection of 0.5 ng SEB at various solution concentrations is demonstrated. Table 6.2 shows that the 0.5 ng of SEB can be completely recovered from 0.1, 1.0, 10, and 100 ml of loading samples respectively using the peptide column. As the control, no SEB was detected from the column without SEB in the loading. In the routine ELISA, 0.5 ng of SEB is analyzed at a concentration of 5 ng/ml in 100 μl of solution to obtain reliable results. When the SEB solution is diluted and the concentration is as low 5pg/ml, it is of the detection range of ELISA. The diluted samples were loaded into the peptide column and the bound SEB was eluted and enriched and collected in 100 μl of solution. The SEB was completely recovered, so that the concentration in the enriched samples was approximately 5 ng/ml and easily detected by ELISA. Since the lowest concentration sample in Table 6.2 was 5.0 pg/ml, and it was enriched 1000 fold to 5.0 ng/ml, the detection limit for this SPE-ELISA is 1000 fold higher than can be achieved without enrichment.

6.3.3 Column Capacity

The capacity of peptide ligand YYWLHH for SEB binding has been determined (Wang and Carbonell, 2003). The binding experimental data were well fitted to the bi-Langmuir equation. There are two noncompetitive binding sites on the ligand YYWLHH for SEB, one has the maximum capacity of 8.5 mg/g with high affinity to SEB, and the other has

the maximum capacity of 34.4 mg/g but with low affinity. The total maximum capacity for SEB is 42.9 mg/g. ~32 mg peptide beads were packed in a column. As a result, the column capacity is ~1.37mg of SEB, which is much higher than that of immuno-affinity columns (Delaunay et al., 2000; Lapeyre et al., 2001). For the capture of 0.5 ng of SEB, only a small part of the high affinity binding sites were occupied.

6.3.4 Column Reusability

It has been found that the recovery of SEB was not affected after ten runs of loading, washing, elution, and regeneration for column YYWLHH using pulse injection of 0.05mg of SEB in 100 μl of sample. No experiments have been carried out with more than ten runs. Kaufman reported that a peptide column FLLVPL for fibrinogen purification could be subjected over 180 cycles running without loss of recovery (Kaufman et al., 2002). Because of the high capacity of the peptide column, the enrichment of a small amount of SEB, e.g. 0.5 ng, from diluted samples are likely to be unaffected even though the capacity drops significantly. Therefore, a peptide-affinity extraction column should be more durable than a peptide affinity column for protein purification.

6.4 Conclusion

The use of peptide affinity columns has been demonstrated for protein purification. This chapter presents the application of a peptide column YYWLHH in a solid-phase

extraction mode to enrich trace SEB to improve its detection. Due to its high affinity and capacity, the peptide column can retain trace SEB and release it in a small volume of elution buffer even if the sample volume is 1000 times larger than the original one. By using ELISA, the concentrated SEB was easier to analyze. The peptide-affinity SPE coupled ELISA extended the detection limit from 5 ng/ml to 5 pg/ml and would be well suited for toxin detection.

6.5 Reference

Archer DL, Young EE. 1988. Contemporary issues: diseases with food vector. Clin Microbiol Rev 1:377-398.

Balaban N, Rasooly A. 2000. Review: Staphylococcal enterotoxins. Int J Food Microbiol 61:1-10.

Balaban N, Rasooly A. 2001. Analytical chromatography for recovery of small amounts of staphylococcal enterotoxins from food. Int J Food Microbiol 64:33-40.

Buettner JA, Dadd CA, Baumbach GA, Masecar BL, Hammond DJ. 1996. Chemically derived peptide libraries: A new resin and methodology for lead identification. Int J Peptide Protein Res 47:70-83.

Delaunay N, Pichon V, Hennion M. 2000. Immunoaffinity solid-phase extrction for the trace-analysis of low-molecular-mass analytes in complex sample matrices. J Chromatogr B 745:15-37.

Enserink M, Malakoff D. 2001. Bioterrorism: Congress weighs select agent update. Science 294:1438-1438.

Franz DR, Jahrling PB, Friedlander AM, McClain DJ, Hoover DL, Bryne WR, Pavlin JA, Christopher CW, Eitzen EM. 1997. Clinical recognition and management of patients exposed to biological warfare agents. J Am Med Assoc 278:399-411.

Gurgel PV, Carbonell RG, Swaisgood HE. 2001. Fractionation of whey proteins with a hexapeptide ligand affinity resin. Bioseparation 9:385-392.

Huang PY, Carbonell RG. 1995. Affinity purification of proteins using ligands derived from peptide libraries. Biotechnol Bioeng 47:288-297.

James C. 2000. Solid phase extraction. In: Venn RF, editor. Principles and practice of bioanalysis. New York: Taylor & Francis. p 28-43.

Kaufman DB, Hentsch ME, Baumbach GA, Buettner JA, Dadd CA, Huang PY, Hammond DJ, Carbonell RG. 2002. Affinity purification of fibrinogen using a ligand from a peptide library. Biotechnol Bioeng 77:278-289.

Lapeyre C, Maire T, Messio S, Dragacci S. 2001. Enzyme immunoassay of staphylococcal enterotoxins in dairy products with cleanup and concentration by immunoaffinity column. J AOAC Int 84:1587-1592.

Li H, Llera A, Malchiodi EL, Mariuzza RA. 1999. The structural basis of T cell activation by superantigens. Annu Rev Immunol 17:435-466.

Liska I. 2000. Fifty years of solid-phase extraction in water analysis - historical development and overview. J Chromatogr A 885:3-16.

Stevenson D. 2000. Immuno-affinity solid-phase extraction. J Chromatogr B 745:39-48.

Wang G, Carbonell RG. 2003. Characterization of a peptide ligand that binds selectively to staphylococcal enterotoxin B (SEB). Chapter 4.

Table 6.1 Effect of loading flow rate on the recovery of SEB

Flow rate (ml/min)	Flow velocity (cm/min)	Peak area (μV-Sec)
0.05	1.44	5046058
0.15	4.33	5030411
0.30	8.67	4971579
0.50	14.44	5007227
1.00	28.87	4419025
1.50	43.33	3683751

Table 6.2 Recovery of 0.5 ng of SEB from samples with different volumes

SEB in the loading (ng)	Volume (ml)	Concentration (ng/ml)	Recovery* (ng)
0	N/A	0	0
0.5	0.1	5	0.537±0.037
	1.0	0.5	0.690±0.109
	10	0.05	0.659±0.194
	100	0.005	0.523±0.052

*: All bound SEB eluted in 100 μl of 2% acetic acid and then neutralized before doing ELISA.

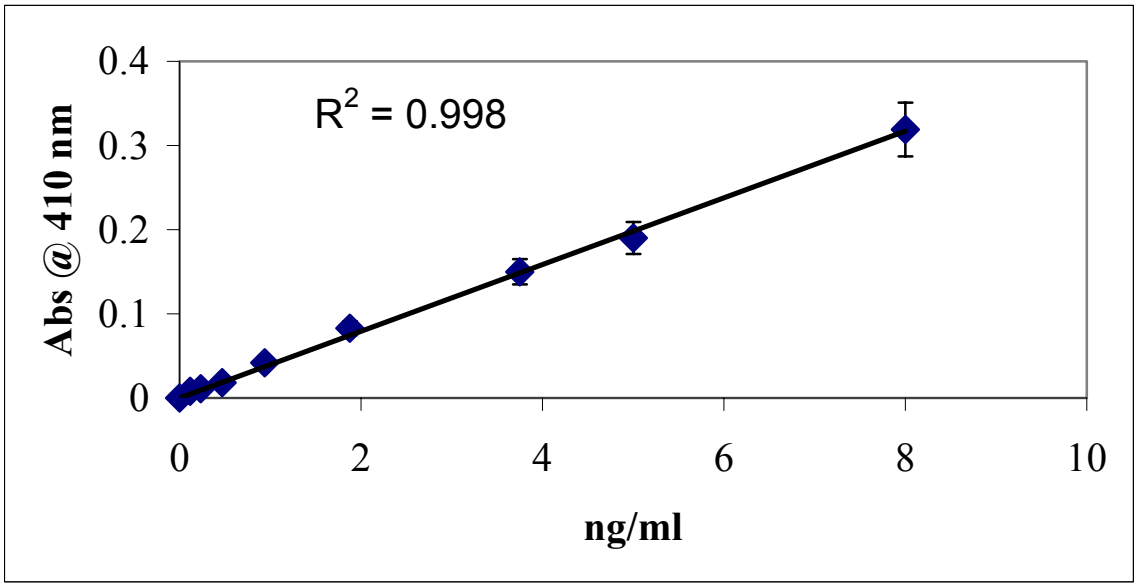

Figure 6.1 ELISA standard curve for SEB detection

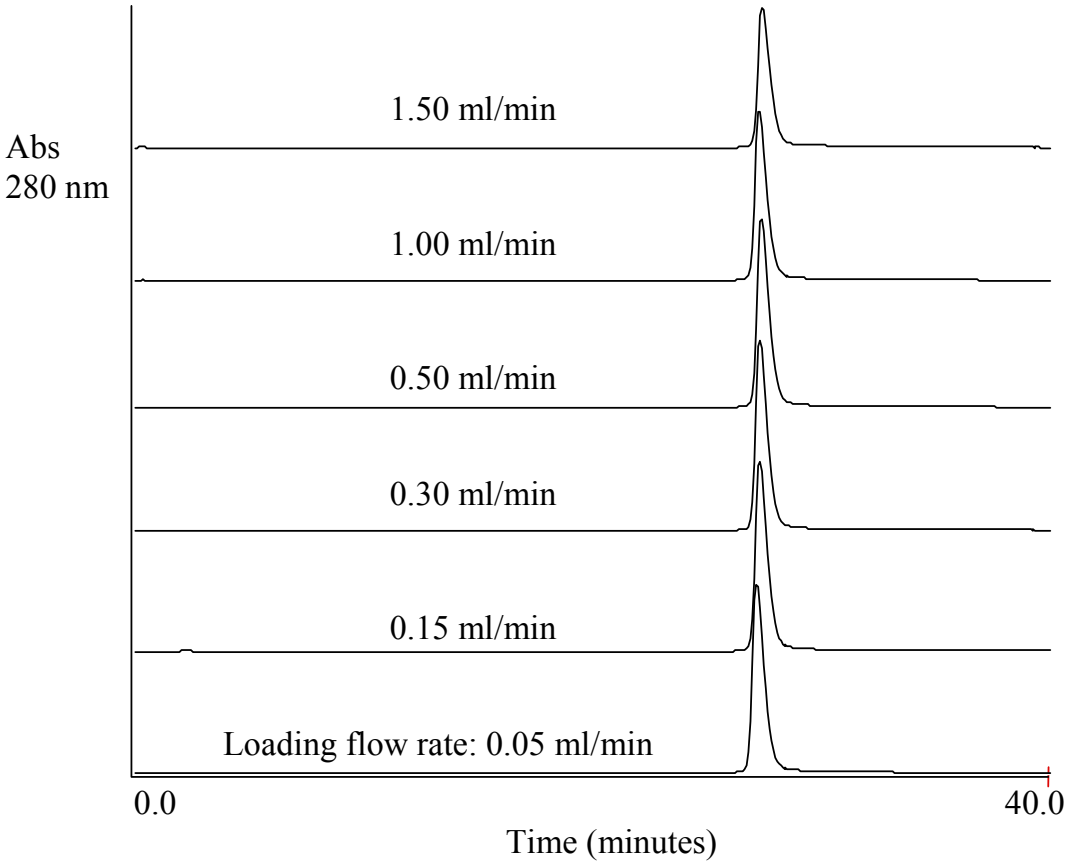

Figure 6.2 Effect of loading flow rate on SEB binding

CHAPTER 7

CONCLUSIONS AND RECOMMENDATIONS FOR FUTURE WORK

7.1 Conclusions

7.1.1 Identification of Peptide Ligands that Bind SEB by Screening Combinatorial Peptide Libraries

A short peptide ligand, YYWLHH, which selectively binds SEB, was identified from a combinatorial peptide library by using a multi-tier screening process. The whole screening process consists three of consecutive steps, namely, the primary, secondary, and tertiary screening. In the primary screening against ^{14}C-labled SEB, twelve peptide leads that bound possibly for SEB were picked up from approximately 1.7 million lead compounds in a hexamer peptide library. The secondary screening employed a batch format to confirm the binding of SEB with/without other competitive proteins and consequently found only one peptide (YYWLHH) bound SEB significantly from the twelve positive peptides. In the tertiary screening, peptide beads bearing ligand YYWLHH were packed into a column and then studied for SEB binding in a chromatography format. It was found that the interaction between SEB and peptide YYWLHH is not electrostatic because 1M of salt cannot elute the bound SEB. The facts that SEB cannot bind to hydrophobic control columns suggest that the interaction between SEB and peptide YYWLHH is specific.

7.1.2 Cross Reactivity with Other Bacterial Superantigens

All SEs share significant sequence homology and have similar three-dimensional structure, and therefore a ligand that binds one of them could show cross reactivity to others. The cross reactivity of column YYWLHH has been studied against three other bacterial toxins, SEA, SEC1, and TSST1. SEB shows 31%, 67%, and 16% sequence homology with SEA, SEC1, and TSST1 respectively. It was found that peptide column YYWLHH showed cross reactivity to TSST1 possibly due to the similarity in tertiary structure, but minor cross reactivity to SEA and SEC1.

7.1.3 Purification of SEB Using A Peptide Affinity Column

In order to demonstrate the selectivity and specialty of peptide column YYWLHH, we carried out one-step purification of SEB from *E. coli* lysate, BSA, and *Staphylococcal aureus* fermentation broth respectively. Some BSA and several hydrophobic proteins in *E. coli* lysate bound to the peptide column nonspecifically. However, a good level of resolution of the SEB peak and the nonspecific elution peak was obtained because nonspecifically bound proteins exhibit different binding mechanisms when compared with SEB. SEB is produced from *Staphylococcal aureus* fermentation. By using the peptide column YYWLHH, SEB was purified successfully from *Staphylococcal aureus* cell extract with high recovery and purity. In the breakthrough purification of SEB, where the peptide column was

overloaded with cell extract, an unknown protein was gradually accumulated in the column and then eluted after the SEB peak in the elution buffer (2% acetic acid).

7.1.4 Binding of Native vs. Nicked SEB

The most likely binding site in the SEB molecule for ligand YYWLHH was derived from studying the binding of native and nicked SEB. Native proteases in SEB preparations can break down the disulfide loop in the SEB molecule to form two nicked toxins. The peptide column YYWLHH cannot retain these two nicked toxins and only showed affinity to native SEB. This indicates that the binding site in the SEB molecule for the peptide ligand is probably associated with the disulfide loop. Aromatic amino acids occur at both ends of the disulfide loop and the disulfide bond could bring these hydrophobic residues to form a hydrophobic pocket, which favors hydrophobic interactions with YYWLHH. Meanwhile, there are some charged and polar amino acids inside the disulfide loop which can potentially hydrogen bond or have weak polar interactions with the peptide ligand. Therefore, the driving force for the SEB binding to ligand YYWLHH might be a combination of hydrophobic interactions, hydrogen bonding, and weak polar interactions.

7.1.5 Modeling Peptide Affinity Chromatography: An Investigation on Adsorption Isotherm, Mass transfer, and Binding Kinetics

The bi-Langmuir isotherm was more suitable than the Langmuir isotherm to fit the experimental data for SEB binding. It suggests that there are two noncompetitive binding

sites on the resins, namely, a high-energy binding site with a small capacity and a low-energy binding site with a large capacity.

Modeling peptide affinity chromatography can help us understand the rates of binding of SEB to peptide ligand and obtain design parameters for a column that can be used either to purify, remove or detect this toxin and other pathogens. The general rate (GR) model was used to fit the breakthrough curve in a YYWLHH column for SEB binding. This model considered all the mass transfer resistances in chromatography, namely, axial dispersion, film mass transfer, pore diffusion, and intrinsic adsorption-desorption kinetics. The mass transfer parameters (axial dispersion and pore coefficients) were determined by pulse experiments using HETP analysis under unretained conditions. The film mass transfer coefficient was estimated from a specific correlation. According to the bi-Langmuir isotherm, Langmuir kinetics, which is second order in adsorption and first order in desorption, can describe SEB adsorption-desorption at either binding site. The intrinsic rate constants were estimated by fitting the breakthrough curve with the GR model using nonlinear regression. The finite element method and the orthogonal collocation method were used to discretize the bulk phase partial differential equation and the pore phase partial differential equation, respectively. An analysis of the number of transfer units revealed that film and intraparticle mass transfer and intrinsic adsorption were rate-limiting steps.

7.1.6 Effect of Peptide Density

The peptide density on the resin's surface had a significant impact on the resin's performance. It was found that with increasing peptide density the dissociation constants first increased to reach a maximum value, then decreased. This phenomenon indicates that there might be a transition in binding mechanism with increase in peptide density. At a relatively low peptide density, each peptide ligand is likely to bind the cleft of each SEB molecule and the surface density favors 1:1 peptide/protein interactions. With increases in peptide density, the binding of SEB to peptide ligand might be hindered due to steric effects leading to an increase in the dissociation constant. When the peptide density reaches a specific value, the peptides may form a hydrophobic layer on the resin's surface and each SEB molecule tends to adjust its conformation to contact several peptides. Therefore, the binding mechanism changes to multipoint binding from single point binding. This can lead to a decrease in the dissociation constant with increase in peptide density. A decrease and then a minimum value of the maximum capacity were observed first with increase in peptide density due to steric effects on the 1:1 peptide/protein interactions. Subsequently, the maximum capacity increased with increase in peptide density due to the change to multipoint binding mechanism.

The GR model was used to fit the breakthrough curves to obtain the rate of binding at different peptide densities. It was found that the rate constants experienced the same change as the dissociation constants did with increase in peptide density, and the intrinsic adsorption was always the rate-limiting step for peptide resins with the density ranging from 6 to 220 μmol/g.

7.1.7 Column Design for Pathogen Log Removal

Design criteria were analyzed for an adsorptive column aimed at reducing the concentration of an infectious pathogen from a known volume of a process stream by several logs in a fixed amount of time. The general rate (GR) model of chromatography was used in the analysis, including all major transport and kinetic steps in the adsorption process. Two design options were analyzed, one fixing the column length and varying the fluid velocity, and the other fixing the fluid velocity and varying the column length. The results indicate that the reduction in SEB concentration is highly dependent on the residence time in the column, which is in turn dependent on the flow rate and column geometry. The theory, with no adjustable parameters, was shown to predict with great accuracy the effect of residence time on the log removal of SEB from an aqueous stream using an affinity resin with the peptide YYWLHH.

The impacts of mass transfer and kinetics on protein purification that is aimed at high yields and purity have been well investigated. But there is little information of these effects on column design for pathogen log removal, which is more stringent than the column design for protein purification. It turned out that film and pore diffusion and adsorption-desorption kinetics had significant impacts on the residence time and column geometry and thereby were limiting factors in column design for SEB removal.

7.1.8 Peptide Affinity Solid-Phase Extraction for SEB Detection

Due to its high affinity and capacity for SEB binding, peptide ligand YYWLHH can be used to selectively capture and concentrate SEB from food and environmental samples so that analytical and detection methods for SEB, such as HPLC, ELISA or MS, can obtain reliable results. One example is to improve the detection limit of ELISA by using a solid-phase extraction column packed with peptide YYWLHH for SEB enrichment. It has been shown that the peptide column can completely capture SEB from diluted samples and release them in a very small volume of the elution buffer, 2% acetic acid. As a result, the detection of SEB by ELISA is no longer limited by the low sample concentrations. In addition, the peptide column can be run many times without loss of efficiency. The peptide-affinity solid-phase extraction significantly extends the application range of ELISA. The SEB detection limit of the combined SPE-ELISA method was 1000 fold lower (5 pg/ml as opposed to 5 ng/ml).

7.2 Recommendations for Future Work

7.2.1 Improved Primary Screening

The primary screening can be improved if more information of the structure of the target molecule is available. Generally, peptide loops that connect α helices and β sheets in protein molecules are flexible in conformation and are exposed to the solvent and thereby responsible for ligand binding (Branden and Tooze, 1998). We have already seen that an

intact disulfide loop in the SEB molecule is required for the binding of SEB to peptide YYWLHH in chapter 3. An alternate screening strategy is to use synthesized peptides that are the same as the specific loop instead of the whole molecule in the primary screening. The main problem in the primary screening is that there are too many false positive signals. The reason to attribute to that is that there are nonspecific binding sites besides the specific loop in the protein molecule. The use of the loop region as the target could eliminate the nonspecific bindings to improve the efficiency of the primary screening.

The affinity peptide ligand that binds SEB is YYWLHH. We can synthesize a hexamer peptide library using four amino acids, namely, Y, W, L, and H. This is a small peptide library containing 4^6 peptide sequences. We can screen this library using radiolabeled SEB to see if we can regain the peptide YYWLHH or find a better one.

7.2.2 Soluble Peptide Ligands

The immobilization of peptide ligands YYWLHH on chromatography resins may significantly contribute to the binding of SEB. Previous studies showed that the library-derived peptide for the purification of von Willebrand Factor had an association constant of 1 μM^{-1}, while the association constant was lowered by three orders of magnitude when the peptide ligands were in free solution (Huang et al., 1996). Similarly, the association constant of peptide ligands was lowered three orders for the binding of α-1-proteinase inhibitor (Bastek, 2000) and a single order for fibrinogen (Kaufman et al., 2002) by using soluble instead of immobilized peptide ligands. These suggest that the binding between the target

protein and peptide resin could result from one or a combination of factors, i.e. conformational dependence of the immobilized peptide, interaction with multiple peptides, and binding to the linker arm and/or base resin (Bastek, 2000). On the other hand, the binding of s-protein to soluble hexamer peptide ligands had a larger association constant than that to immobilized peptide ligands because protein-surface interaction can negatively affect the association constant (Huang and Carbonell, 1995). Basically, immobilized peptides show a larger association constant than soluble peptides for multipoint binding due to the relatively higher peptide density at resin's surface, which favors multipoint binding. If the protein/peptide interaction is 1:1 in ratio, protein binding to the immobilized peptide may be prevented by the protein adsorption at neighboring peptides leading to a reduced association constant in comparison with that in free peptides. Therefore, it is better to investigate the interactions between SEB molecules and soluble peptide ligands YYWLHH to further characterize the peptide ligand YYWLHH for SEB binding.

7.2.3 Breakthrough Curves

Modeling chromatography requires a well-packed column to obtain uniform flow velocity to get the breakthrough curve. Because of the extreme toxicity and high cost of SEB, a small column (2.1mm × 30mm) was used to minimize the use of this toxin. The wall effect in this small column may cause the flow velocity to deviate from uniformity at cross-area of the column. Meanwhile, the hold-up volume may not be neglected compared to the column volume. All these nonideal factors violate the assumption that the GR model is

based on and as a result bring errors in the modeling. The breakthrough is becoming more dispersive than that in an ideal column and thus a longer processing time is needed to saturate the column. The rate constants will be underestimated by fitting the breakthrough curve with the GR model using a nonlinear regression. Therefore, in order to minimize the effect of nonideal factors, a column with bigger size, e.g. 4.6mm × 10cm, is recommended to obtain the breakthrough curve if an economic resource of SEB can be obtained.

7.2.4 Resin Reproducibility

For an affinity resin to be cost effective it must be recyclable. Kaufman et al. (2002) showed that the peptide ligand FLLVPE for fibrinogen purification could be subjected to 180 cycles of repeated loading of sample, washing, elution of fibrinogen, cleaning and regeneration without either performance or peptide concentration loss. For the purification or removal of SEB using ligand YYWLHH, the information of resin reproducibility is also required. We found column YYWLHH remain its total binding activity to SEB after ten cycles of repeated loading, washing, elution, clearing, and regeneration. A complete lifetime study of the column YYWLHH should be investigated in the future.

7.3 Reference

Bastek PD. 2000. Purification of alpha-1-proteinase inhibitor using ligands from combinatorial peptide libraries [Doctoral dissertation]. Raleigh, NC: North Carolina State University.

Branden C, Tooze J. 1998. Introduction to protein structure. New York: Garland Publishing, Inc.

Huang PY, Baumbach GA, Dadd CA, Buettner JA, Masecar BL, Hentsch M, Hammond DJ, Carbonell RG. 1996. Affinity purification of von Willebrand Factor using ligands derived from peptide libraries. Bioorg Med Chem 4:699-708.

Huang PY, Carbonell RG. 1995. Affinity purification of proteins using ligands derived from peptide libraries. Biotechnol Bioeng 47:288-297.

Kaufman DB, Hentsch ME, Baumbach GA, Buettner JA, Dadd CA, Huang PY, Hammond DJ, Carbonell RG. 2002. Affinity purification of fibrinogen using a ligand from a peptide library. Biotechnol Bioeng 77:278-289.